

Evaluation of Moment-Curvature Relationship for Reinforced Concrete Beam Element

By

Jiten A. Patel

12MCLC20



DEPARTMENT OF CIVIL ENGINEERING

AHMEDABAD-382481

MAY 2014

Evaluation of Moment-Curvature Relationship for Reinforced Concrete Beam Element

Major Project Report

Submitted in partial fulfillment of the requirements

For the degree of

Master of Technology in Civil Engineering

(Computer Aided Structural Analysis And Design)

By

Jiten Patel

(12MCLC20)

Guided By

Prof. (Dr.)Sharad Purohit



DEPARTMENT OF CIVIL ENGINEERING

INSTITUTE OF TECHNOLOGY

NIRMA UNIVERSITY

AHMEDABAD-382481

MAY 2014

Declaration

This is to certify that

- i) The thesis comprises my original work towards the degree of Master of Technology in Civil Engineering (Computer Aided Structural Analysis and Design) at Nirma University and has not been submitted elsewhere for a degree.
- ii) Due acknowledgement has been made in the text to all other material used.

Jiten A. Patel

Certificate

This is to certify that the Major Project Report entitled ”**Evaluation of Moment-Curvature Relationship for RC Beam Element**” submitted by **Mr. Jiten A. Patel (Roll No: 12MCLC20)**, towards the partial fulfillment of the requirements for the degree of Master of Technology in Civil Engineering (Computer Aided Structural Analysis And Design.) of Nirma University is the record of work carried out by him under our supervision and guidance. The work submitted has in our opinion reached a level required for being accepted for examination. The results embodied in this major project work to the best of our knowledge have not been submitted to any other University or Institution for award of any degree or diploma.

Date:

Prof.(Dr.) Sharad Purohit

Guide and Professor,
Department of Civil Engineering,
Institute of Technology,
Nirma University,
Ahmedabad.

Dr. P. V. Patel

Professor and Head
Department of Civil Engineering,
Institute of Technology,
Nirma University,
Ahmedabad.

Dr. K. Kotecha

Director,
Institute of Technology,
Nirma University,
Ahmedabad.

Examiner

Date of Examination

Abstract

The relationship between Moment and Curvature of Reinforced Concrete sections is an important parameter for Nonlinear Analysis of RC framed structure. This helps in determining strength, stiffness, ductility, and energy dissipation capacity of the RC sections. The moment-curvature relationship would enable us to observe the strength reduction beyond the yield point and degradation of the flexural rigidity. Theory of beam flexure states that curvature is the second derivate of displacement. Moment-Curvature ($M-\theta$) relation is then very important as it helps to calculation of displacement due to the forces acting in to the inelastic elements.

Analytical as well as experimental study is carried out for RC beam section. A well-established models of stress-strain for concrete and steel material are used. Models showing relationship of stress-strain for both confine as well as unconfined concrete are studied. Six deferent stress-strain models are selected. Among those IS 456 Model, Hongnestad Model, Kent and Park Model, IRC Model are pertaining to unconfined concrete and Cusson Model and Mendar Model are pertaining to confined concrete. For steel material King Model is used. A MATLAB based program is developed to derive Moment-Curvature relationship for RC beam elements using above mentioned models for concrete and steel material analytically.

An experimental program is design to evaluate Moment-Curvature relationship for RC beam elements. Both singly and doubly reinforced sections are design with under and over reinforcement for each section. Three sample specimens of dimension 120mm \times 150mm \times 1700mm are prepared for each case leading to total twelve numbers of test specimens. Loads and strain are measured to derive Moment-Curvature for each test specimens.

It is found that well established models of stress-strain for material to derive Moment- Curvature relationship closely match with the Moment-Curvature relationship experimentally. It is noticed that model suggested by IRC 112 shows good agrement with experimentally obtain Moment-Curvature relationship.

Acknowledgements

It gives me immense pleasure in expressing thanks and profound gratitude to **Dr. Sharad Purohit**, Professor, Civil Department, Institute of Technology, Nirma University, Ahmedabad for his valuable guidance and continual encouragement throughout this work. His constant support and interest in the subject equipped me with a great understanding of different aspects of the required architecture for the project work. The appreciation and continual support he has imparted, has been a great motivation to me in reaching a higher goal. His guidance has triggered and nourished my intellectual maturity that I will benefit from, for a long time to come.

It gives me an immense pleasure to thank **Dr. Paresh Patel**, Hon'ble Head of Civil Engineering Department, Institute of Technology, Nirma University, Ahmedabad for his kind support and providing basic infrastructure and healthy research environment.

My deepest thank you is extended to **Dr. Urmil Dave**, PG CL - Coordinator, Department of Civil Engineering, Institute of Technology, Nirma University, Ahmedabad for an exceptional support and continual encouragement throughout the Major Project

A special thank you is expressed wholeheartedly to **Dr K Kotecha**, Hon'ble Director, Institute of Technology, Nirma University, Ahmedabad for the unmentionable motivation he has extended throughout course of this work.

I would also thank the Institution, all faculty members of Civil Engineering Department, Nirma University and my friends for their special attention and suggestions towards the project work.

The blessings of God and family members make the way for completion of Project. I am very much grateful to them.

- **Jiten Patel**
12MCLC20

Abbreviations, Notations and Nomenclature

M	Moment of Reinforced Concrete Elements.
ϕ	Curvature of RC Elements.
f_{ck}	Characteristic Strength of Concrete.
σ_c	Stress at Any Point.
ε_c	Strain at Any Level.
f_{cc}	Characteristic Strength of Confined Concrete.
f_{c0}	Characteristic Strength of Unconfined Concrete.
f_c	Cylinder Strength of Concrete.
f_{cd}	Design Compressive Strength of Concrete.
ε_{co}	Peak Strain for Unconfined Concrete.
ε_{cc}	Peak Strain for Confined Concrete.
ε_{si}	Strain in Steel at Level of i^{th} Bar.
f_l	Lateral Confinement Pressure.
M_{cr}	Moment at Cracking.
ϕ_{cr}	Curvature at Cracking.
f_r	Modulus of Rupture.
I_g	Gross Moment of Inertia.
ρ	Tensile Steel Ratio.
ρ'	Compression Steel Ratio.
m	Modular Ratio.
f_y	Yield Strength of Reinforcement.
k_d	Neutral Axis Depth.
k	Neutral Axis Depth Factor.
a	Depth of Rectangular Stress Block.
M_y	Moment at Yielding.
ϕ_y	Curvature at Yielding.
M_u	Moment at Ultimate.

ϕ_u	Curvature at Ultimate.
C_c	Concrete Compressive Strength.
α	Mean Stress Factor.
γ	Centroid Factor.
T	Tensile Steel.
M_c	Moment of Compressive Force in Concrete About the Neutral Axis.
M_{cs}	Moment of Force in Compressive Steel About the Neutral Axis.
M_t	Moment of Force in Tensile Steel About the Neutral Axis.
A_{st}	Area of Tension Reinforcement.
A_{sc}	Area of Compression Reinforcement.
A_{sx}	Area of Transverse Reinforcement Running in X Direction.
A_{sy}	Area of Transverse Reinforcement Running in Y Direction.
SUR	Singly Under Reinforcement.
SOR	Singly Over Reinforcement.
DUR	Doubly Under Reinforcement.
DOR	Doubly Over Reinforcement.

Contents

Declaration	iii
Certificate	iv
Abstract	v
Acknowledgements	vi
Abbreviations, Notations and Nomenclature	vii
List of Tables	xii
List of Figures	xiv
1 Introduction	1
1.1 General	1
1.2 Introduction	2
1.3 Significance of Moment-Curvature	2
1.4 Objective of Study	3
1.5 Scope of Study	4
1.6 Methodology Carried Out	4
1.7 Organization of Report Work	6
2 Literature review	7
2.1 General	7
2.2 Unconfined Concrete	7
2.3 Confined Concrete	11
2.4 Inelastic Analysis of RC Elements	16
2.5 Summary	18
3 Analytical Evaluation of Moment Curvature	19
3.1 General	19
3.2 Evaluation of Moment-Curvature	19
3.3 Moment-Curvature by Transform Area Method	20

3.3.1	Moment-Curvature at Cracking	20
3.3.2	Moment-Curvature at Yielding	20
3.3.3	Moment-Curvature at Ultimate	21
3.4	Strain Compatibility Method	23
3.4.1	Procedure for Strain Compatibility Method	25
3.5	Computational Tools for Moment Curvature	28
4	Analysis of Moment-Curvature for RC Beam Elements	29
4.1	General	29
4.2	Problem Statement	29
4.3	Analytical Moment-Curvature	31
4.3.1	Transform Area Method	31
4.3.2	Strain Compatibility Method	33
4.4	Moment-Curvature by Computational Tools	42
4.4.1	Moment-Curvature Relationship by RC-Analysis	42
4.4.2	Moment-Curvature Relationship by RESPONSE 2000	43
4.5	Summery	45
5	Experimental Program	46
5.1	General	46
5.2	Concepts for Evaluation of Moment-Curvature	46
5.3	Experimental Problem	49
5.4	Casting of RC Beam	51
5.5	Instrumentation and Test Setup for RC Beam	53
5.6	Testing of RC Specimens	55
5.7	Test Results	57
5.7.1	Test Results for Concrete Properties	57
5.7.2	Experimental Moment-Curvature	59
5.8	Summary	79
6	Results and Discussion	81
6.1	General	81
6.2	Stress-Strain Curves	81
6.3	Experimental and Analytical Comparison of Moment-Curvature	82
6.4	Summary	88
7	Summary and Conclusions	89
7.1	Summary	89
7.2	Conclusions	90
7.3	Future Scope of Work	91
	References	92
A	Matlab Program by Transform Area Method	95

CONTENTS

xi

B Matlab Program by Strain Compatibility Method

101

C Experimental Results

107

List of Tables

4.1	Geometric Specification for Beam	30
4.2	Moment-Curvature for Singly Under Reinforced RC Beam.	35
4.3	Moment-Curvature for Singly Over Reinforced RC Beam.	37
4.4	Moment-Curvature for Doubly Under Reinforced RC Beam.	39
4.5	Moment-Curvature for Doubly Over Reinforced RC Beam.	41
4.6	Moment-Curvature Relationship by Using RC-ANALYSIS.	43
4.7	Moment-Curvature Relationship by Using RESPONSE 2000	44
5.1	Mix Design for M20 Grade Concrete	51
5.2	Cube Strength	57
5.3	Flexure Strength of Concrete	57
5.4	Modulus of Elasticity of Concrete	58
5.5	Moment-Curvature for SUR-1	59
5.6	Moment-Curvature for SUR-2	60
5.7	Moment-Curvature for SUR-3	61
5.8	Average Moment-Curvature for Singly Under Reinforced RC Beam. .	62
5.9	Moment-Curvature for Singly Over Reinforced Beam-1	64
5.10	Moment-Curvature for Singly Over Reinforced beam-2	65
5.11	Moment-Curvature for Singly Over Reinforced beam-3	66
5.12	Average Moment-Curvature for Singly Over Reinforced RC Beam. .	67
5.13	Moment-Curvature for Doubly Under Reinforced beam-1	69
5.14	Moment-Curvature for Doubly Under Reinforced beam-2	70
5.15	Moment-Curvature for Doubly Under Reinforced beam-3	71
5.16	Average Moment-Curvature for Doubly Under Reinforced RC Beam.	72
5.17	Moment-Curvature for Doubly Over Reinforced Beam-1	75
5.18	Moment-Curvature for Doubly Over Reinforced Beam-2	76
5.19	Moment-Curvature for Doubly Over Reinforced Beam-3	77
5.20	Average Moment-Curvature for Doubly Over Reinforced RC Beam. .	78
C.1	Strain in Singly Under Reinforced Beam-1	108
C.2	Strain in Singly Under Reinforced Beam-2	109
C.3	Strain in Singly Reinforced Beam 3	110
C.4	Strain in Singly Over Reinforced Beam-1	111

C.5	Strain in Singly Over reinforced Beam-2	112
C.6	Strain in Singly Over reinforced Beam-3	113
C.7	Strain in Doubly Under Reinforced Beam-1	114
C.8	Strain in Doubly Under Reinforced Beam-2	115
C.9	Strain in Doubly Under Reinforced Beam-3	116
C.10	Strain in Doubly Over Reinforced Beam-1	117
C.11	Strain in Doubly Over Reinforced Beam-2	118
C.12	Strain in Doubly Over Reinforced Beam-3	119

List of Figures

1.1	Idealized Moment-Curvature Relation [1]	3
1.2	Flow of The Study	5
2.1	Proposed Stress-Strain Model for Confined and Unconfined Concrete by Kent and Park [4].	9
2.2	Stress-Strain Relation for Monotonic Loading of Confined and Unconfined Concrete by Mander [8]	14
2.3	Stress-Strain Relation for Monotonic Loading of Confined and Unconfined Concrete by cusson [14].	15
3.1	Stress-Strain Curve for Steel [3]	24
3.2	Section With Strain, Stress and Force Distribution [3]	25
3.3	Flow Chart of Computer Program	27
4.1	Cross Section of Beam (a) Singly Under Reinforced (b) Singly Over Reinforced	30
4.2	Cross Section of Beam (a) Doubly Under Reinforced (b) Doubly Over Reinforced	31
4.3	Moment-Curvature Relationship for Singly Reinforced Beam	32
4.4	Moment-Curvature Relationship for Doubly Reinforced Beam	32
4.5	Various Stress-Strain Models	34
4.6	Moment-Curvature for Singly Under Reinforced Beam	36
4.7	Moment-Curvature for Singly Over Reinforced Beam	38
4.8	Moment-Curvature for Doubly Under Reinforced Beam	40
4.9	Moment-Curvature for Doubly Over Reinforced Beam	42
4.10	Moment-Curvature Relationship from RC-ANALYSIS	43
4.11	Moment-Curvature Relationship from RESPONSE 2000	45
5.1	Curvature of Member [3]	47
5.2	Moment-Curvature Relationship for Singly Reinforced Section	48
5.3	Experimental Program	49
5.4	Cross Section of Beam (a) Singly Under Reinforced (b) Singly Over Reinforced	50

5.5	Cross Section of Beam (a) Doubly Under Reinforced (b) Doubly Over Reinforced	51
5.6	3D View of Formwork for Beam	52
5.7	Casting of Specimens for Deriving Concrete Properties	52
5.8	Formwork and Reinforcement Cage of RC Specimens.	53
5.9	Instrumentation and Test Setup.	53
5.10	Test Setup and Instrumentation Used for Experiments	54
5.11	Testing of Specimens	55
5.12	Failure of RCC Beams	55
5.13	Failure Patterns of RCC Beams	56
5.14	Moment-Curvature For Singly Under Reinforced Beam	63
5.15	Stain at Tension and Compression Zone	63
5.16	Moment-Curvature relationship for Singly Over Reinforced beam . . .	68
5.17	Concrete and Steel Strain of Doubly Under Reinforced Beam	68
5.18	Moment-Curvature Doubly Under Reinforced	73
5.19	Compression Strain and Tensile Strain in Doubly Under Reinforced Beam	74
5.20	Moment-Curvature Doubly Over Reinforced	79
5.21	Compression Strain and Tensile Strain in Doubly Over Reinforced Beam	79
6.1	Stress-Strain Models	82
6.2	Moment-Curvature for Singly Under Reinforced Beam	83
6.3	Moment-Curvature for Singly Over Reinforced Beam	84
6.4	Moment-Curvature for Doubly Under Reinforced Beam	85
6.5	Moment-Curvature for Doubly Over Reinforced Beam	87
6.6	Compressive and tensile strain in concrete and steel respectively . . .	88

Chapter 1

Introduction

1.1 General

Reinforced concrete (RC) is the one of the most widely used structural material. Because of the non-homogeneity of the reinforced concrete, various methods for its analysis and design are used. However linear behavior is valid for a region of small response. At ultimate load condition material and geometrical non-linearity occurs which calls for non-linear analysis of structure. In present days, there is a turn in design philosophy from linear static approaches to performance based approaches. Nonlinear analysis required relationship of Moment-Curvature for section so it play important role. Moment-Curvature relationship for the section is the initial input of the Non-Linear analysis. The Moment-Curvature relationship of RC section demonstrates the strength, ductility, stiffness and energy dissipation capacity of the structural section subjected to bending. The Moment-Curvature also give as the clear view of strength reduction beyond the peak point and degradation of the flexural rigidity. In present report, a computer program is developed to evaluate Moment-Curvature relation for RC rectangular beam section analytically. An experimental program is also design to obtain Moment-Curvature for RC beam experimentally. Then experimental results are compared with the analytical results.

1.2 Introduction

Most of buildings and bridges are designed to exceed their elastic limits when attacked by the design earthquake. Exceeding elastic limits for reinforced concrete sections means cracking of concrete, yielding of reinforcement, crushing of concrete and eventual collapse of the section. The nonlinear flexural behavior of reinforced concrete sections can be assessed by a special type of section analysis called Moment-Curvature analysis. The outcome of this analysis is the relation between applied moment and related curvature in the section.

”Moment-Curvature analysis is a method to accurately determine the load-deformation behavior of the concrete section using nonlinear material stress-strain relationship.”

For given axial load there exists an extreme compression fiber strain and a section curvature at which the nonlinear stress distribution is in equilibrium with the applied axial load. A unique bending moment can be calculated at this section curvature from the stress distribution. The extreme concrete compression stain and section curvature can be iterated until a range of moment-curvature values are obtain.

1.3 Significance of Moment-Curvature

The design of the structure is carried out by limit state method even though the analysis of structure is done by the conventional elastic theory, for taking in to account the material nonlinearity. This method is good for determinate as well as indeterminate structure even under factor load conditions till the Moment -Curvature relationship remain linear. For under reinforced section it is valid till the reinforcement steel is not yielded. However, once yielding has take place (at any section), the behavior of a structure enters in an inelastic phase, and the simplified conventional linear elastic structural analysis is no longer valid. There is a called for inelastic analysis of structure. One has to determine the bending moments for loading beyond the yielding stage. In simplified limit analysis the moment-curvature relation is an idealized

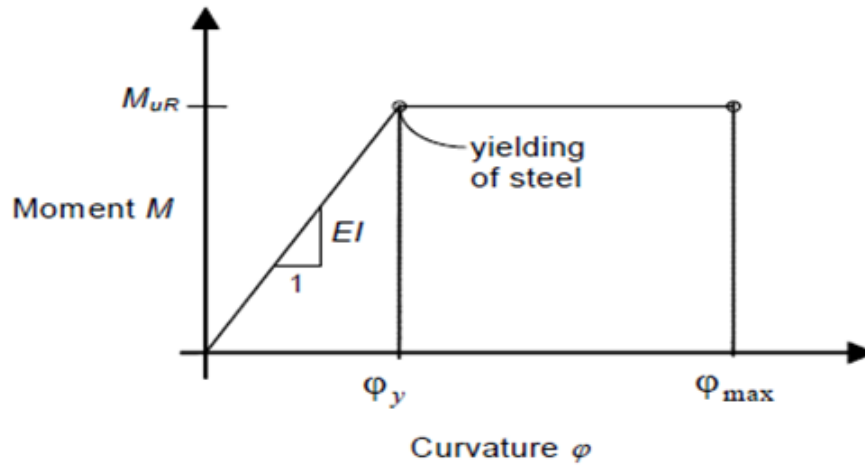


Figure 1.1: Idealized Moment-Curvature Relation [1]

bilinear elasto-plastic relation as shown in Fig. 1.1.

1.4 Objective of Study

Objectives of the present study have been identified as follows:

- To understand the various stress-strain models for confine and unconfined concrete.
- To develop computer program to calculate analytical Moment-Curvature.
- To carry out experiment to determine relation between Moment and curvature for RC beam elements.
- To explore various computational tools for Moment Curvature.

1.5 Scope of Study

In order to achieving the above objectives the scope of study are as under:

- To study need of Moment-Curvature relationship in Non-Linear analysis.
- To study various nonlinear stress-strain models for concrete and steel.
- It also include the preparation for RC specimens for deriving experimental Moment-Curvature relationship.
- To study about instrumentation for measuring the curvature in RC beam elements
- To develop a computer program to determine the moment curvature relationship for RC rectangular beam element using Matlab.
- To study the different available tools which are used for finding Moment - Curvature for RC Beam Element.
- Comparison of results obtain by experiments and analytically.

1.6 Methodology Carried Out

Methodology adopted in present study are as shown in Fig. 1.2. Here, study was divided in to two parts part-I include the experimental work and part-II include analytical work. Experiment work includes casting of specimens, preparation for instrumentation and testing of specimens and part-II include analytical evaluation of moment curvature by transform area method and strain compatibility method.

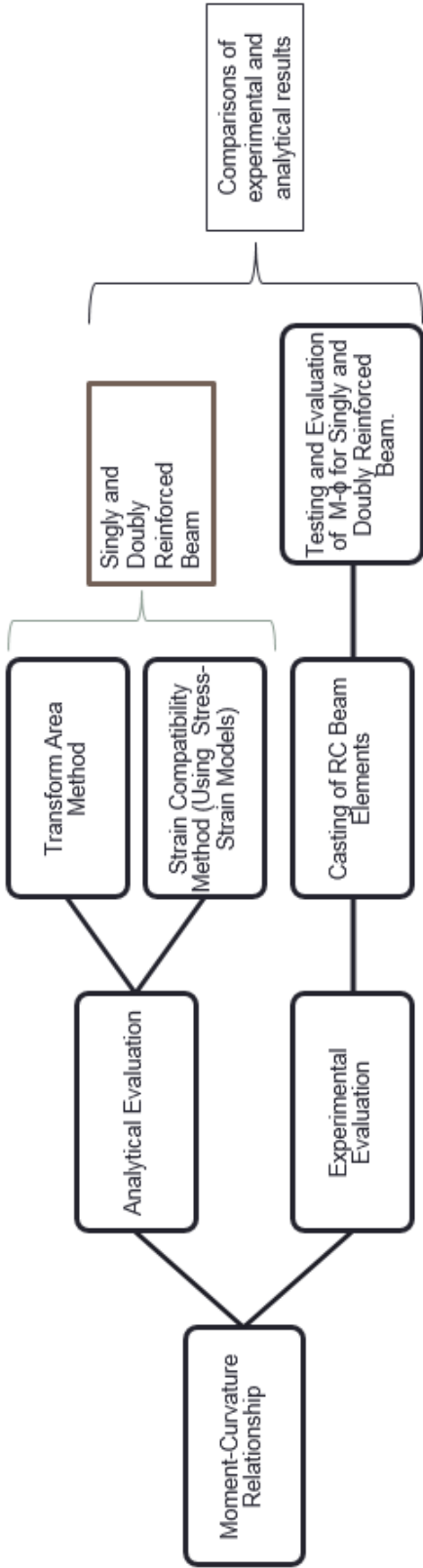


Figure 1.2: Flow of The Study

1.7 Organization of Report Work

Chapter 2 starts with a literature review which include three parts. In first part description of various stress-strain curve for concrete and steel are included. In second part the experimental evolution of moment-Curvature relationship is given. And in third part is dealing with the evolution of analytical Moment-Curvature relationship.

Chapter 3 includes the theoretical evolution of Moment Curvature relationship for unconfined concrete as well as confined concrete. these chapter also deals with the various methods for evaluation of Moment-Curvature.

Chapter 4 includes the problem statements and Moment-Curvature relationship was evaluated for the designed RC beam elements by using various mathematical stress-strain models. In this chapter, a Moment-Curvature relationship was also developed by using various available tools.

Chapter 5 discusses about the experimental setup and experimental evaluation of the moment curvature relationship for RC beam Element.

Chapter 6 includes the experimental results for concrete properties as well as experimental Moment-Curvature. It also deals with the comparison of analytical Moment-Curvature and experimental Moment-Curvature.

Chapter 7 deals with the summery of the study. It also include the conclusions and future scope of the work.

Chapter 2

Literature review

2.1 General

This chapter deals with the most relevant literature available on the study of Moment-Curvature relationship. It includes the study of different existing confined and unconfined stress-strain models for concrete. It also deals with the literature available for evaluation of moment and curvature for reinforced beam and column elements.

2.2 Unconfined Concrete

IS Code Model[7], IS456 suggests a standard constitutive model for concrete. The constitutive behavior of concrete in compression is assumed to be parabolic up to strain 0.002 and then it follows a straight horizontal line up to failure. It ignores the degradation of concrete at strains beyond 0.002. Thus the constitutive relation is expressed as follow:

For $0 < \varepsilon_c < 0.002$

$$\sigma_c = f_{ck} \left[\left(\frac{2\varepsilon_c}{\varepsilon_{co}} \right) - \left(\frac{\varepsilon_c}{\varepsilon_{co}} \right)^2 \right] \quad (2.1)$$

For $0.002 < \varepsilon_c < 0.004$

$$\sigma_c = f_{ck} \quad (2.2)$$

Where, σ_c = stress in concrete at any point of strain; ε_c = strain at any point; ε_{co} = strain at which parabolic part ends = 0.002; f_{ck} = characteristic compressive strength of concrete.

Hognestad Model[6] The Hognestad model includes the damage parameter of concrete. The stress-strain curve before maximum stress reached is a parabola and then the falling branch behavior is adopted depending on the limit of useful strain the relations is expressed as under;

For $0 < \varepsilon_c < 0.002$

$$\sigma_c = f_{ck} \left[\left(\frac{2\varepsilon_c}{\varepsilon_{co}} \right) - \left(\frac{\varepsilon_c}{\varepsilon_{co}} \right)^2 \right] \quad (2.3)$$

For $0.002 < \varepsilon_c < 0.004$

$$\sigma_c = f_{ck} [1 - 100(\varepsilon_c - \varepsilon_{co})] \quad (2.4)$$

Kent and Park (1971) [4] proposed a stress-strain equation for both unconfined and confined concrete. In their model they used Hognestad's (1951) equation to more completely describe the post-peak stress-strain behavior. In this model the ascending branch is represented by modifying the Hognestad second degree parabola by replacing $0.85f_c'$ by f_c' and ε_{co} by 0.002.

$$\sigma_c = f_c \left[\left(\frac{2\varepsilon_c}{\varepsilon_{co}} \right) - \left(\frac{\varepsilon_c}{\varepsilon_{co}} \right)^2 \right] \quad (2.5)$$

The post peak branch was assumed to be straight line whose slope was defined primarily as a function of concrete strength.

$$\sigma_c = f_c [1 - Z(\varepsilon_c - \varepsilon_{co})] \quad (2.6)$$

Where,

$$Z = \frac{0.5}{\varepsilon_{50u} - \varepsilon_{co}} \quad (2.7)$$

$$\varepsilon_{50u} = \frac{3 + 0.29f_c}{145f_c - 1000} \quad (2.8)$$

ε_{50u} =the strains corresponding to the stress equal to 50% of the maximum concrete strength for unconfined concrete. The Kent and park model is represented in Fig. 2.1

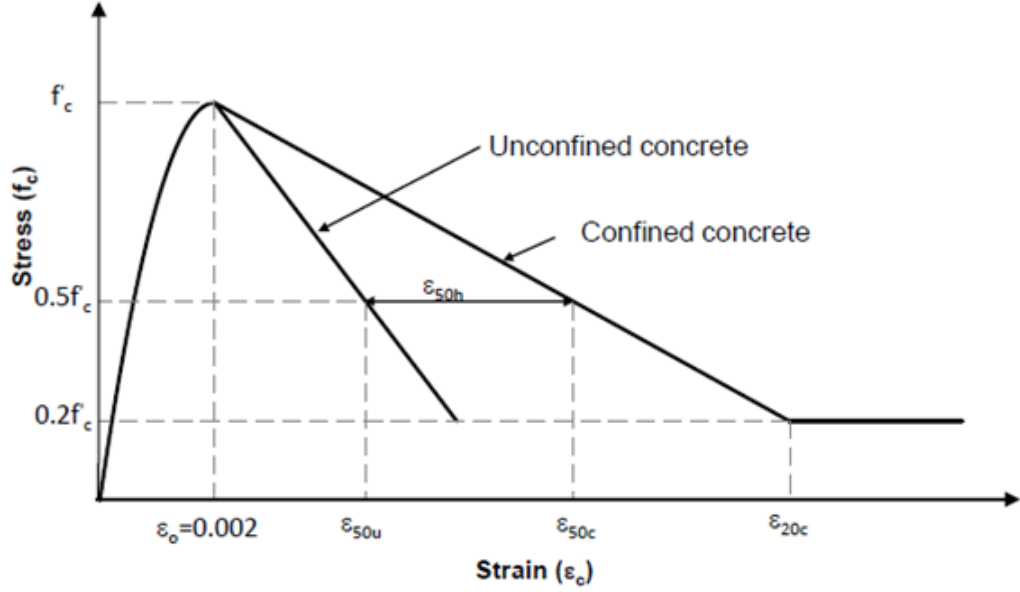


Figure 2.1: Proposed Stress-Strain Model for Confined and Unconfined Concrete by Kent and Park [4].

IRC 112 Model[8] The parabolic rectangular stress-strain block described by the IRC 112 model is valid for all situations and expression for ascending portion are as under;

$$\sigma_c = f_{cd} \left[1 - \left(1 - \left(\frac{\varepsilon_c}{\varepsilon_{c2}} \right)^2 \right) \right] \quad (2.9)$$

Post peak behavior of the curve describe by follow;

$$\sigma_c = f_{cd} \quad (2.10)$$

$$f_{cd} = \frac{0.67f_{ck}}{1.5} \quad (2.11)$$

Where, f_{cd} = design compressive strength of concrete; σ_c = stress in concrete at any point of strain; ε_c = strain at any point; ε_{c2} = strain at reaching characteristic strength=0.002; ε_{cu2} = Ultimate strain=0.0035; f_{ck} = characteristic compressive strength of concrete.

Popovics (1973) [10] proposed a single equation to describe unconfined concrete stress-strain behavior. A major appeal of this model is that it only requires three parameters to control the entire pre and post peak behavior, specifically f_{ck} , ε_{co} and E_c .

$$\frac{\sigma_c}{f_{ck}} = \frac{n\left(\frac{\varepsilon_c}{\varepsilon_{co}}\right)}{(n-1) + \left(\frac{\varepsilon_c}{\varepsilon_{co}}\right)^n} \quad (2.12)$$

In which the power 'n' can be expressed as an approximate function of the compressive strength of normal-weight concrete as;

$$n = 0.4 \times 10^{-3}f_{ck} + 1.0 \quad (2.13)$$

Popovics equation works well for most normal strength concrete ($f_{ck} \leq 55$ MPa), but it lacks the necessary control over the slope of the post-peak branch for high strength concrete.

Thorenfeldt et al. (1987) [12] made modifications to the Popovics (1973)[10] relation to adjust the descending branch of the concrete stress-strain relation. The authors proposed the following equation for the unconfined concrete stress-strain relation.

$$\frac{\sigma_c}{f_{ck}} = \frac{n\left(\frac{\varepsilon_c}{\varepsilon_{co}}\right)}{(n-1) + \left(\frac{\varepsilon_c}{\varepsilon_{co}}\right)^{nk}} \quad (2.14)$$

In above eq. for $(\varepsilon_c/\varepsilon_{co}) < 1$ value of k is taken as 1 and for $(\varepsilon_c/\varepsilon_{co}) > 1$ value of k is taken as greater than 1. Thus by adjusting the value of 'k' the post-peak branch

of the stress-strain relation can be made steeper. This approach can be used for high strength concrete.

One shortcoming of those models are that they ignore the level of confinement provided by the lateral reinforcement. The useful strain in concrete depends on the confinement of concrete. So in present study confined model were also included to study the effect of the confinement.

2.3 Confined Concrete

Kent and **Park** (1971) [4] **modified** their stress-strain model for including effect of the confinement. Based on the results from tests on square columns by **Roy** and **Sozen**, it was shown that confining the concrete with rectangular or square hoops was not very effective and there was no substantial increase in the concrete compressive strength due to confinement because of this the maximum stress in the confined concrete is assumed same as that unconfined concrete so thus the ascending branch of the model is represented by the same second degree of parabola.

The slope of the post-peak branch is affected by the confinement. The empirical equation for descending branch of the stress-stain relation is given by,

$$\sigma_c = f_c[1 - Z(\varepsilon_c - \varepsilon_o)] \quad (2.15)$$

where,

$$Z = \frac{0.5}{\varepsilon_{50h} + \varepsilon_{50u} - \varepsilon_o} \quad (2.16)$$

$$\varepsilon_{50u} = \frac{3 + 0.29f_c}{145f_c - 1000} \quad (2.17)$$

$$\varepsilon_{50h} = \varepsilon_{50c} - \varepsilon_{50u} \quad (2.18)$$

$$\varepsilon_{50h} = \frac{3}{4}p''\sqrt{\frac{b''}{s}} \quad (2.19)$$

where ε_{50c} and ε_{50u} are the strains corresponding to the stress equal to 50% of the maximum concrete strength for confined and unconfined concrete respectively.

b'' is the width of the confined core. S is the spacing of the confine reinforcement p'' is the volumetric ratio of the confine hoops to the volume of the concrete core measured to the outside of the perimeter hoops and is given by

$$p'' = \frac{2(b'' + d'')As''}{b''d''s} \quad (2.20)$$

d'' is the depth of the confine core and As'' is the cross sectional area of the hoop bars. It is assumed that concrete can sustain some stress at indefinitely large strains. However, the failure of the member would occur before the strains in concrete become impractically high. Hence, for this model it was assumed that the concrete can sustain a stress of $0.2f_c'$ from a strain of ε_{20c} to infinite strain. Fig. 2.1 shows the proposed stress-strain model by Kent and Park.

Mander et al. (1988) [8] tested a full scale rectangular, square and circular column to study the effect of the transverse reinforcement on the confinement effectiveness and overall performance. From the test he observed that if the peak strain and stress co-ordinates could be found then the performance over the entire range of stress-strain curve was similar. And it was not depends on the arrangement of confinement reinforcement. Author decide the failure criteria base on **William** and **Warnker** model and **Schicert** and **Winkle** model to generate a confine model. He used **Popvics** model to describe entire stress-strain model.

$$\frac{\sigma_c}{f_{ck}} = \frac{n\left(\frac{\varepsilon_c}{\varepsilon_{co}}\right)}{(n-1) + \left(\frac{\varepsilon_c}{\varepsilon_{co}}\right)^n} \quad (2.21)$$

$$n = \frac{Ec}{Ec - E_{sec}} \quad (2.22)$$

$$E_c = 5000\sqrt{f_{ck}} \quad (2.23)$$

$$E_{sec} = \frac{f_{cc'}}{\varepsilon_{cc}} \quad (2.24)$$

ε_{cc} is the stain at the maximum compressive strength of confined concrete f_{cc}' .

$$\varepsilon_{cc} = \varepsilon_{co} \left[1 + 5 \left(\frac{f_{cc'}}{f_{c'}} - 1 \right) \right] \quad (2.25)$$

f_{cc}' is the compressive strength of confine concrete. For circular section:

$$f_{cc'} = f_{ck} \left(-1.254 + 2.254 \sqrt{1 + \frac{7.94 f_{l'}}{f_{ck}} - \frac{2 f_{l'}}{f_{ck}}} \right) \quad (2.26)$$

in which $f_{l'}$ is the confinement pressure and is given by

$$f_{l'} = \frac{1}{2} K_e \rho_s f_{yh} \quad (2.27)$$

ρ_s = ratio of volume of transvers confining steel to volume of confine concrete core.

f_{yh} = yield strength of the transverse reinforcement. K_e = Confinement coefficient.

For rectangular section:

$$f_{cc} = f_{co} + 4.1 \times f_{le} \quad (2.28)$$

$$f_{le} = \sqrt{f_{le_x}^2 + f_{le_y}^2} \quad (2.29)$$

$$f_{le_x} = \frac{k_e \times A_{sx} \times F_y}{s \times d_c} \quad (2.30)$$

$$f_{le_y} = \frac{k_e \times A_{sy} \times F_y}{s \times b_c} \quad (2.31)$$

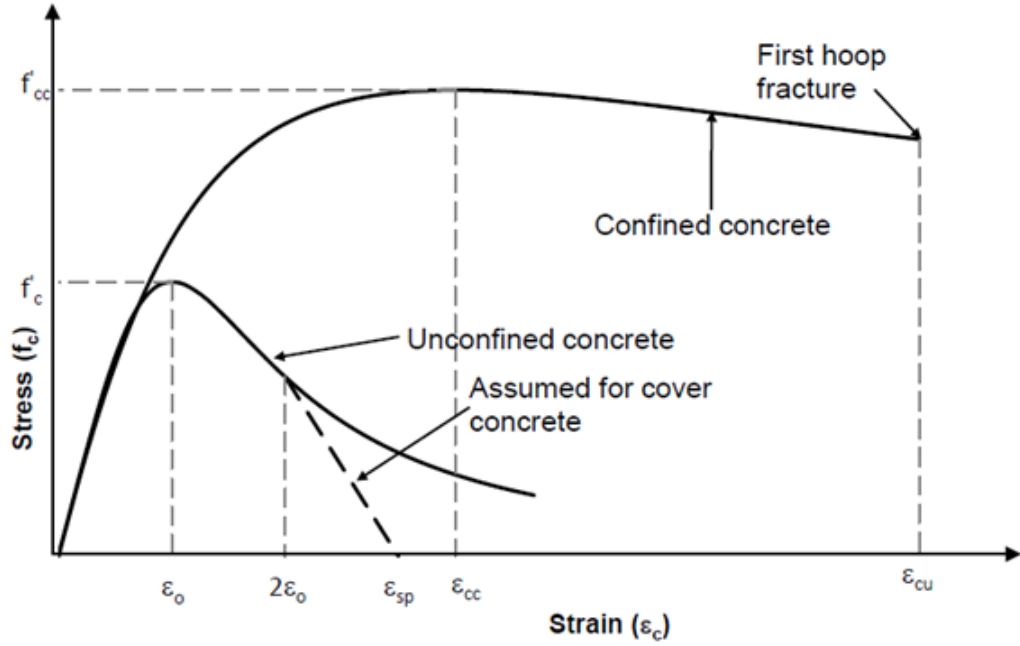


Figure 2.2: Stress-Strain Relation for Monotonic Loading of Confined and Unconfined Concrete by Mander [8]

$$k_e = \frac{(1 - \sum_{i=1}^n \frac{(w_i)^2}{6b_c d_c})(1 - \frac{s'}{2b_c})(1 - \frac{s'}{2d_c}))}{1 - \rho_{cc}} \quad (2.32)$$

Where, b_c and d_c are the core dimensions. ρ_{cc} = ratio of area of longitudinal reinforcement to area of core of section. S' = Spacing between hoops. A_{sx} and A_{sy} are total area of transverse steel running in the x and y directions, respectively. The Mander et al. (1988) model does not handle the post-peak branch of high strength concrete particularly well and requires some modification. Fig. 2.2 shows stress-strain curve proposed by the Mander.

Cusson et al. (1995) [14] conducted an experiment on 50 large scale high strength concrete column to develop stress-strain model which includes the effect of concrete compressive strength, tie yield strength, tie configuration, transverse reinforcement ratio, tie spacing and longitudinal reinforcement ratio. Based on the experimental results he proposed following sets of equations. The ascending part (OA) Fig.

2.3 is a relationship originally proposed by **Popovics** [8] for concrete and written as:

$$\sigma_c = f_{cc} \left(\frac{K \left(\frac{\varepsilon_c}{\varepsilon_{cc}} \right)}{K - 1 + \left(\frac{\varepsilon_c}{\varepsilon_{cc}} \right)^K} \right) \quad (2.33)$$

where,

$$K = \frac{E_c}{E_c - \frac{f_{cc}}{\varepsilon_{cc}}} \quad (2.34)$$

Here, K controls the initial slope and the curvature of the ascending branch. E_c =tangent modulus of concrete. The descending part (ABC) Fig. 2.3 of the stress-strain curve is a modification of the relationship proposed by the **Fafitis and shah** [23] for confined HSC and is described as under:

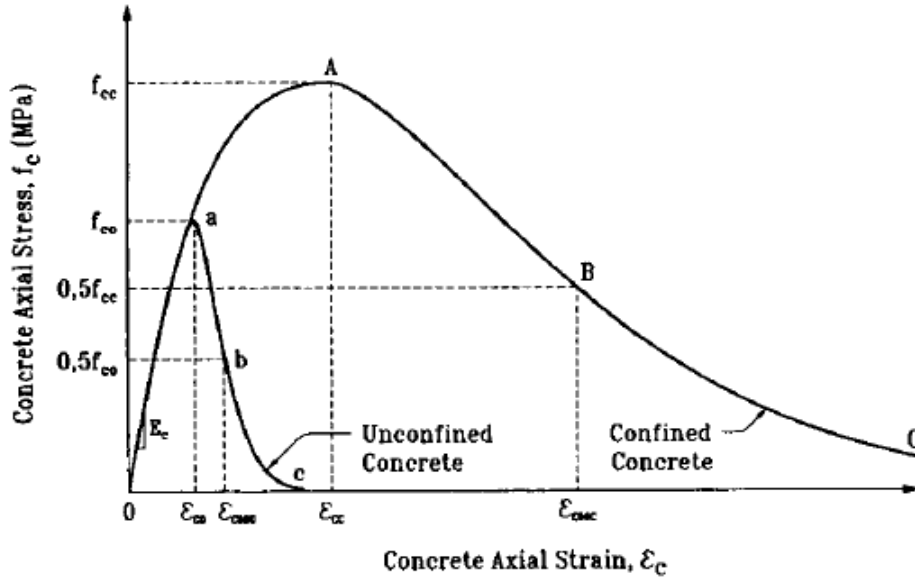


Figure 2.3: Stress-Strain Relation for Monotonic Loading of Confined and Unconfined Concrete by **cusson** [14].

$$\sigma_c = f_{cc} e^{k_1(\varepsilon_c - \varepsilon_{cc})^{1.5}} \quad (2.35)$$

$$k_1 = \frac{\ln 0.5}{(\varepsilon_{c50c} - \varepsilon_{cc})^{1.5}} \quad (2.36)$$

k_1 control the general slope of the descending branch of the curve.

Li et al. (2000) [5] conducted an experimental investigation on circular and square reinforced concrete columns to study the behavior of high-strength concrete columns confined by normal and high-yield strength transverse reinforcement and with different confinement ratio and configurations. From the tests they concluded that volumetric ratio and the yield strength of confining reinforcement significantly affect the shape of the stress-strain curve. Based on their experimental study, Li et al. (2001) proposed a three branch stress-strain model for high strength concrete confined by either normal or high-yield strength transverse reinforcement. The equations are:

$$\sigma_c = \begin{cases} E_c \varepsilon_c + \left(\frac{f_{ck} - E_c \varepsilon_{co}}{\varepsilon_{co}^2} \right) \varepsilon_c^2 & 0 < \varepsilon_c \leq \varepsilon_{co} \\ f_{cc'} - \frac{(f_{cc'} - f_{ck})}{(\varepsilon_{cc} - \varepsilon_{co})^2} (\varepsilon_c - \varepsilon_{co})^2 & \varepsilon_{co} < \varepsilon_c \leq \varepsilon_{cc} \\ f_{cc'} - \frac{\beta f_{cc'}}{\varepsilon_{cc}} (\varepsilon_c - \varepsilon_{cc})^2 \geq 0.4 f_{cc'} & \varepsilon_c > \varepsilon_{cc} \end{cases}$$

The term β controls the slope of the post-peak branch of the stress-strain model. The maximum confined concrete compressive strength is given by

$$f_{cc'} = f_{ck} \left(-1.254 + 2.254 \sqrt{1 + \frac{7.94 f_l'}{f_{c'}} - \frac{2 \alpha_s f_l'}{f_{c'}}} \right) \quad (2.37)$$

Where

$$\alpha_s = \begin{cases} (21.2 - 0.35 f_{ck}) \frac{f_l'}{f_{ck}} & f_{ck} \leq 52 \text{Mpa} \\ 3.1 \frac{f_l'}{f_{ck}} & f_{ck} > 52 \text{Mpa} \end{cases}$$

Where f_l' is the effective lateral confining pressure, calculated using the equations proposed by Mander et al. (1988).

2.4 Inelastic Analysis of RC Elements

Shamim A. Sheikh [22] developed the computer program by using four stress-strain model (i.e Mander model, Fafitis model, Sheikh and Uzumeri model, and modified Kent and park model.) to predict the moment curvature relationship for the column

section under axial load. By comparing the experimental results with the analytical results he found that the model by Mander et al. overestimate the moment curvature for RC element and analytical results from the modified Kent and Park model underestimate the sectional capacity.

Srikanth et al. (2007) [17] found out the analytical Moment-Curvature behavior for statically determinate RC beam elements by considering effect of the confinement reinforcement in the compression zone. Author developed Moment-Curvature relationship by using six different stress-strain model as a stress block. Analytical Moment-Curvature obtain from different model was compared with the experimental results. Author has found that the results obtain from the Cusson and Mendis model are very closer from the experimental results. Srikanth also carried out parametric study to find out the effect of various parameters on the Moment-Curvature relationship.

Noor [25] developed experimental program to find ductility for simply supported beam subjected to the two point loading. Noor considered moment-curvature relation, depth of neutral axis and strain in the material as a performance criteria. Here author found out the effect of the high strength steel and high strength concrete on the ductility and moment curvature. Noor concluded that by using high strength steel ductility and stiffness were increased and in the case of high strength concrete it was decreased.

Kwak et al. (2000) [16] carried out the material nonlinear analysis of RC beam using Moment-Curvature instead of using sophisticated layered approach because it has some limitation in application to large structure with many degree of freedom. Kent and Park and later extended by Scott [11] model was used as a stress block for the concrete in the computer program of Moment Curvature. Kwak found the moment- Curvature at three different point such as cracking, yielding and ultimate.

Suarez et al. [20] Developed tool known as RC-analysis to find out the Moment-Curvature for RC square, rectangular and circular column and rectangular RC beam element. RC-analysis models nonlinear behavior of confined concrete, unconfined con-

crete and reinforcing bars to obtain curvature response. The shear strength plot is obtain by modified Kowalsky and priestly model. From the moment curvature plot different response limit states can be identified. The stress-strain relation for reinforcing steel is same used by the king program.

2.5 Summary

Present study include different stress-strain blocks for confine and unconfined concrete member. Literature review shows that Mander[9] and Cusson [12] gives close solution to the experimental solution.

In literatures L/d ratio for simply supported beams were taken around 10. And b/d ratio was taken around 0.5 to 0.9.

Literature also shows that as the concrete grade is increased probability of brittle failure of RC section is also increased.

Chapter 3

Analytical Evaluation of Moment Curvature

3.1 General

This chapter deals with the analytical evaluation of Moment Curvature of RC rectangular beam element. A matlab program is developed to evaluate the Moment-Curvature relationship for rectangular RC beam element by transformed area method as well as by strain compatibility method. Here the stress-strain curves which are used in this study are also discuss. This chapter is include various computational tools available for Moment-Curvature relationship for confine as well as unconfined RC elements.

3.2 Evaluation of Moment-Curvature

Moment-Curvature can be evaluate by using Theoretical Method or Strain Compatibility method anad Transform area method. The transform area method is simple but approximate method to evaluate moment curvature while strain compatibility method is accurate but iterative method. In strain compatibility method material models used as a stress block. Following section explain in detail about the evalua-

tion of Moment-Curvature by these two methods.

3.3 Moment-Curvature by Transform Area Method

In transform area method, Moment-Curvature relation is found out for three different points say cracking, yielding and ultimate to plot whole curve. Each state is described in details in following sections.

3.3.1 Moment-Curvature at Cracking

When the stress in the concrete reached equal to the modulus of the rupture of section, the first onset crack is occur and critical moment is calculated by using following equation;

$$M_{cr} = \frac{f_r I_g}{y_t} \quad (3.1)$$

Where, f_r is the modulus of rupture of concrete, I_g is the moment of inertia of gross section considering the contribution from reinforcements, and y_t is the distance of extreme tension fiber from neutral axis of the section. Considering the contribution of reinforcements to moment of inertia. Corresponding curvature can be find out by using following equation;

$$\phi = \frac{f_r}{E_c y} \quad (3.2)$$

This gives the cracking point on the curve (M_{cr} , ϕ_{cr}). Where, E_c is modulus of elasticity of concrete.

3.3.2 Moment-Curvature at Yielding

As the moment is increased the cracks in the tension zone propagates through the cross-section. The moment-curvature relation is linear till the tension reinforcement yields. At yielding, strain in the tension reinforcement is ε_y and neutral axis shifts towards the compression area. The neutral axis at yielding is given as distance kd from

extreme compression fiber, where the depth factor \mathbf{k} is calculated using expression in case of doubly reinforced section;

$$k = \sqrt{(\rho + \rho')^2 m^2 + 2 \left(\rho + \frac{\rho' d'}{d} \right) m - (\rho + \rho')} \quad (3.3)$$

In case of singly reinforced section \mathbf{k} is calculated by calculating roots of following equation;

$$k^2 + 2m\rho k - 2m\rho = 0 \quad (3.4)$$

Where ρ and ρ' are the tension and compression steel ratios, m is the modular ratio, and d and d' are the distance of compression and tension steel from extreme compression fiber. Moment is given by following equation;

$$M_y = jd f_y A_s \quad (3.5)$$

Where, f_y is the yielding of the reinforcement. A_s is the tension reinforcement and jd is the distance from centroid of compressive forces in the steel and concrete to the centroid of tension. Corresponding curvature is given by following equation;

$$\phi_y = \frac{\varepsilon_s}{(d - kd)} \quad (3.6)$$

This gives the cracking point on the curve (M_y, ϕ_y) .

3.3.3 Moment-Curvature at Ultimate

After yielding of tension steel, stress remains constant but strain keeps increasing until compressive strain in extreme fiber of concrete reaches its maximum value. In order to address the nonlinearity in concrete at high strains, Whitney-block is used to convert the parabolic stress distribution in concrete to an equivalent rectangular stress-block representation. The ultimate Curvature and moment of doubly reinforced section for the case where the tension steel is yielding may be found using following

equations;

$$a = \frac{A_s f_y - A'_s f_y}{0.85 f'_c b} \quad (3.7)$$

$$M = 0.85 f'_c a b \left(d - \frac{a}{2} \right) + A'_s f_y (d - d') \quad (3.8)$$

The ultimate Curvature and moment of singly reinforced section for the case where the compression steel is yielding may be found using following set of equations. Equivalent depth of the rectangular stress block can be calculated by solving following equation;

$$\left(\frac{0.85 f'_c}{0.003 E_c \rho} \right) a^2 + a d - 0.85 d^2 = 0 \quad (3.9)$$

Ultimate moment can be calculated by;

$$M_u = 0.85 f'_c a b (d - 0.5a) \quad (3.10)$$

where, d is the effective depth of the section. f'_c is the concrete compressive strength. E_c is the modulus of the elasticity of concrete. b is the width of the section. Corresponding Curvature is given by

$$\phi_u = \frac{0.85 \varepsilon_c}{a} \quad (3.11)$$

Where, ε_c is ultimate strain in concrete at maximum stress. Assumption of yielding in tension reinforcement is now checked by ensuring:

$$\varepsilon'_s = \varepsilon_c \left(\frac{c - d'}{c} \right) \leq \varepsilon_y \quad (3.12)$$

If the above condition is satisfied then assumption made is true and obtained value of defines the ultimate state on the moment-curvature curve (M_u , ϕ_u). A Matlab program was written to calculate the moment-curvature values for three states as per principles explained in above sections. Code is attached in the appendix.

3.4 Strain Compatibility Method

By strain compatibility method, Moment Curvature for the RC section with flexural and axial load can be derived on bases of the assumptions similar to those used for the determination of the flexural strength. Assumptions are as under :

- Plane section before bending remain plane after bending.
- The tensile strength of concrete is neglected.
- Stress- strain curves for steel and concrete are known.
- The steel is perfectly bonded.
- The variation of the strain across the section is taken as a linear up to failure.
- The stress-stain relation proposed in a model is taken as a stress block.

The curvature associated with the large range of bending moment can be find out by using above assumptions, from the equation of equilibrium, strain compatibility and stress-strain models for concrete and steel. f_y = yielding strength of steel f_c "=strength of concrete in a member . For a given concrete strain in the extreme compression fiber ε_{cm} and neutral axis depth kd , the steel strain (i.e ε_{s1} and ε_{s2}) can be determine by using similar triangular strain diagram.

$$\varepsilon_{si} = \varepsilon_{cm} \frac{kd - d_i}{kd} \quad (3.13)$$

The stress corresponding strain can be determine by using stress-strain curve for steel. Fig. 3.1 show typical stress-stain curves for steel. Then steel force can be found out by multiplying stress in to steel and area of the steel. Fig. 3.2 shows distribution of the forces. For given concrete strain ε_{cm} in the compressive fiber, the concrete compressive force is given by

$$C_c = \alpha f_c'' b k d \quad (3.14)$$

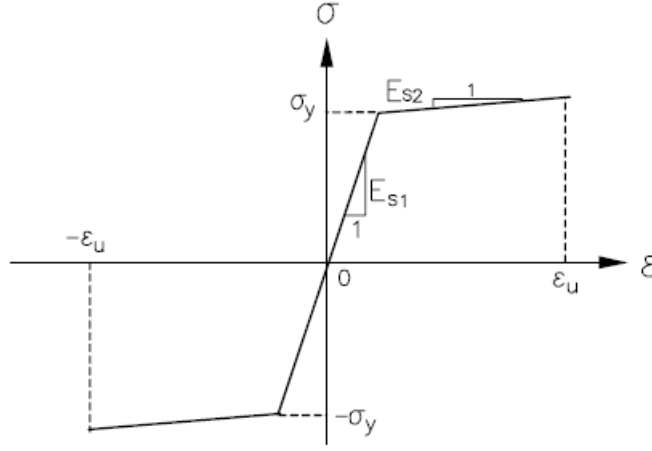


Figure 3.1: Stress-Strain Curve for Steel [3]

It is acting at γkd from the extreme compression fiber. α is the mean stress factor. γ is the centroid factor. α and γ is given by following eq.

$$\alpha = \frac{\int_0^{\varepsilon_{cm}} f_c d\varepsilon_c}{f_c'' \varepsilon_{cm}} \quad (3.15)$$

$$\gamma = 1 - \frac{\int_0^{\varepsilon_{cm}} \varepsilon_c f_c d\varepsilon_c}{\varepsilon_{cm} \int_0^{\varepsilon_{cm}} f_c d\varepsilon_c} \quad (3.16)$$

If the stress in the concrete f_c can be written in terms of the strain ε_c , the concrete force and its line of action may be determine from above equation. The force equilibrium equations can be written as follow;

$$P = \alpha f_c'' bkd + \sum_{i=1}^n f_{si} A_{st} \quad (3.17)$$

$$M = \alpha f_c'' bkd \left(\frac{h}{2} - \gamma kd \right) + \sum_{i=1}^n f_{si} A_{st} \left(\frac{h}{2} - d_i \right) \quad (3.18)$$

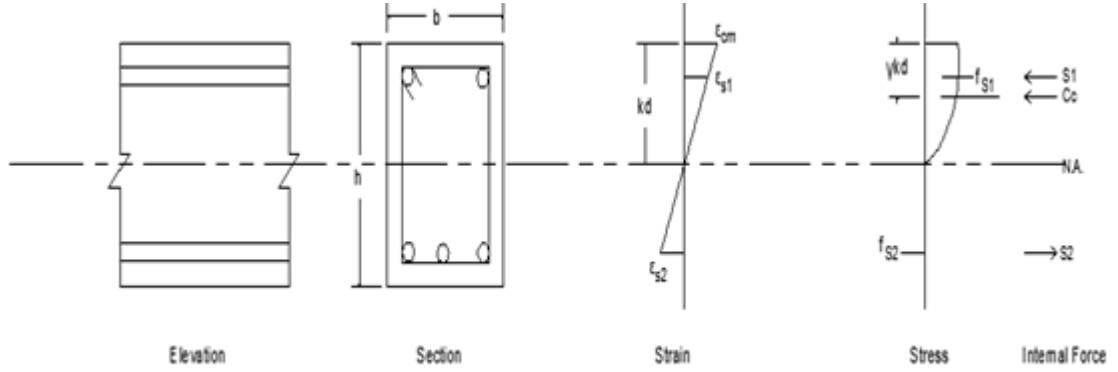


Figure 3.2: Section With Strain, Stress and Force Distribution [3]

Where, M is the Moment and P is the axial load. Here in this case it was taken as zero. Corresponding curvature is given by following equation;

$$\phi = \frac{\varepsilon_{cm}}{kd} \quad (3.19)$$

3.4.1 Procedure for Strain Compatibility Method

For deriving the complete moment-curvature relationship for RC rectangular beam element, discrete values of concrete strains (ε_c) were selected such that even distributions of points on the plot, both before and after the maximum were obtained. The procedure used in computation is given below:

- The extreme fiber concrete compressive strain was assumed (i.e. 1/10 of ultimate strain).
- For the value of assume strain N.A. depth, kd was assumed. Say 0.5d.
- For this value of N.A., compressive forces C_c in concrete was calculated by using stress-strain models for concrete.
- The strain in tension and compression steel was calculated base on the strain compatibility.

- Based on the strain in the tension steel, corresponding stresses were calculated from the stress-strain curve of steel.
- The total tensile force (T) in tensile steel was calculated.
- Same procedure was repeated for compressive steel to calculate compressive force in compression steel.
- The total compression force C ($C=C_c+C_t$) acting in the compression zone was calculated.
- If $C=T$ then assumed value of N.A. depth was corrected and M and ϕ calculated otherwise the N.A. depth was modified until the $C=T$ was achieved.
- Same procedure was repeated till the assumed strain is equal to the ultimate strain.

Now, the total moment about N.A. was given by:

$$M=M_c + M_{cs} + M_t$$

where,

M_c = Moment of compressive force in concrete about the N.A.

M_{cs} = Moment of force in compressive steel about the N.A.

M_t = Moment of force in tensile steel about the N.A.

Corresponding curvature is given by using Eqn. 3.19.

A Matlab code is developed for evaluation of Moment-Curvature relationship by using various stress-strain model for concrete as well as steel. Code is attached in appendix. Flow chart of the matlab program is shown in Fig 3.3.

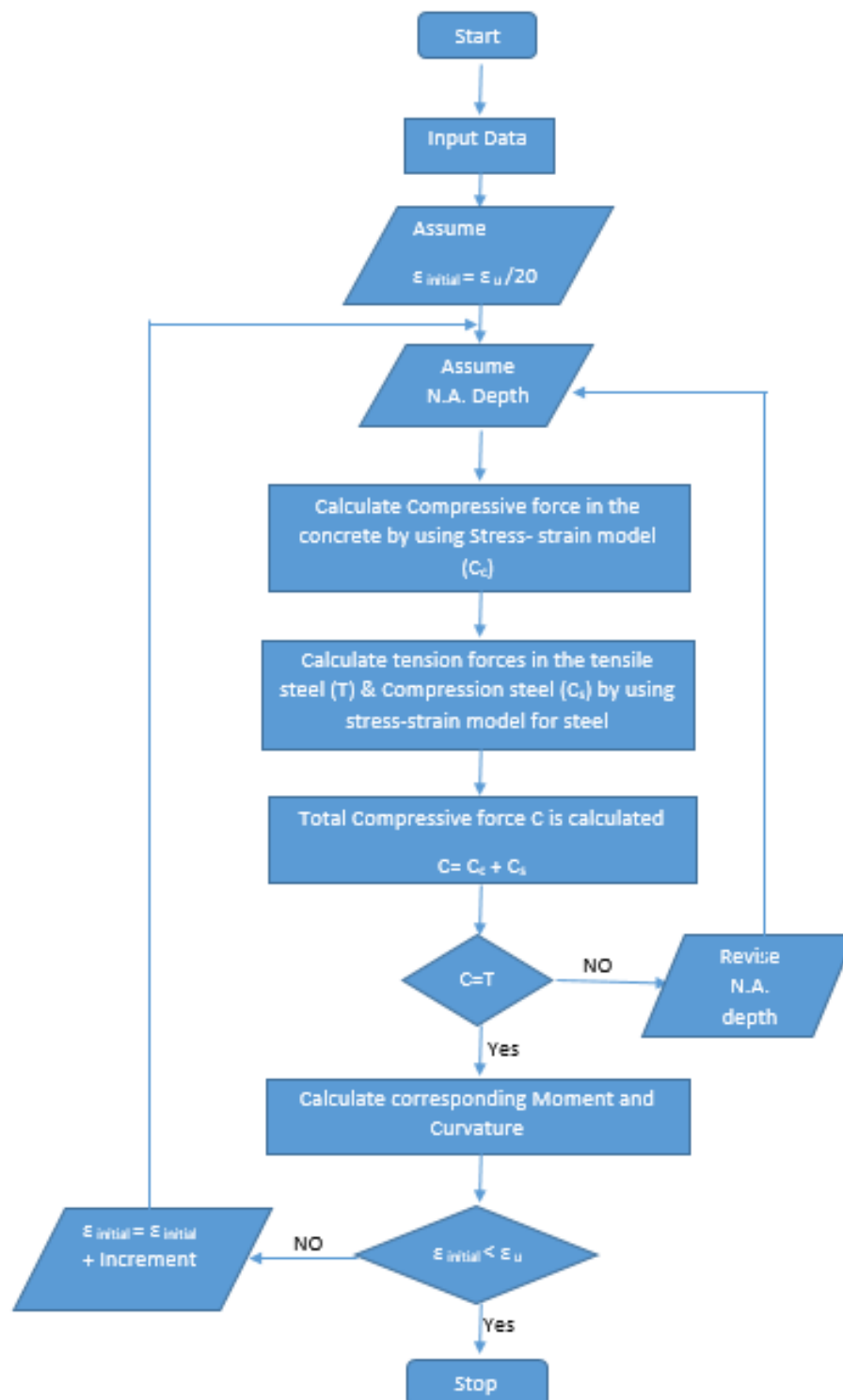


Figure 3.3: Flow Chart of Computer Program

3.5 Computational Tools for Moment Curvature

- **CUMBIA** is a software written in Matlab language by **Luis A. Montejo**, North Carolina State University. The software is able to perform monotonic moment-curvature analysis and force-displacement response of reinforced concrete column.
- **Response 2000** is a software developed by **Evan Bentz and Michael P. Collins**, University of Toronto. It is used for sectional analysis program that will calculate the strength and ductility of a reinforced concrete cross-section subjected to shear, moment, and axial load. All three loads are considered simultaneously to find the full load-deformation response using the modified compression field theory. He used popovics and thorenfeldt equation for basic stress-strain block.
- **RC-Analysis** is a software developed by **Suarez V. A. and Hurtado J. C.**. It is used for moment-curvature and shear strength analysis of reinforced concrete sections.
- **XSECTION, CONSEC, UCFyber** are also used to predict moment curvature relationship.

In the present study, RC-Analysis and Response 2000 are used in order to determine moment-curvature relationship for a beam section. Yield curvature and ultimate curvature are obtained using these tools.

Chapter 4

Analysis of Moment-Curvature for RC Beam Elements

4.1 General

Development of the software programs requires clear understanding of programming language and the domain knowledge. Matlab is used for the coding of the program. The entire program is based on the formal mathematical models which have been coded for stress-strain block. Results obtain by analytical method are compared to the experimental results. This chapter includes the problem statement. It also deals with the analytical evaluation of Moment-Curvature of designed RC rectangular beam element by using transform area method and strain compatibility method.

4.2 Problem Statement

In present study four different type of rectangular specimens (Singly Under Reinforced beam, Singly Over Reinforced, Doubly Under Reinforced and Doubly Over Reinforced) were designed to calculate Moment-Curvature. From the literature it is found that b/d and L/d ratio for the simply supported beam was taken between 0.5 to 0.9 and 10 respectively. Where, L is the span of the beam, d is the depth of the

Table 4.1: Geometric Specification for Beam

Description	SUR	SOR	DUR	DOR
b (mm)	120	120	120	120
D (mm)	150	150	150	150
d (mm)	135	135	135	135
f_{ck} (MPa)	20	20	20	20
f_y (MPa)	415	415	415	415
A_{sc} (mm^2)	2-6 ϕ	2-6 ϕ	2-8 ϕ	2-8 ϕ
A_{st} (mm^2)	3-8 ϕ	3-10 ϕ	2-10 ϕ +1-8 ϕ	3-10 ϕ
Xu (mm)	63.01	112.9	45.21	71.59
M (KNm)	5.9	10.51	6.64	10.9
P (KN)	23.6	42.04	35.32	43.6

beam and b is the width of the beam. So in present study, b/d ratio of the beam was taken as 0.8 and L/d ratio was taken as 10. Dimensions of the RC specimens were $120\text{ mm} \times 150\text{ mm} \times 1700\text{ mm}$, where span of the beam was taken as 1500 mm . General specifications of beams are shown in Table 4.1. Fig. 4.1 shows the cross section and reinforcement details for singly under as well as over reinforced beam. and Fig. 4.2 shows the cross section and reinforcement detail for Doubly under reinforced as well as Doubly over reinforced RC beam element.

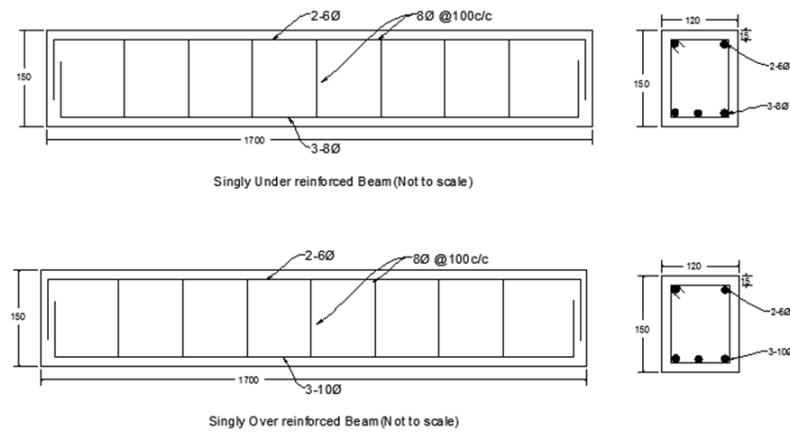


Figure 4.1: Cross Section of Beam (a) Singly Under Reinforced (b) Singly Over Reinforced

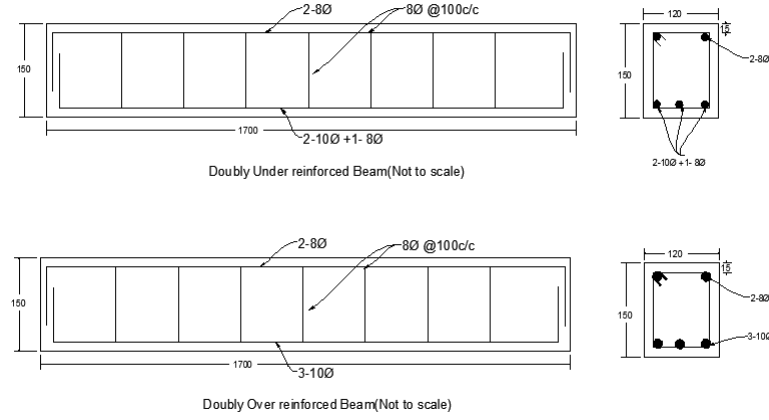


Figure 4.2: Cross Section of Beam (a) Doubly Under Reinforced (b) Doubly Over Reinforced

4.3 Analytical Moment-Curvature

In this section Moment-Curvature was evaluated for selected problem by using transform area method as well as strain compatibility method. Transform area method is the simple but approximate method where strain compatibility method is accurate method for beam under flexure and axial load. But this method is iterative method.

4.3.1 Transform Area Method

In present study, it is assumed that 100 mm spacing between ties is small for any confining effects so beam can be treated as an unconfined section for obtaining moment-curvature relationship[3]. Plots obtained from the matlab are as shown in Fig. 4.3 and Fig. 4.4. From Fig. 4.3, it is observed that in case of singly under reinforced RC beam there is a minor drop in moment carrying capacity after the yielding of the reinforcement. In this case ultimate moment carrying capacity is less compare to the singly over reinforced section but the ultimate curvature is more. In case of singly over reinforced section, degradation in strength after peak is comparatively more.

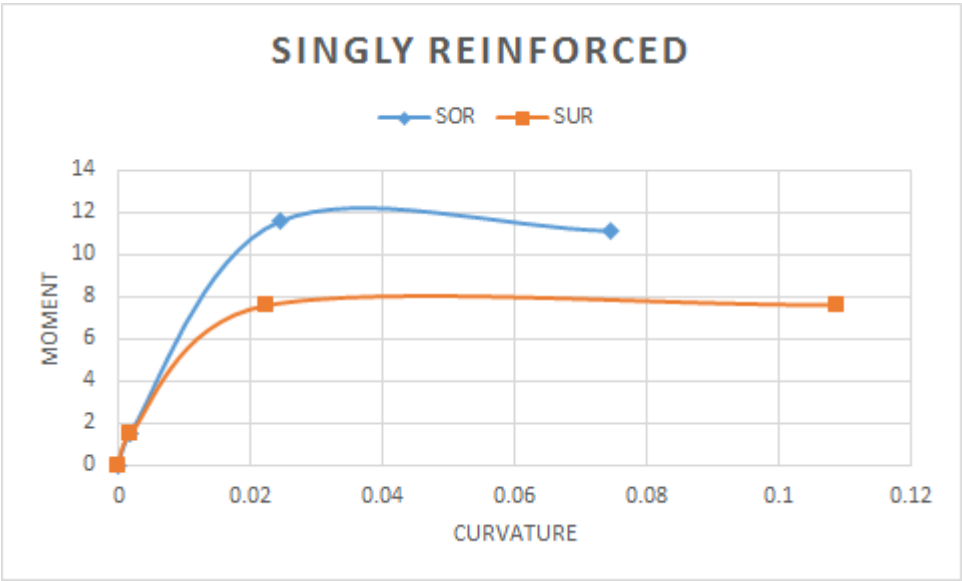


Figure 4.3: Moment-Curvature Relationship for Singly Reinforced Beam

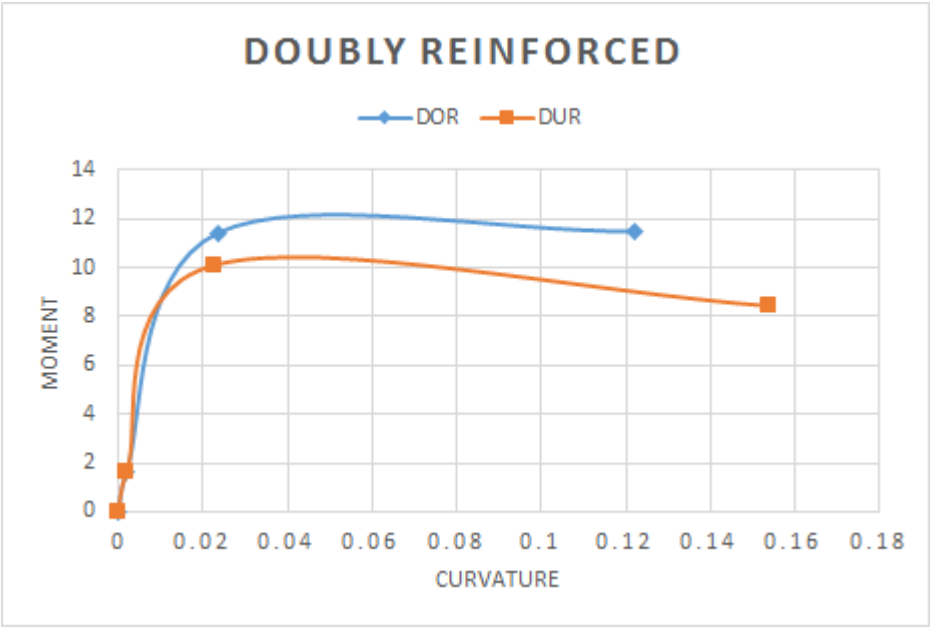


Figure 4.4: Moment-Curvature Relationship for Doubly Reinforced Beam

Curvature ductility, the ratio of ultimate curvature to the curvature at yielding of reinforcement, is 4.88 in case of singly under reinforced beam and 2.80 in case of singly over reinforced section. So even though singly over reinforced section has more moment carrying capacity ductility is less as compare to the Singly under reinforced section.

From Fig. 4.4, in both the case (Under reinforced and Over reinforced) of doubly reinforced beam, degradation in strength after peak is less compare to the singly over reinforced section. Curvature ductility for doubly under reinforced section is 6.72 and for doubly over reinforced section is 5.2.

4.3.2 Strain Compatibility Method

To evaluate Moment-Curvature relationship for RC rectangular beam elements by Strain Compatibility Method, six different existing confine as well as unconfine mathematical stress-strain models were used as stress block. Among these six models IS 456 Model, Hognestad Model, Kent and Park Model and IRC 112 Models were unconfined concrete models. Cusson Model and Mander Model were confined concrete model. One shortcoming of unconfined models are that it ignores the level of confinement provided by the lateral reinforcement. The useful strain in concrete depends on the confinement of concrete so to study the effect of the confinement on the Moment-Curvature confine stress-strain models were also used. Fig. 4.5 shows various stress-strain models which were used in present study.

Table 4.2 shows Moment-Curvature relationship at different strain level by using all six stress-strain models as a stress block for singly under reinforced beam. Cusson Model and Mander Model are for confined concrete as the effective strain in concrete depends on the confinement of concrete so they were used to study the effect of the confinement on the Moment-Curvature relationship. Fig. 4.6 shows Moment-Curvature for singly under reinforced beam. From Fig. 4.6, it is observed that Moment-Curvature plot for singly under reinforced (SUR) remain linear in elastic

Model	Ascending Branch	Decending Branch
IS 456 Model	$f_c = f'_c \left(\left(\frac{2\varepsilon_c}{\varepsilon_{c0}} \right) - \left(\frac{\varepsilon_c}{\varepsilon_{c0}} \right)^2 \right)$	$f_c = f'_c$
Hognestad Model	$f_c = f'_c \left(\left(\frac{2\varepsilon_c}{\varepsilon_{c0}} \right) - \left(\frac{\varepsilon_c}{\varepsilon_{c0}} \right)^2 \right)$	$f_c = f'_c [1 - 100(\varepsilon_c - \varepsilon_{c0})]$
Kent and Park Model	$f_c = f'_c \left(\left(\frac{2\varepsilon_c}{\varepsilon_{c0}} \right) - \left(\frac{\varepsilon_c}{\varepsilon_{c0}} \right)^2 \right)$	$f_c = f'_c [1 - Z(\varepsilon_c - \varepsilon_{c0})]$ $\varepsilon_{50u} = \frac{3 + 0.29f'_c}{145f'_c - 1000}$ $Z = \frac{0.5}{\varepsilon_{50u} - \varepsilon_{c0}}$
IRC 112 Model	$f_c = f_{cd} \left[1 - \left[1 - \frac{\varepsilon_c}{0.002} \right]^2 \right]$ $f_{cd} = \frac{0.67f_{ck}}{1.5}$	$f_c = f_{cd}$ $f_{cd} = \frac{0.67f_{ck}}{1.5}$
Cusson Model	$f_c = f_{cc} \left[\frac{K \left(\frac{\varepsilon_c}{\varepsilon_{c0}} \right)}{K - 1 + \left(\frac{\varepsilon_c}{\varepsilon_{c0}} \right)^K} \right]$ $K = \frac{E_c}{E_c - (f_{cc}/\varepsilon_{cc})}$	$f_c = f'_c \exp[k_1(\varepsilon_c - \varepsilon_{c0})^{1.5}]$ $k_1 = \frac{\ln 0.5}{(\varepsilon_{c50c} - \varepsilon_{c0})^{1.5}}$
Mander Model	$f_c = \frac{f'_{cc} X r}{r - 1 + X^r}$ $X = \left(\frac{\varepsilon_c}{\varepsilon_{cc}} \right)$ $\varepsilon_{cc} = \varepsilon_{c0} \left[1 + 5 \left(\frac{f'_{cc}}{f_{c0}} - 1 \right) \right]$ $r = \frac{E_c}{E_c - (f'_{cc}/\varepsilon_{cc})}$	

Figure 4.5: Various Stress-Strain Models

zone and remain horizontal in inelastic zone. This is due to the increase in lever-arm in to the RC beam after the yield. Here, 0.00105 was consider as a yielding strain for all models excluding IRC 112 Models. In IRC model 0.0014 was consider as a yielding strain. Curvature ductility, ratio of ultimate curvature to curvature at yield for SUR beam was observed 4.3, 3.66, 2.54, 2.72, 4.71, and 5.22 form IS Code Model, Hognestad Model, Kent and Park Model, IRC Model, Cusson Model and Mander Model respectively. Curvature ductility obtain for SUR from IS code Model and Mander Model are near to the Curvature ductility obtain from Transform area method.

Table 4.2: Moment-Curvature for Singly Under Reinforced RC Beam.

Strain	IS CODE MODEL		Hongnestad		Kent and Park Model		IRC 112		Cussion		Mander Model	
	M (kNm)	ϕ (rad/m)	M (kNm)	ϕ (rad/m)	M (kNm)	ϕ (rad/m)	M (kNm)	ϕ (rad/m)	M (kNm)	ϕ (rad/m)	M (kNm)	ϕ (rad/m)
0	0	0	0	0	0	0	0	0	0	0	0	0
0.00035	4.2851	0.0112	4.2851	0.0112	4.2311	0.0112	2.7829	0.008	4.378	0.0114	4.2502	0.0112
0.0007	8.1257	0.0214	8.1257	0.0214	8.0242	0.0215	5.2642	0.0154	8.3835	0.0219	8.0437	0.0215
0.00105	8.5359	0.04	8.5359	0.04	8.4732	0.04	7.4191	0.0221	8.4854	0.0426	8.4702	0.04
0.0014	8.4112	0.0627	8.4112	0.0627	8.3485	0.0627	9.2155	0.0282	8.3664	0.067	8.3442	0.0632
0.00175	8.3576	0.0847	8.3576	0.0847	8.2912	0.0848	9.1619	0.0378	8.3066	0.0921	8.2731	0.088
0.0021	8.3485	0.1033	8.3567	0.1022	8.3037	0.1005	9.138	0.0461	8.2758	0.1163	8.2291	0.1133
0.00245	8.3485	0.1205	8.3792	0.1151	8.3705	0.1058	9.138	0.0538	8.2645	0.1391	8.2041	0.1384
0.0028	8.3485	0.1377	8.4046	0.1267	8.463	0.1077	9.138	0.0615	8.2582	0.1603	8.1866	0.1632
0.00315	8.3485	0.1549	8.4306	0.1371	8.5776	0.1063	9.138	0.0692	8.2576	0.1804	8.1768	0.1873
0.0035	8.3485	0.1722	8.4616	0.1463	8.7268	0.1017	9.138	0.0769	8.2569	0.2006	8.1698	0.2107

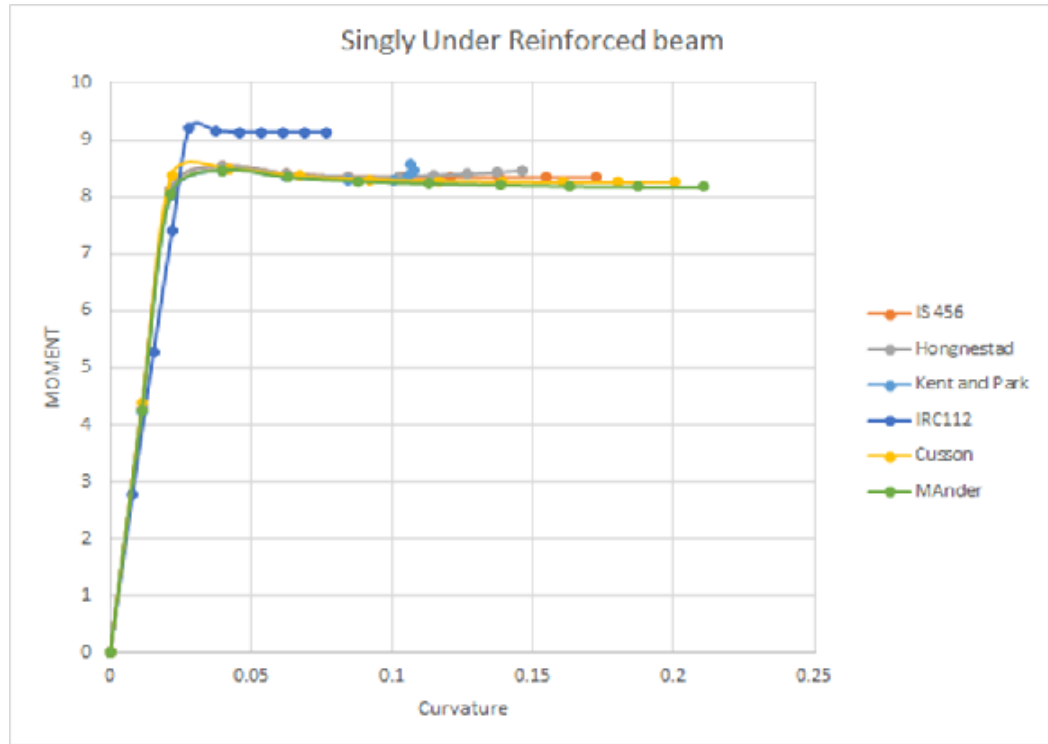


Figure 4.6: Moment-Curvature for Singly Under Reinforced Beam

From Fig. 4.6, it is observed IRC 112 model shows more ultimate moment but less curvature than other models. Neutral axis depth is inversely proposed to the curvature. Here neutral axis depth was observed more than other models because of this curvature is less compared to the other models. After the yielding of reinforcement slight increased in moment than drop in moment carrying capacity was observed.

Table 4.3 shows the Moment and corresponding curvature at different strain level for singly over reinforced beam (SOR) for all six concrete models. Fig. 4.7 shows Moment-Curvature plot for SOR. Here Moment-curvature is linear in elastic zone but minor drop was observed in strength after the peak. Curvature ductility calculated for SOR was 4.3, 3.66, 2.63, 1.72, 4.7 and 5.25 from IS Code Model, Hognestad Model, Kent and Park Model, IRC Model, Cusson Model and Mander Model respectively. Curvature ductility obtain for SUR from Hognestad Model are near to the Curvature ductility obtain from Transform area method.

Table 4.3: Moment-Curvature for Singly Over Reinforced RC Beam.

Strain	IS CODE		Hongnestad		Kent and		IRC 112		Cussion Model		Mander Model	
	M (kNm)	ϕ (rad/m)	M (kNm)	ϕ (rad/m)	M (kNm)	ϕ (rad/m)	M (kNm)	ϕ (rad/m)	M (kNm)	ϕ (rad/m)	M (kNm)	ϕ (rad/m)
0	0	0	0	0	0	0	0	0	0	0	0	0
0.00035	5.2846	0.0093	5.2846	0.00925	4.7809	0.0087	3.3886	0.0068	5.4021	0.0094	5.2375	0.0093
0.0007	10.0097	0.0178	10.0097	0.01777	9.0509	0.0167	6.3967	0.013	10.3337	0.0182	9.9009	0.0179
0.00105	14.0606	0.0256	14.0606	0.02559	12.7669	0.024	8.9926	0.0188	13.9359	0.0273	13.9354	0.0257
0.0014	13.7596	0.0401	13.7596	0.0401	13.9602	0.0341	11.1353	0.024	13.6481	0.0429	13.6204	0.0405
0.00175	13.6296	0.0542	13.6296	0.05423	13.809	0.0461	12.7728	0.0285	13.5059	0.0589	13.4515	0.0564
0.0021	13.6065	0.0661	13.6219	0.06544	13.8221	0.055	13.857	0.0324	13.4316	0.0744	13.3485	0.0726
0.00245	13.6065	0.0771	13.6809	0.07364	13.9819	0.0592	14.6977	0.036	13.3962	0.0891	13.2824	0.0887
0.0028	13.6065	0.0881	13.7409	0.08109	14.1675	0.0619	15.4428	0.0396	13.3864	0.1026	13.2414	0.1046
0.00315	13.6065	0.0992	13.8092	0.08774	14.3889	0.0633	15.5336	0.0443	13.3877	0.1154	13.2169	0.12
0.0035	13.6065	0.1102	13.8821	0.09363	14.6638	0.0632	15.5336	0.0492	13.3845	0.1283	13.1991	0.1351



Figure 4.7: Moment-Curvature for Singly Over Reinforced Beam

From Fig. 4.7, it is observed that the slope of the Moment-Curvature plot in elastic zone is more compare to the case of singly under reinforced beam. Here also IRC 112 shows more ultimate moment and less curvature. Mander and Cusson models shows more degradation in strength compare to other models.

Table 4.4 shows the Moment-Curvature at different strain level for Doubly Under Reinforced beam(DUR) for all six concrete models. Fig. 4.8 shows Moment-Curvature plot for DUR. Here Moment-curvature is liner up to the yielding of reinforcement but after this sudden drop was observed in strength. In case of Moment-Curvature obtain by using Cusson Model and Mander Model drop in strength was not drastically as it was in other models. Curvature ductility calculated for DUR was 4.9, 4.4, 3.644, 3.72, 5.105 and 5.525 form IS Code Model, Hognestad Model, Kent and Park Model, IRC Model, Cusson Model and Mander Model respectively.

Table 4.4: Moment-Curvature for Doubly Under Reinforced RC Beam.

Strain	IS CODE MODEL		Hongnestad		Kent and Park Model		IRC 112		Cussion		Mander Model	
	M (kNm)	ϕ (rad/m)	M (kNm)	ϕ (rad/m)	M (kNm)	ϕ (rad/m)	M (kNm)	ϕ (dar/m)	M (kNm)	ϕ (rad/m)	M (kNm)	ϕ (rad/m)
0	0	0	0	0	0	0	0	0	0	0	0	0
0.00035	4.8385	0.0103	4.9306	0.0102	4.8729	0.0103	3.276	0.0077	4.9711	0.0104	4.8905	0.0103
0.0007	9.1793	0.0198	9.3597	0.0197	9.2525	0.0198	6.233	0.0149	9.5218	0.0202	9.2642	0.0198
0.00105	10.7518	0.0335	10.9149	0.0335	10.8605	0.0334	8.8506	0.0216	10.8172	0.0352	10.8403	0.0335
0.0014	10.337	0.0532	10.5077	0.0532	10.4489	0.0532	11.1035	0.0277	10.4564	0.056	10.4335	0.0536
0.00175	10.0775	0.073	10.2556	0.073	10.1985	0.0729	10.9308	0.038	10.2522	0.0775	10.2076	0.0751
0.0021	9.8422	0.091	10.0228	0.0904	9.9488	0.0891	10.3956	0.0493	10.1065	0.0988	10.0627	0.0972
0.00245	9.6218	0.1087	9.764	0.1054	9.6332	0.0993	9.9136	0.0611	9.9769	0.1195	9.9587	0.1194
0.0028	9.4195	0.127	9.5091	0.1204	9.2904	0.1082	9.4548	0.074	9.8476	0.1396	9.8714	0.1415
0.00315	9.2319	0.1459	9.2502	0.1355	8.9357	0.1157	9.0263	0.088	9.7129	0.1595	9.7925	0.1634
0.0035	9.0634	0.1652	8.9913	0.1505	8.5797	0.1217	8.6294	0.103	9.5948	0.1797	9.7153	0.1851

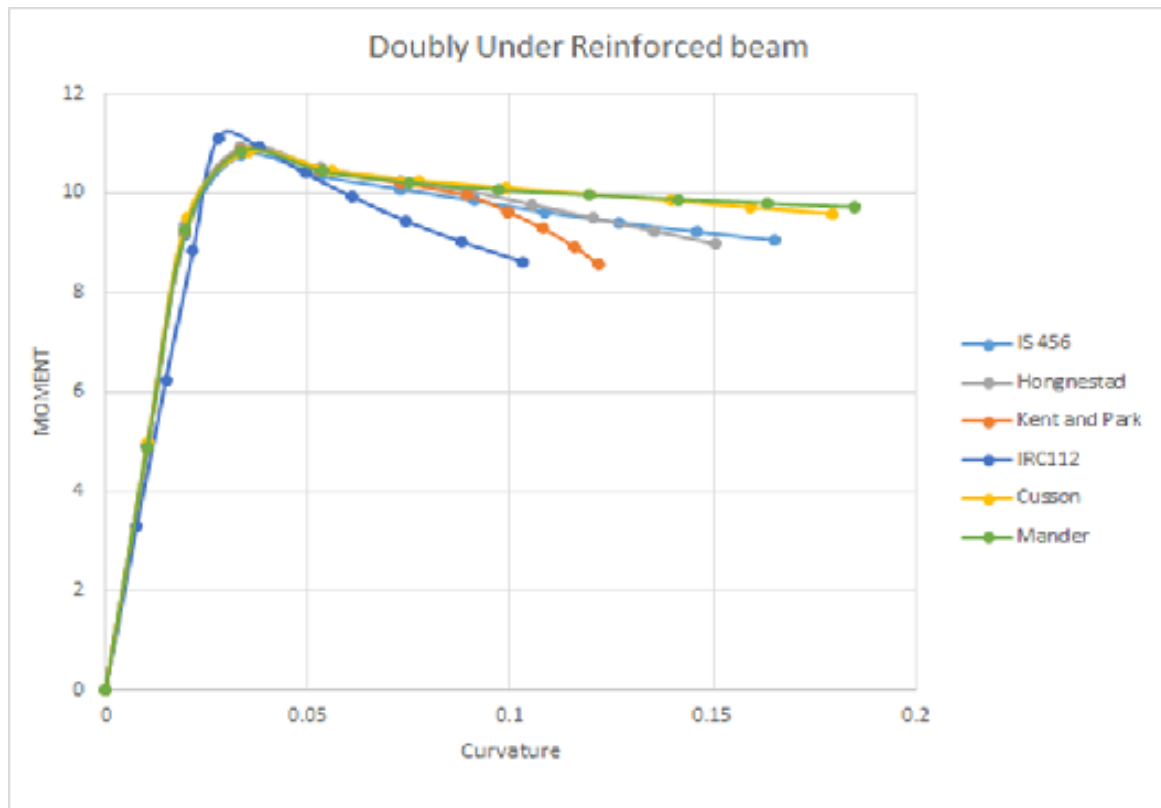


Figure 4.8: Moment-Curvature for Doubly Under Reinforced Beam

From Fig. 4.8, In case of doubly under reinforced section IRC 112 shows maximum degradation in strength after the peak. Here also IRC shows more ultimate moment and less curvature.

Table 4.5 shows the Moment-Curvature for Doubly Over Reinforced beam (DOR) for confine as well as unconfine concrete models. Fig. 4.9 shows Moment-Curvature for DUR. Here also Moment-curvature is linear up to the yielding of reinforcement but after this sudden drop was observed in strength. Curvature ductility calculated for DOR was 5.05, 4.6, 3.64, 2.62, 5.3 and 5.8 from IS Code Model, Hongnestad Model, Kent and Park Model, IRC Model, Cusson Model and Mander Model respectively.

Table 4.5: Moment-Curvature for Doubly Over Reinforced RC Beam.

Strain	IS CODE		Hognestad		Kent and		IRC 112		Cussion		Mander Model	
	M (kNm)	ϕ (rad/m)	M (kNm)	ϕ (rad/m)	M (kNm)	ϕ (rad/m)	M (kNm)	ϕ (rad/m)	M (kNm)	ϕ (rad/m)	M (kNm)	ϕ (rad/m)
0	0	0	0	0	0	0	0	0	0	0	0	0
0.00035	5.1603	0.0097	5.2578	0.0097	5.1931	0.0097	3.4877	0.0073	5.2964	0.0099	5.2154	0.0098
0.0007	9.7897	0.0187	9.9815	0.0187	9.857	0.0187	6.6342	0.0142	10.1448	0.0191	9.8788	0.0188
0.00105	12.589	0.0293	12.773	0.0293	12.6873	0.0293	9.4183	0.0205	12.6042	0.0309	12.6851	0.0293
0.0014	12.0118	0.0468	12.208	0.0468	12.1202	0.0468	11.8114	0.0263	12.0891	0.0494	12.1165	0.0472
0.00175	11.6408	0.0646	11.8488	0.0646	11.7665	0.0646	13.2151	0.0327	11.77	0.0688	11.7637	0.0666
0.0021	11.3318	0.0808	11.551	0.0802	11.468	0.0791	12.6149	0.0422	11.5379	0.0883	11.5202	0.0867
0.00245	11.0435	0.097	11.2573	0.0937	11.1517	0.0881	12.0739	0.0523	11.3344	0.1074	11.3311	0.1071
0.0028	10.7797	0.1137	10.96	0.1073	10.8252	0.0958	11.5456	0.0634	11.1436	0.126	11.1729	0.1276
0.00315	10.5331	0.131	10.6673	0.1209	10.5078	0.102	11.0319	0.0756	10.9596	0.1444	11.031	0.1481
0.0035	10.3089	0.1489	10.3751	0.1346	10.2055	0.1067	10.8489	0.0857	10.7863	0.1634	10.8983	0.1685

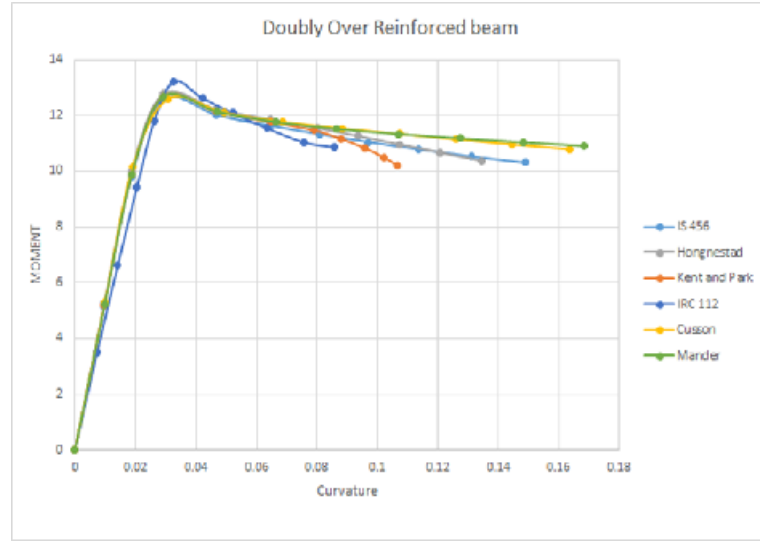


Figure 4.9: Moment-Curvature for Doubly Over Reinforced Beam

From Fig. 4.9, In case of doubly over reinforced section IRC 112 shows maximum degradation in strength after the peak. Here also IRC shows more ultimate moment and less curvature. As Mander and Cusson models includes the effect of the confinement it shows less degradation in strength after the peak.

4.4 Moment-Curvature by Computational Tools

In present study, among various available computational tools RESPONSE 2000 and RC-analysis were used to evaluate Moment-Curvature for design problem.

4.4.1 Moment-Curvature Relationship by RC-Analysis

Table 4.6 shows the Moment and corresponding Curvature for different strain level. These values were obtained by using RC-ANALYSIS which used Mander model for concrete and king model for steel. The curvature ductility obtained by this tools were 5.73, 4.17, 5.72 and 5.62 for SUR, SOR, DUR and DOR. Fig 4.10 shows moment-curvature relationship for beam elements. This tool considers the effect of the shear

also so it under estimate the moment carrying capacity of the section.

Table 4.6: Moment-Curvature Relationship by Using RC-ANALYSIS.

Strain	SUR		SOR		DUR		DOR	
	M (kNm)	ϕ (rad/m)	M (kNm)	ϕ (rad/m)	M (kNm)	ϕ (rad/m)	M (kNm)	ϕ (rad/m)
0	0	0	0	0	0	0	0	0
0.00112	6.73885	0.02808	8.02358	0.02257	7.96076	0.02427	8.29511	0.02304
0.00223	6.9637	0.08239	10.33318	0.05464	9.20419	0.06543	10.34796	0.05811
0.00335	7.4642	0.12518	10.33489	0.09218	9.42523	0.10619	10.4271	0.0974
0.00446	7.71671	0.16127	10.57575	0.12142	9.70586	0.14023	10.7437	0.12946

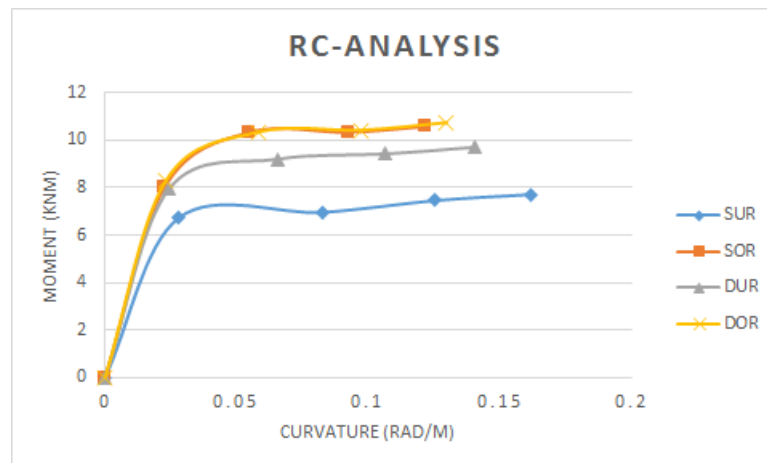


Figure 4.10: Moment-Curvature Relationship from RC-ANALYSIS

4.4.2 Moment-Curvature Relationship by RESPONSE 2000

Fig. 4.11 shows moment-curvature relationship for all four type of RC beam elements which were derived by using **RESPONSE 2000**. Table 4.7 shows Moment and corresponding curvature obtain from **RESPONSE 2000** tool. **RESPONSE 2000** was used Popovics model for the concrete. Compression field theorem was used to derive Moment-Curvature relationship.

Table 4.7: Moment-Curvature Relationship by Using RESPONSE 2000

SUR		SOR		DUR		DOR	
M (kNm)	ϕ (rad/m)	M (kNm)	ϕ (rad/m)	M (kNm)	ϕ (rad/m)	M (kNm)	ϕ (rad/m)
0	0	0	0.00000	0	0.00000	0	0.00000
0.76	0.00088	0.787	0.00088	0.796	0.00088	0.805	0.00088
1.396	0.00221	1.529	0.00221	1.511	0.00221	1.554	0.00221
1.782	0.00354	2.046	0.00354	1.992	0.00354	2.078	0.00354
2.131	0.00488	2.532	0.00488	2.44	0.00488	2.57	0.00488
2.472	0.00621	3.009	0.00621	2.88	0.00621	3.053	0.00621
2.81	0.00754	3.484	0.00754	3.317	0.00754	3.534	0.00754
3.147	0.00888	3.956	0.00888	3.752	0.00888	4.012	0.00888
3.484	0.01021	4.426	0.01021	4.186	0.01021	4.489	0.01021
3.819	0.01154	4.894	0.01154	4.618	0.01154	4.962	0.01154
4.154	0.01288	5.357	0.01288	5.048	0.01288	5.433	0.01288
4.488	0.01421	5.817	0.01421	5.476	0.01421	5.901	0.01421
4.843	0.01563	6.302	0.01563	5.928	0.01563	6.394	0.01563
5.23	0.01720	6.829	0.01720	6.421	0.01720	6.931	0.01720
5.654	0.01891	7.4	0.01891	6.957	0.01891	7.514	0.01891
6.114	0.02081	8.015	0.02081	7.538	0.02081	8.144	0.02081
6.449	0.02289	8.674	0.02289	8.165	0.02289	8.821	0.02289
6.794	0.02518	9.377	0.02518	8.74	0.02518	9.547	0.02518
6.751	0.02769	9.972	0.02769	9.032	0.02769	10.13	0.02769
6.78	0.03046	10.156	0.03046	9.071	0.03046	10.181	0.03046
6.807	0.03351	10.199	0.03351	9.106	0.03351	10.222	0.03351
6.833	0.03686	10.236	0.03686	9.14	0.03686	10.259	0.03686
6.865	0.04055	10.269	0.04055	9.168	0.04055	10.29	0.04055
6.95	0.04460	10.295	0.04460	9.236	0.04460	10.332	0.04460
7.035	0.04906	10.402	0.04906	9.342	0.04906	10.446	0.04906
7.124	0.05397	10.505	0.05397	9.448	0.05397	10.558	0.05397
7.214	0.05936	10.604	0.05936	9.554	0.05936	10.667	0.05936
7.297	0.06530	10.667	0.06530	9.629	0.06530	10.737	0.06530
7.341	0.07183	10.686	0.07183	9.662	0.07183	10.765	0.07183
7.378	0.07901	10.681	0.07901	9.675	0.07901	10.771	0.07901
7.43	0.08691	10.667	0.08691	9.715	0.08691	10.788	0.08691
7.477	0.09560	10.685	0.09560	9.758	0.09560	10.828	0.09560
7.519	0.10516	10.697	0.10516	9.798	0.10516	10.866	0.10516
7.556	0.11568	-	-	9.835	0.11568	10.904	0.11568
7.587	0.12725	-	-	9.871	0.12725	-	-

5.7, 3.8, 5.03 and 4.59 were evaluated curvature ductility by RESPONSE 2000 for SUR, SOR, DUR and DOR RC elements respectively. These values are much closer to the values obtain by Cusson and Hongnstand model.

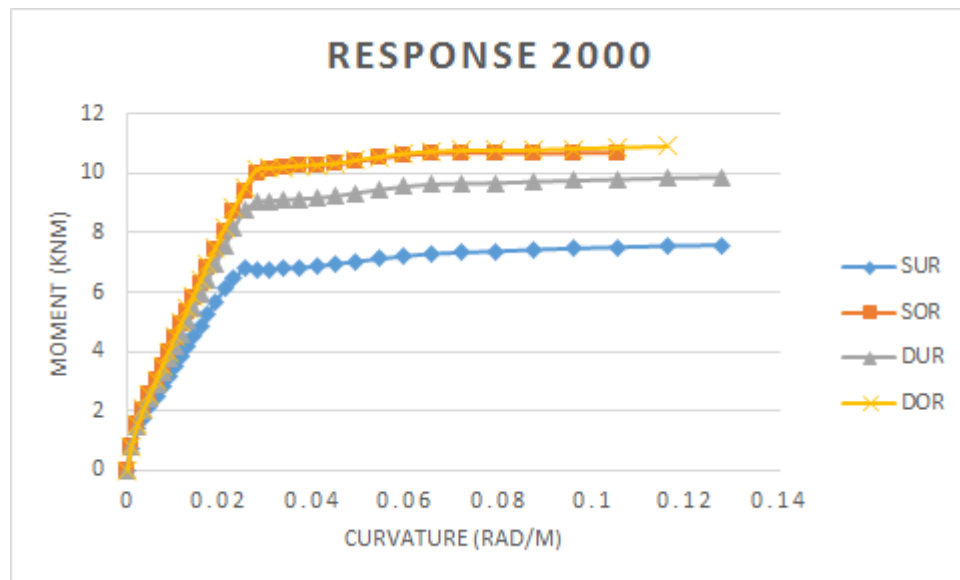


Figure 4.11: Moment-Curvature Relationship from RESPONSE 2000

4.5 Summery

This chapter discussed the various methods for analytically evaluation of Moment-Curvature relationship. The transform area method is the approximate method while the strain compatibility method is accurate but iterative method. Response 2000, which is based on the Popovics model is gives the Moment-curvature near to the Kent and park model. and RC-Analysis is also include the shear effect on the RC beam so it under estimate the moment carrying capacity of the beam. By calculating moment curvature for any beam one can estimate the curvature ductility also estimate the degradation in strength after the peak.

Chapter 5

Experimental Program

5.1 General

This chapter deals with the experimental evaluation of Moment-Curvature. The experimental program was design to compare the experimental values to the values obtain by analytical Methods. The experimental program consist of casting and testing of twelve RC beams of M20 grade concrete and Fe 415 grade steel. Two point loading was applied in middle one third portion. The beams were testes as a simply supported beams.

5.2 Concepts for Evaluation of Moment-Curvature

By using Moment-Curvature relationship we can estimate stiffness, ductility, energy dissipation and strength beyond the post peak of the stress-stain curve for any RC elements. Here Fig 5.1 shows an initially straight element of RC member having equal end moments and axial force. Let R is the radius of the curvature. It is measured from the neutral axis of the section. Neutral axis is located at depth kd from the top fiber of RC element. ε_c and ε_s is the concrete strain in the extreme compression fiber and strain in the steel respectively. Then considering only small length dx of the member, the rotation between two ends is given by following equation;

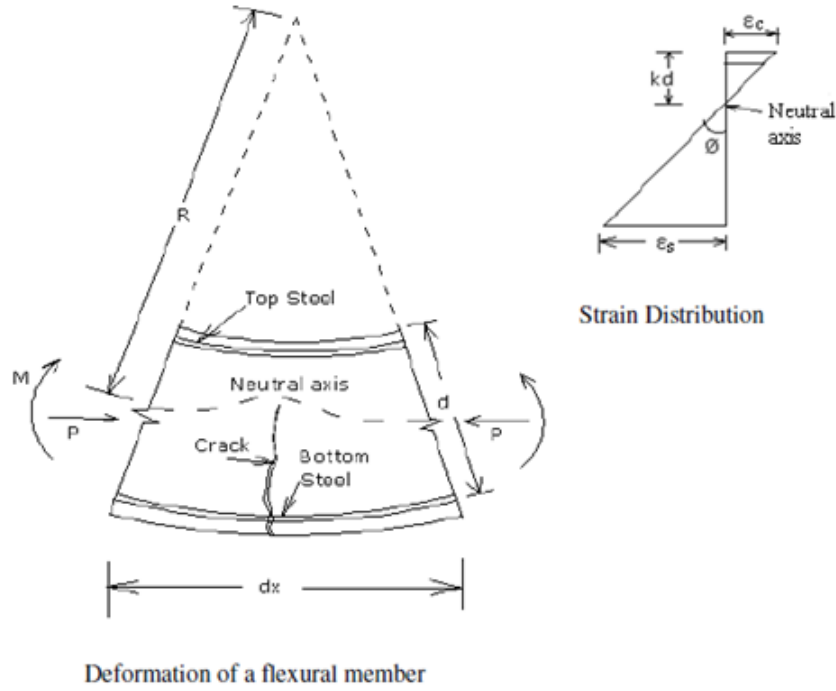


Figure 5.1: Curvature of Member [3]

$$\frac{dx}{R} = \frac{\varepsilon_c dx}{kd} = \frac{\varepsilon_s dx}{d(1-k)} \quad (5.1)$$

$$\frac{1}{R} = \frac{\varepsilon_c}{kd} = \frac{\varepsilon_s}{d(1-k)} \quad (5.2)$$

$$\phi = \frac{1}{R} = \frac{\varepsilon_c}{kd} = \frac{\varepsilon_s}{d(1-k)} = \frac{\varepsilon_c + \varepsilon_s}{d} \quad (5.3)$$

Here, $\frac{1}{R}$ is the curvature of the elements and is denoted by ϕ . It is also called as rotation per unit length of member.

Curvature is also called as a gradient of the stain profile. It can be vary along the length of the member because of the fluctuation of the neutral axis depth and strains between the cracks. If the strain at the critical section of RC beam are measured as the bending moment is increased to failure, the curvature can be calculated by equation 5.3. Fig 5.2 shows Moment Curvature for RC beam failing in tension and

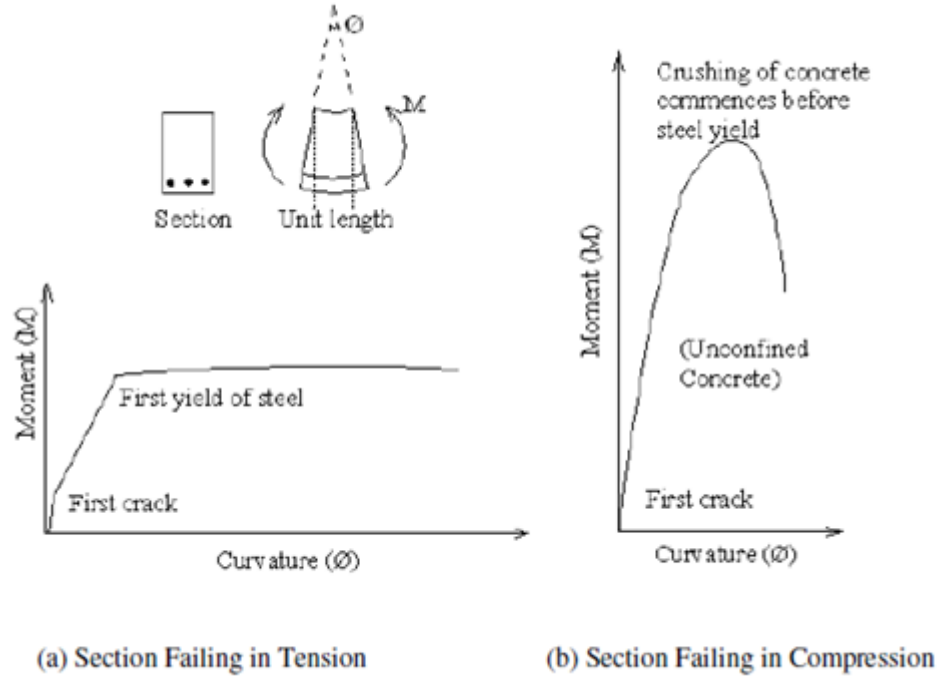


Figure 5.2: Moment-Curvature Relationship for Singly Reinforced Section

compression. Both the curves are linear in the initial stage. Relation between moment and curvature is given by classical elastic equation.

$$EI = MR = \frac{M}{\phi} \quad (5.4)$$

Where, EI is the flexural rigidity of the section. With increase in moment, cracking of the concrete reduces the flexural rigidity of the sections, the reduction in rigidity being greater for the lightly reinforced section than for the more heavily reinforced section. The behavior of section after cracking is dependent mainly on the steel content. Lightly reinforced sections shows Fig. 5.2 (a) results in practically linear $M-\phi$ curve up to point of steel yielding. When steel yields, a large increase in curvature occurs at nearly constant bending moment, the moment rising slowly to a maximum due to an increase in the internal lever arm, then decreasing. In heavily reinforced

sections shows in Fig. 5.2 (b), on the other hand, the $M-\phi$ becomes nonlinear when the concrete enters in inelastic part of stress-strain relationship, and failure can be quite brittle unless the concrete is confined by closed stirrups at close centers. If the concrete is not confined, the concrete crushes at a relatively small curvature before the steel yields, causing an immediate decrease in the moment-carrying capacity. To ensure ductile behavior in practice, steel contents less than the balanced design value are always used for beams [3].

5.3 Experimental Problem

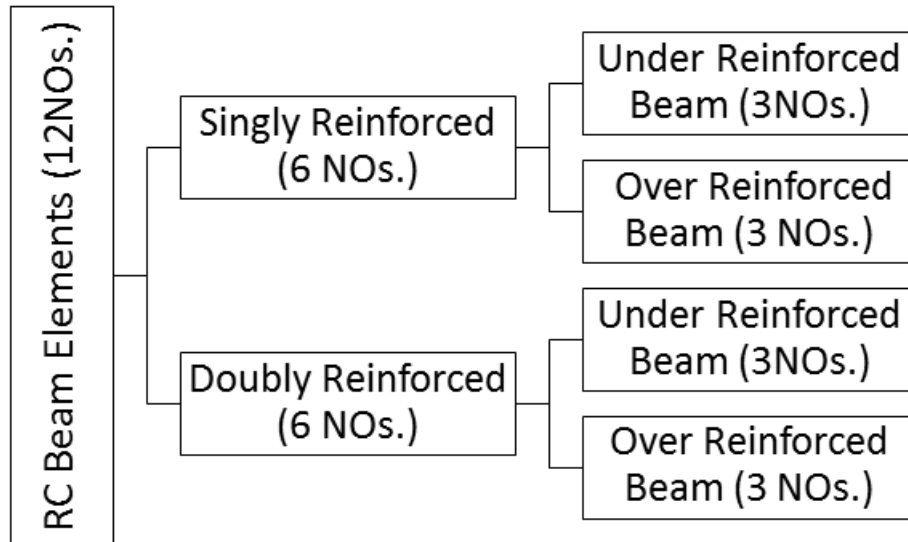


Figure 5.3: Experimental Program

The experimental program includes the casting of twelve RC rectangular beam of M20 grade concrete and Fe 415 grade steel. Dimensions of the sections were decided on the base of available literatures. In the literature, it was found that the L/d ratio of the simply supported beams was taken around 10 and b/d ratio was taken around 0.5 to 0.8. Where, L is the span of beam, d is the depth of the section and b is the width of the section. So in present study first of all L/d ratio was assumed. it was taken as

10 and b/d ratio was taken as 0.8. Hence overall dimensions of the beams 120mm X 150mm X 1700mm were selected. Here clear span of the beam was taken as a 1500mm.

In present study, all the beams were designed by using limit state method. Here, four different types of beams were design like Singly Under Reinforced, Singly Over Reinforced, Doubly Under Reinforced and Doubly Over Reinforced. Fig 5.3 shows the layout of experimental program.

Clear cover of the beams were taken as 15mm. In present study in the case of singly reinforced beams 2-6mm dia bar used as a hanger bar at the top. Two legged 8mm dia stirrups were used at 100mm c/c in all twelve beams. The details of the beams are as shown in Table 4.1. The cross sectional and reinforcement details of the beams are as in Fig. 5.4) and Fig. 5.5.

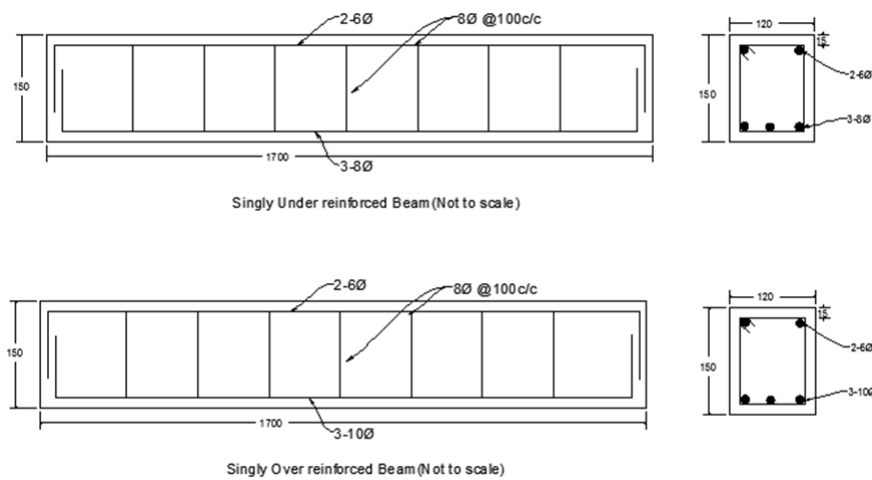


Figure 5.4: Cross Section of Beam (a) Singly Under Reinforced (b) Singly Over Reinforced

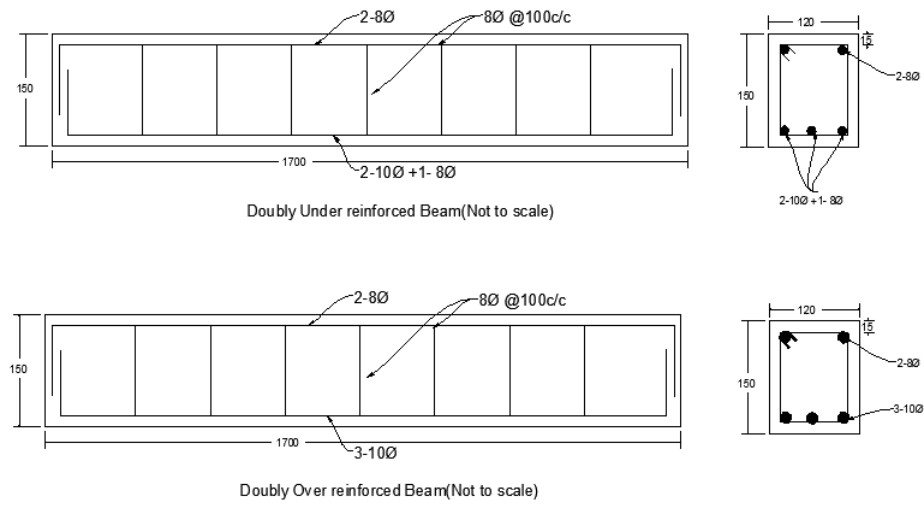


Figure 5.5: Cross Section of Beam (a) Doubly Under Reinforced (b) Doubly Over Reinforced

Table 5.1: Mix Design for M20 Grade Concrete

SR. No.	Descri.	Wt (kg/m ³)	Wt (kg/beam)
1	Cement	371	12
2	Water	214.14	7
3	20 mm	710.16	22
4	10 mm	473.44	15
5	F.A.	725.43	22.2

5.4 Casting of RC Beam

Fig. 5.6 shows 3D view and cross section of the formwork. Formwork was prepared from the wooden sheet. Wooden clamps were also prepared for the ensuring the dimensional stability during the casting of the specimens. Two sets of the formwork was prepared so that two specimens could be casted at a time.

Mix design for M20 grade concrete was prepared. Mix design are shown in Table 5.1. During the casting of the specimens for measuring the cube strength at 7 days and 28 days, six cubes (150mm × 150 mm × 150 mm) were casted. Three cylinder (150

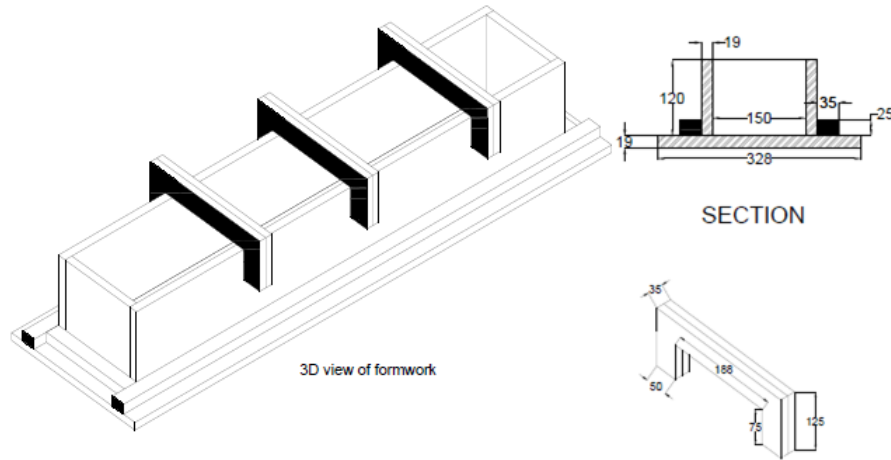


Figure 5.6: 3D View of Formwork for Beam

mm \times 300 mm) and three beams(100 mm \times 100 mm \times 500 mm) were also casted for measuring the modulus of elasticity of concrete and flexure strength of concrete. Cube strength, Modulus of elasticity of concrete and flexure strength of concrete will be used in the analytical solution for the moment curvature of the RC beam. Fig. 5.7(a) shows drum mixer. And Fig. 5.7(b) shows casted specimens for measuring concrete properties.



(a)



(b)

Figure 5.7: Casting of Specimens for Deriving Concrete Properties



Figure 5.8: Formwork and Reinforcement Cage of RC Specimens.

Fig. 5.8(a) shows reinforcement cage and Fig. 5.8(b) shows casted reinforced concrete beam specimens.

5.5 Instrumentation and Test Setup for RC Beam

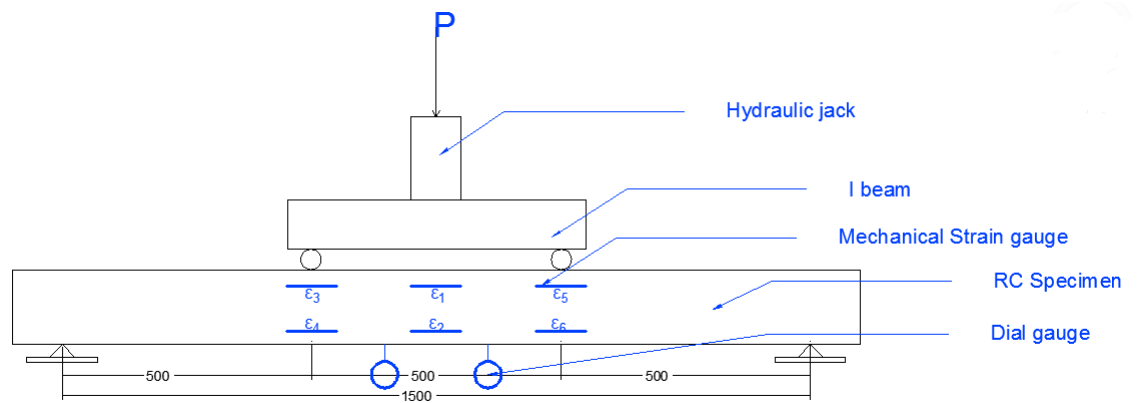


Figure 5.9: Instrumentation and Test Setup.

Fig. 5.9 shows the test set up and instrumentation diagram for all four type of RC beams. Test setup was design in such way so that in middle one third of the

beam was in pure bending zone and flexure failure was occurred in this portion. Two point load applied in the middle one third portion. As the curvature is the strain gradient, in present experiment the main focus was kept on measuring the strain in the RC rectangular beam elements. For measuring strain at the level of core, strain was measure at the top and bottom reinforcement level. Total six mechanical strain gauges were used. Among these three were fixed at top and remining were fixed at bottom.



Figure 5.10: Test Setup and Instrumentation Used for Experiments

Strain was measured by using mechanical strain gauge having 10 cm gauge length. Fig. 5.10(a) shows test setup of the experiments and also shows position of strain points at where strain was going to measure. Fig. 5.10(b) shows mechanical strain gauge. d is the distance between top and bottom strain gauge. In present experiment it was kept as 90mm.

Experimental curvature is measure by using equation 5.3. Where, ε_c is the concrete strain which was taken as a average concrete strain from the top three strain gauge and ε_s is the bottom strain or tension steel strain and was taken as a average strain from the bottom three strain gauge.



Figure 5.11: Testing of Specimens

5.6 Testing of RC Specimens



Figure 5.12: Failure of RCC Beams

Fig. 5.11 shows the testing of RC beam elements. Readings were taken at each 4 kN increment of load till the beam was failed. Corresponding Curvature were calculated from the top and bottom average strain. Corresponding moment was calculated from the load value. Then experimental Moment-Curvature relationship

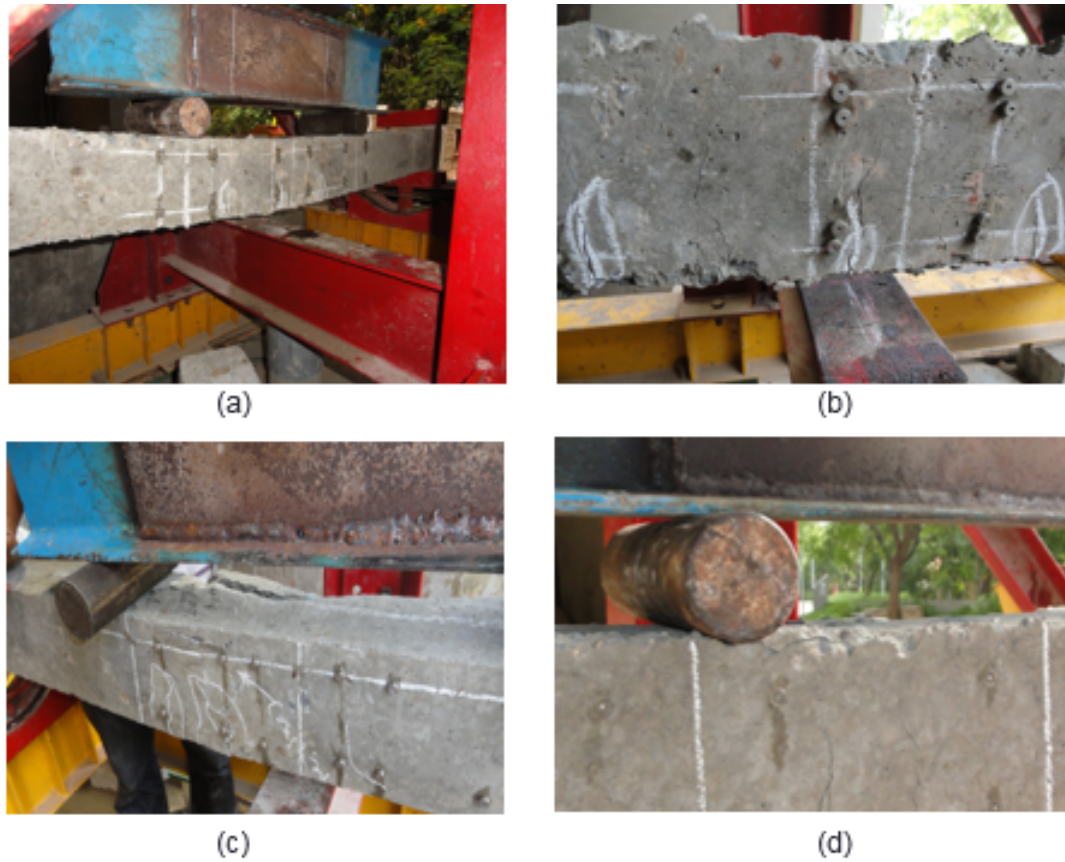


Figure 5.13: Failure Patterns of RCC Beams

was plotted. To measure the deflection for the RC beam deflection gauge was used near the center of the beam. It was observed that all the beams were failed in the flexure. And cracks were observed in middle one third portion of the beams. Shear failure was not observed. Fig. 5.12 shows failure pattern of the beam elements. Fig. 5.12(a) shows the cracks in the tension zone and Fig. 5.12(b) shows deflected shape of beam after testing. Fig. 5.13(a) and 5.13(b) shows failure of specimens. Fig. 5.13(c) and 5.13(d) shows the compression failure of the RC beams.

5.7 Test Results

This section discussed the test results for concrete properties as well as the Moment-Curvature.

5.7.1 Test Results for Concrete Properties

In present experiment cubes ($150\text{mm} \times 150\text{mm} \times 150\text{mm}$), cylinders($150\text{mm} \times 300\text{mm}$) and beams ($100\text{mm} \times 100\text{mm} \times 500\text{mm}$) were also tested to find out the concrete properties. These properties were used in the analytical solution for Moment-Curvature. Table 5.2 shows 7 days and 28 days cube results. Table 5.5 and Table 5.4 shows the flexure strength of concrete and Modulus of elasticity of concrete which were used in the computer program to evaluate Moment-Curvature relationship analytically.

Table 5.2: Cube Strength

7 Days Cube strength			
Sr No	Wt (kg)	Strength (Mpa)	Average Strength (MPa)
1	8.54	22.2	21.8
2	8.62	21.4	
3	8.79	21.9	
28 bays Cube strength			
1	8.68	25	25.7
2	8.74	26.4	
3	8.69	25.7	

Table 5.3: Flexure Strength of Concrete

M20	Load (kN)	Flexure Strength	Average
	15	3.39	3.09
	12	2.71	
	14	3.17	

Table 5.4: Modulus of Elasticity of Concrete

L=212mm			
P (kN)	dl_1(mm)	dl_2 (mm)	dl_3(mm)
50	1	1	2
100	3	2	3
150	4	5	4
200	6	6	7
250	7	8	8
300	10	9	10
350	13	12	12
400	17	16	15
450	20	22	22
$E_c(\text{kN/mm}^2)$	24.69	23.436	24.34
$E_c(\text{kN/mm}^2)$	24.15		

After the testing of the cube specimens, average 7 day cube strength was observed 21.8 MPa. And 28 days cube strength was observed 25.7MPa. Cube strength was used in transform area method as well as strain compatibility method. Flexure strength of beam was found 3.03 and Modulus of elasticity of concrete was found 24.15 kN/mm². These two were used only in transform area method.

5.7.2 Experimental Moment-Curvature

Twelve specimens were tested and experimental Moment-Curvature relationship was obtain for all the RC specimens.

Table 5.5: Moment-Curvature for SUR-1

Load (kN)	M (kNm)	Top Strain $\times 10^{-3}$	Bottom Strain \times 10^{-3}	$\phi \times 10^{-2}$ (rad/m)
0	0	0	0	0
4	0.5	-0.0200	0.0533	0.0772
8	1	-0.0800	0.1133	0.2035
12	1.5	-0.1667	0.1600	0.3439
16	2	-0.1867	0.2467	0.4561
20	2.5	-0.2533	0.4067	0.6947
24	3	-0.2733	0.4867	0.8000
28	3.5	-0.3667	0.6200	1.0386
32	4	-0.4400	0.7400	1.2421
36	4.5	-0.5333	0.8067	1.4105
40	5	-0.6067	0.8333	1.5158
44	5.5	-0.7133	0.9400	1.7404
48	6	-0.7533	1.0667	1.9158
52	6.5	-0.8933	1.2333	2.2386
56	7	-0.9800	1.4600	2.5684
60	7.5	-1.1133	1.8733	3.1439
64	8	-1.3533	3.5667	5.1789
68	8.5	-1.4867	6.6267	8.5404
70	8.75	-1.7133	8.9933	11.2702
70	8.75	-2.0333	11.1600	13.8877
70	8.75	-2.1067	16.9333	20.0421

Table 5.5 shows Moment and corresponding Curvature for singly under reinforced beam 1. Here the Ultimate Moment was observed 8.75 kNm and Ultimate curvature was observed 0.2 rad/m. First crack was observed at 40kN load. Table 5.6 shows Moment and corresponding Curvature for singly under reinforced beam 2. In this case ultimate Moment was observed 8.625 kNm and Ultimate curvature was observed

0.191 rad/m. At 44kN load first crack was observed and similarly Table 5.7 shows the Moment-Curvature relationship for Singly under reinforced beam 3. Ultimate Moment was observed 8.625 kNm and Ultimate curvature was observed 0.166 rad/m. At 42kN load first crack was observed. Table also shows the compression and tension strain of the concrete at each increment of load and moment.

Table 5.6: Moment-Curvature for SUR-2

Load (kN)	M (kNm)	Top Strain \times 10^{-3}	Bottom Strain \times 10^{-3}	$\phi \times 10^{-2}$ (rad/m)
0	0	0.0000	0.0000	0.0000
4	0.5	-0.0133	0.0333	0.0519
8	1	-0.1000	0.2067	0.3407
12	1.5	-0.1933	0.3933	0.6519
16	2	-0.2933	0.5067	0.8889
20	2.5	-0.3267	0.5267	0.9481
24	3	-0.2333	0.4867	0.8000
28	3.5	-0.3800	0.7067	1.2074
32	4	-0.5267	0.6467	1.3037
36	4.5	-0.6400	0.7600	1.5556
40	5	-0.7267	0.8800	1.7852
44	5.5	-0.8067	1.0333	2.0444
48	6	-0.9067	1.1400	2.2741
52	6.5	-1.0200	1.2867	2.5630
56	7	-1.1200	1.4467	2.8519
60	7.5	-1.2267	1.5800	3.1185
64	8	-1.3467	2.1533	3.8889
68	8.5	-1.3867	2.9267	4.7926
69	8.625	-1.7267	6.8667	9.5481
69	8.625	-2.0467	9.9200	13.2963
69	8.625	-2.1133	15.0867	19.1111

Table 5.8 shows the average Moment and corresponding curvature for singly under reinforced beam. Ultiment moment and corresponding curvture was observed 8.67 kNm and 0.186 rad/m. Fig 5.14 shows Moment-Curvature relationship for all three

Singly Under Reinforced beam. Fig 5.14 also represent the average $M-\phi$ relationship. The experimental plot of the $M-\phi$ diagram starts with the elastic region which is signified by its large slope, followed by plastic region which occurs after yielding and is signified by its parabolic shape and proceeded by ultimate and failures. In case of average Moment-Curvature, it is almost linear in elastic zone but after yielding it follows parabolic path and than horizonatal path which represent more increment in curvature for nearly constant moment.

Table 5.7: Moment-Curvature for SUR-3

Load (kN)	M (kNm)	Top Strain \times 10^{-3}	Bottom Strain \times 10^{-3}	$\phi \times 10^{-2}$ (rad/m)
0	0	0.0000	0.0000	0.0000
4	0.5	-0.0200	0.0333	0.0056
8	1	-0.0800	0.1133	0.2035
12	1.5	-0.2067	0.1867	0.4140
16	2	-0.2333	0.3533	0.6175
20	2.5	-0.2133	0.4800	0.7298
24	3	-0.3333	0.7533	1.1439
28	3.5	-0.5000	0.6400	1.2000
32	4	-0.5200	0.8933	1.4877
36	4.5	-0.6067	1.0533	1.7474
40	5	-0.6733	1.2000	1.9719
44	5.5	-0.7333	1.2067	2.0421
48	6	-0.8400	1.3067	2.2596
52	6.5	-0.9600	1.4267	2.5123
56	7	-1.0333	1.5933	2.7649
60	7.5	-1.1400	2.4200	3.7474
64	8	-1.2200	4.3533	5.8667
68	8.5	-1.4200	6.4600	8.2947
69	8.625	-1.5667	8.6467	10.7509
69	8.625	-2.0733	9.4533	12.1333
69	8.625	-2.1800	13.5800	16.5895

Fig. 5.15 shows the strain in the compression zone and tension zone for all three

Table 5.8: Average Moment-Curvature for Singly Under Reinforced RC Beam.

Load (kN)	M (kNm)	Top Strain \times 10^{-3}	Bottom Strain \times 10^{-3}	$\phi \times 10^{-2}$ (rad/m)
0	0	0.0000	0.0000	0.0000
4	0.5	-0.0178	0.0400	0.0617
8	1	-0.0867	0.1444	0.2493
12	1.5	-0.1889	0.2467	0.4699
16	2	-0.2378	0.3689	0.6542
20	2.5	-0.2644	0.4711	0.7909
24	3	-0.2800	0.5756	0.9146
28	3.5	-0.4156	0.6556	1.1487
32	4	-0.4956	0.7600	1.3445
36	4.5	-0.5933	0.8733	1.5712
40	5	-0.6689	0.9711	1.7576
44	5.5	-0.7511	1.0600	1.9423
48	6	-0.8333	1.1711	2.1498
52	6.5	-0.9578	1.3156	2.4379
56	7	-1.0444	1.5000	2.7284
60	7.5	-1.1600	1.9578	3.3366
64	8	-1.3067	3.3578	4.9782
68	8.5	-1.4311	5.3378	7.2092
69.3	8.67	-1.6689	8.1689	10.5231
69.3	8.67	-2.0511	10.1778	13.1058
69.3	8.67	-2.1333	15.2000	18.5809

Singly Under Reinforced beam. Negative value indicate the concrete strain while the positive values represent steel strain. Concrete strain is closer the steel strain till the yeilding that shows good bonding between steel and concrete. After the yeilding there was drasticaly increment was observed in the tensile strain.

As the yielding has occured there was sudden increment in deflection was observed. As the deflection was incresed the rigidity of the RC beam was decreased.

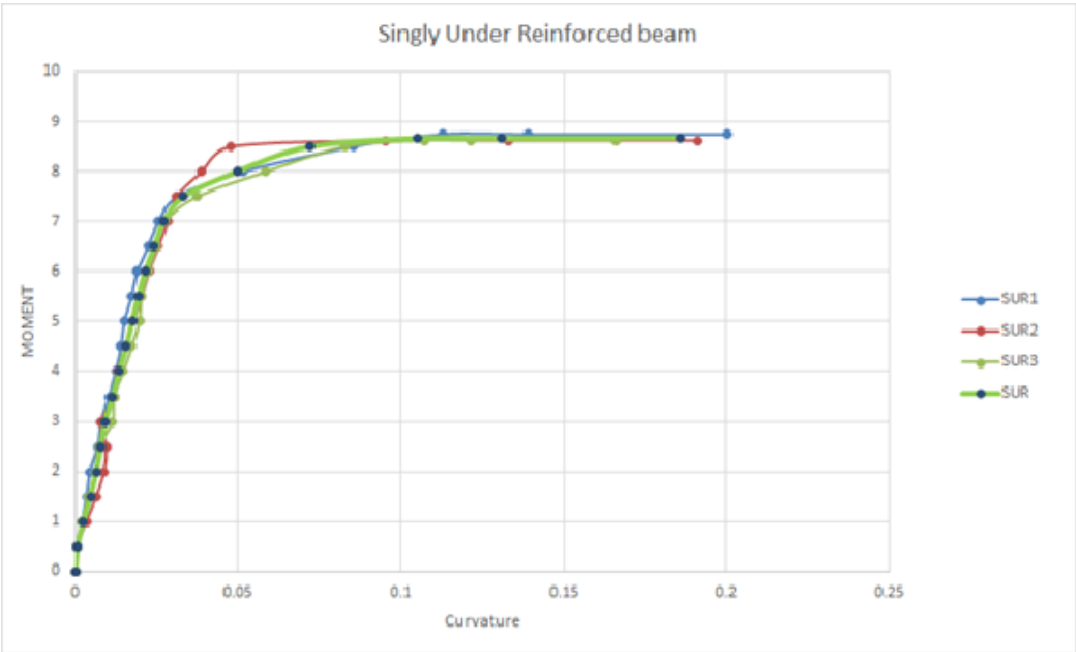


Figure 5.14: Moment-Curvature For Singly Under Reinforced Beam

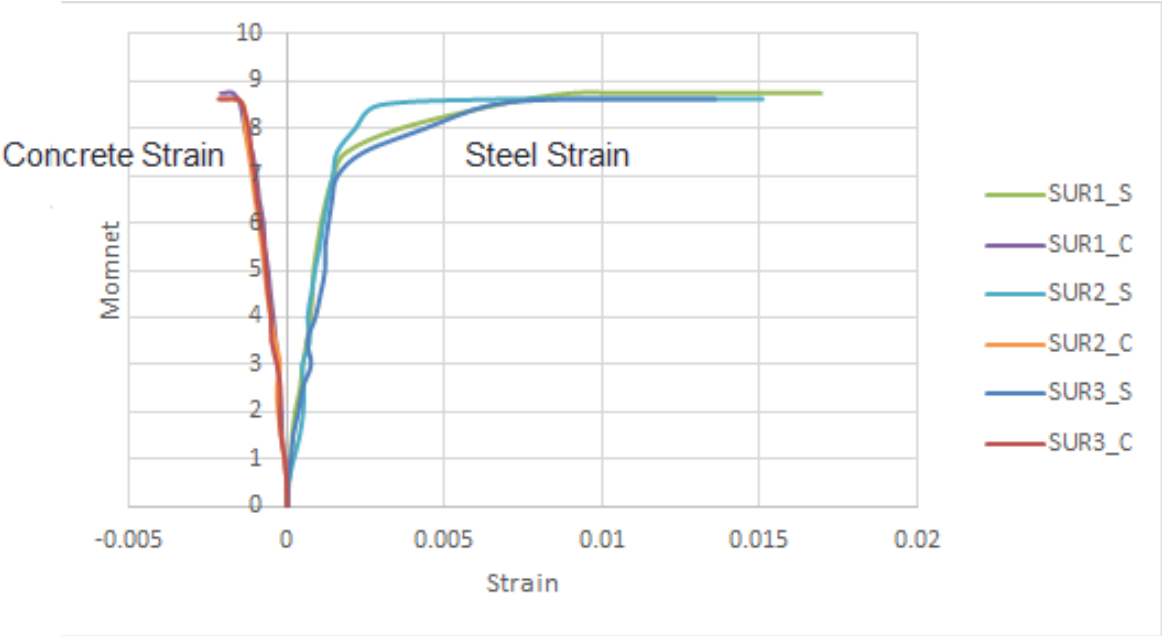


Figure 5.15: Stain at Tension and Compression Zone

Table 5.9: Moment-Curvature for Singly Over Reinforced Beam-1

Load (kN)	M (kNm)	Top Strain \times 10^{-3}	Bottom Strain \times 10^{-3}	$\phi \times 10^{-2}$ (rad/m)
0	0	0	0	0
4	0.5	-0.013	0.033	0.052
8	1	-0.080	0.127	0.230
12	1.5	-0.080	0.200	0.311
16	2	-0.113	0.307	0.467
20	2.5	-0.160	0.293	0.504
24	3	-0.147	0.400	0.607
28	3.5	-0.220	0.493	0.793
32	4	-0.280	0.533	0.904
36	4.5	-0.473	0.540	1.126
40	5	-0.487	0.467	1.059
44	5.5	-0.373	0.587	1.067
48	6	-0.427	0.680	1.230
52	6.5	-0.513	0.773	1.430
56	7	-0.520	0.840	1.511
60	7.5	-0.560	0.887	1.607
64	8	-0.600	0.960	1.733
68	8.5	-0.593	1.033	1.807
72	9	-0.553	1.093	1.830
76	9.5	-0.667	1.107	1.970
80	10	-0.727	1.253	2.200
84	10.5	-0.787	1.340	2.363
88	11	-0.800	1.440	2.489
92	11.5	-0.933	1.527	2.733
96	12	-1.040	1.467	2.785
100	12.5	-1.033	1.407	2.711
104	13	-1.007	1.753	3.067
108	13.5	-1.153	2.107	3.622
112	14	-1.233	3.233	4.963
113	14.125	-1.660	7.287	9.941
113	14.125	-2.060	9.593	12.948

Table 5.10: Moment-Curvature for Singly Over Reinforced beam-2

Load (kN)	M (kNm)	Top Strain \times 10^{-3}	Bottom Strain \times 10^{-3}	$\phi \times 10^{-2}$ (rad/m)
0	0	0	0	0
4	0.5	-0.027	0.053	0.089
8	1	-0.053	0.093	0.163
12	1.5	-0.053	0.120	0.193
16	2	-0.100	0.287	0.430
20	2.5	-0.187	0.333	0.578
24	3	-0.240	0.413	0.726
28	3.5	-0.213	0.447	0.733
32	4	-0.293	0.693	1.096
36	4.5	-0.247	0.680	1.030
40	5	-0.333	0.753	1.207
44	5.5	-0.400	0.813	1.348
48	6	-0.427	0.907	1.481
52	6.5	-0.493	0.980	1.637
56	7	-0.507	1.000	1.674
60	7.5	-0.573	1.113	1.874
64	8	-0.640	1.200	2.044
68	8.5	-0.747	1.233	2.200
72	9	-0.847	1.353	2.444
76	9.5	-0.953	1.507	2.733
80	10	-1.033	1.573	2.896
84	10.5	-1.113	1.727	3.156
88	11	-1.187	1.847	3.370
92	11.5	-1.273	2.027	3.667
96	12	-1.327	2.173	3.889
100	12.5	-1.447	2.420	4.296
104	13	-1.553	3.040	5.104
108	13.5	-1.653	4.400	6.726
110	13.75	-1.680	5.793	8.304
109	13.625	-1.993	7.887	10.978
110	13.75	-2.087	9.527	12.904

Table 5.11: Moment-Curvature for Singly Over Reinforced beam-3

Load (kN)	M (kNm)	Top Strain \times 10^{-3}	Bottom Strain \times 10^{-3}	$\phi \times 10^{-2}$ (rad/m)
0	0	0	0	0
4	0.5	-0.020	0.033	0.059
8	1	-0.067	0.140	0.230
12	1.5	-0.100	0.180	0.311
16	2	-0.140	0.273	0.459
20	2.5	-0.173	0.313	0.541
24	3	-0.187	0.427	0.681
28	3.5	-0.233	0.500	0.815
32	4	-0.340	0.440	0.867
36	4.5	-0.413	0.520	1.037
40	5	-0.453	0.460	1.015
44	5.5	-0.433	0.607	1.156
48	6	-0.500	0.633	1.259
52	6.5	-0.507	0.680	1.319
56	7	-0.547	0.727	1.415
60	7.5	-0.553	0.807	1.511
64	8	-0.600	0.873	1.637
68	8.5	-0.620	0.920	1.711
72	9	-0.707	1.040	1.941
76	9.5	-0.713	1.127	2.044
80	10	-0.793	1.200	2.215
84	10.5	-0.880	1.313	2.437
88	11	-0.920	1.300	2.467
92	11.5	-0.993	1.467	2.733
96	12	-1.133	1.673	3.119
100	12.5	-1.207	1.860	3.407
104	13	-1.313	2.507	4.244
108	13.5	-1.440	3.367	5.341
112	14	-1.707	5.113	7.578
113	14.125	-1.887	5.947	8.704
113	14.125	-2.147	8.920	12.296

Table 5.12: Average Moment-Curvature for Singly Over Reinforced RC Beam.

Load (kN)	M (kNm)	Top Strain <i>times</i> 10^{-3}	Bottom Strain <i>times</i> 10^{-3}	ϕ <i>times</i> 10^{-2} (rad/m)
0	0	0	0	0
4	0.5	-0.020	0.040	0.067
8	1	-0.067	0.120	0.207
12	1.5	-0.078	0.167	0.272
16	2	-0.118	0.289	0.452
20	2.5	-0.173	0.313	0.541
24	3	-0.191	0.413	0.672
28	3.5	-0.222	0.480	0.780
32	4	-0.304	0.556	0.956
36	4.5	-0.378	0.580	1.064
40	5	-0.424	0.560	1.094
44	5.5	-0.402	0.669	1.190
48	6	-0.451	0.740	1.323
52	6.5	-0.504	0.811	1.462
56	7	-0.524	0.856	1.533
60	7.5	-0.562	0.936	1.664
64	8	-0.613	1.011	1.805
68	8.5	-0.653	1.062	1.906
72	9	-0.702	1.162	2.072
76	9.5	-0.778	1.247	2.249
80	10	-0.851	1.342	2.437
84	10.5	-0.927	1.460	2.652
88	11	-0.969	1.529	2.775
92	11.5	-1.067	1.673	3.044
96	12	-1.167	1.771	3.264
100	12.5	-1.229	1.896	3.472
104	13	-1.291	2.433	4.138
108	13.5	-1.416	3.291	5.230
111.33	13.92	-1.540	4.713	6.948
111.67	13.96	-1.847	7.040	9.874
112	14	-2.098	9.347	12.716

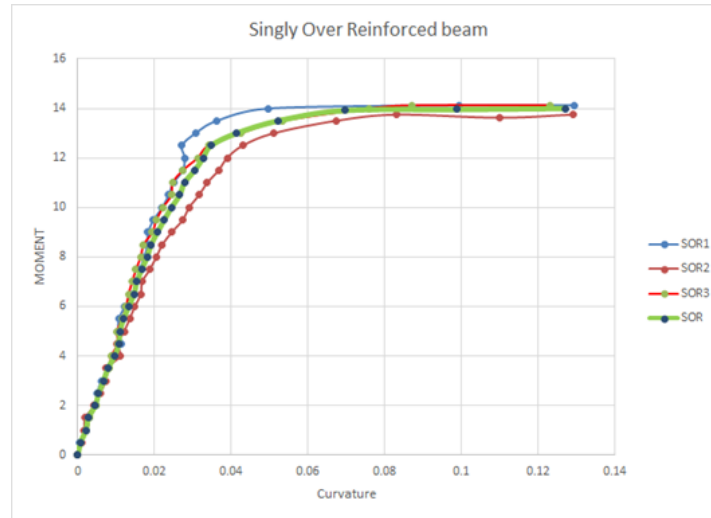


Figure 5.16: Moment-Curvature relationship for Singly Over Reinforced beam

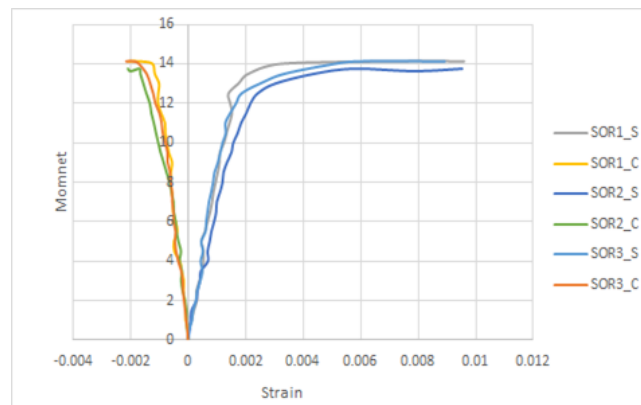


Figure 5.17: Concrete and Steel Strain of Doubly Under Reinforced Beam

Table 5.9 shows Moment and Curvature for singly over reinforced beam-1. Ultimate Moment and curvature was observed 14.125 kNm and 0.129 rad/m. Table 5.10 shows Moment and corresponding Curvature for singly over reinforced beam-2. Here, ultimate moment and corresponding Curvature was observed 13.75 kNm and 0.129 rad/m and Table 5.11 shows the Moment and corresponding curvature for Singly Over Reinforced beam-3. 14.125 kNm and 0.123 rad/m was observed ulti-

mate moment and curvature for singly over reinforced beam-3. Those tables are also shows concrete strain and steel strain for each increment of load. Fig. 5.16 shows the Moment-Curvature relationship for all three Singly Over Reinforced beam. It also shown average Moment-Curvature for rc beam. Fig. 5.17 shows the strain in RC element at the top and bottom reinforcement level.

Table 5.13: Moment-Curvature for Doubly Under Reinforced beam-1

Load (kN)	M (kNm)	Top Strain \times 10^{-3}	Bottom Strain \times 10^{-3}	$\phi \times 10^{-2}$ (rad/m)
0	0	0	0	0
4	0.5	-0.013	0.033	0.052
8	1	-0.073	0.087	0.178
12	1.5	-0.167	0.120	0.319
16	2	-0.193	0.147	0.378
20	2.5	-0.280	0.233	0.570
24	3	-0.593	0.253	0.941
28	3.5	-0.593	0.307	1.000
32	4	-0.600	0.373	1.081
36	4.5	-0.533	0.427	1.067
40	5	-0.660	0.540	1.333
44	5.5	-0.740	0.487	1.363
48	6	-0.720	0.647	1.519
52	6.5	-0.847	0.720	1.741
56	7	-0.893	0.827	1.911
60	7.5	-1.087	0.880	2.185
64	8	-1.167	0.913	2.311
68	8.5	-1.240	1.020	2.511
72	9	-1.293	1.167	2.733
76	9.5	-1.313	1.580	3.215
80	10	-1.387	1.927	3.681
84	10.5	-1.507	2.180	4.096
87	10.875	-1.660	4.780	7.156
83	10.375	-1.873	6.660	9.481
80	10	-2.160	12.287	16.052

Table 5.14: Moment-Curvature for Doubly Under Reinforced beam-2

Load (kN)	M (kNm)	Top Strain \times 10^{-3}	Bottom Strain \times 10^{-3}	$\phi \times 10^{-2}$ (rad/m)
0	0	0	0	0
4	0.5	-0.020	0.013	0.037
8	1	-0.047	0.060	0.119
12	1.5	-0.160	0.133	0.326
16	2	-0.180	0.300	0.533
20	2.5	-0.153	0.360	0.570
24	3	-0.227	0.373	0.667
28	3.5	-0.273	0.500	0.859
32	4	-0.400	0.647	1.163
36	4.5	-0.480	0.707	1.319
40	5	-0.560	0.767	1.474
44	5.5	-0.633	0.853	1.652
48	6	-0.640	0.920	1.733
52	6.5	-0.727	0.907	1.815
56	7	-0.847	0.993	2.044
60	7.5	-0.953	1.080	2.259
64	8	-1.040	1.147	2.430
68	8.5	-1.147	0.987	2.370
72	9	-1.073	1.187	2.511
76	9.5	-1.173	1.280	2.726
80	10	-1.340	1.733	3.415
84	10.5	-1.547	3.813	5.956
88	11	-1.940	5.833	8.637
82	10.25	-2.053	8.373	11.585
78	9.75	-2.240	11.867	15.674

Table 5.12 shows the average Moment and corresponding Curvature for all three singly over reinforced beam. Here, average ultimate moment and corresponding Curvature was observed 14 kNm and 0.127 rad/m. Table 5.13 represent Moment and corresponding Curvature for doubly under reinforced beam-1. From Table 5.13 ultimate Moment and Curvature was 10.875 kNm and 0.715 rad/m. Here first crack was observed at 60 kN load. Table 5.14 shows Moment-Curvature for doubly under reinforced beam-2.

Table 5.15: Moment-Curvature for Doubly Under Reinforced beam-3

Load (kN)	M (kNm)	Top Strain \times 10^{-3}	Bottom Strain \times 10^{-3}	$\phi \times 10^{-2}$ (rad/m)
0	0	0	0	0
4	0.5	-0.020	0.000	0.022
8	1	-0.073	0.053	0.141
12	1.5	-0.140	0.127	0.296
16	2	-0.213	0.193	0.452
20	2.5	-0.327	0.260	0.652
24	3	-0.393	0.320	0.793
28	3.5	-0.513	0.440	1.059
32	4	-0.613	0.520	1.259
36	4.5	-0.667	0.573	1.378
40	5	-0.740	0.653	1.548
44	5.5	-0.820	0.707	1.696
48	6	-0.727	0.867	1.770
52	6.5	-0.793	0.947	1.933
56	7	-0.907	1.047	2.170
60	7.5	-0.980	1.153	2.370
64	8	-1.047	1.187	2.481
68	8.5	-1.227	1.307	2.815
72	9	-1.267	1.420	2.985
76	9.5	-1.360	1.687	3.385
80	10	-1.380	2.147	3.919
84	10.5	-1.647	3.887	6.148
87	10.875	-1.747	7.560	10.341
83	10.375	-1.980	9.867	13.163
78	9.75	-2.213	13.660	17.637

Table 5.16: Average Moment-Curvature for Doubly Under Reinforced RC Beam.

Load (kN)	M (kNm)	Top Strain \times 10^{-3}	Bottom Strain \times 10^{-3}	$\phi \times 10^{-2}$ (rad/m)
0	0	0	0	0
4	0.5	-0.018	0.016	0.037
8	1	-0.064	0.067	0.146
12	1.5	-0.156	0.127	0.314
16	2	-0.196	0.213	0.454
20	2.5	-0.253	0.284	0.598
24	3	-0.404	0.316	0.800
28	3.5	-0.460	0.416	0.973
32	4	-0.538	0.513	1.168
36	4.5	-0.560	0.569	1.254
40	5	-0.653	0.653	1.452
44	5.5	-0.731	0.682	1.570
48	6	-0.696	0.811	1.674
52	6.5	-0.789	0.858	1.830
56	7	-0.882	0.956	2.042
60	7.5	-1.007	1.038	2.272
64	8	-1.084	1.082	2.407
68	8.5	-1.204	1.104	2.565
72	9	-1.211	1.258	2.743
76	9.5	-1.282	1.516	3.109
80	10	-1.369	1.936	3.672
84	10.5	-1.567	3.293	5.400
87.33	10.92	-1.782	6.058	8.711
82.67	10.33	-1.969	8.300	11.410
78.67	9.83	-2.204	12.604	16.454

In case of Beam-2 11 kNm and 0.864 rad/m were the observed ultimate moment and curvature. At the load of 56 kN first crack was observed. Table 5.15 shows the Moment Curvature for doubly under reinforced beam-3. Here, ultimate Moment and Curvature was observed 10.875 kN and 0.103 rad/m. Those tables also include strain in concrete as well as strain in steel for Doubly Under Reinforced beam. Table 5.16 shows average moment and curvature for doubly under reinforce RC beam. Average ultimate Moment and curvature of doubly under reinforced beam was observed 10.92 kNm and 0.871 rad/sec. Fig. 5.18 shows the Moment-Curvature relationship for all three doubly under reinforced beam as well as average Moment-Curvature. Here, Moment-Curvature is linear up to yielding of reinforcement after this it follows parabolic path. In the case of doubly under reinforced beam degradation in strength was observed after the peak strength. Fig. 5.19 shows the strain in RC element at the top and bottom reinforcement level. Strain were liner up to the yeild then it follow parabolic path. Here also drop in streghth was observed.

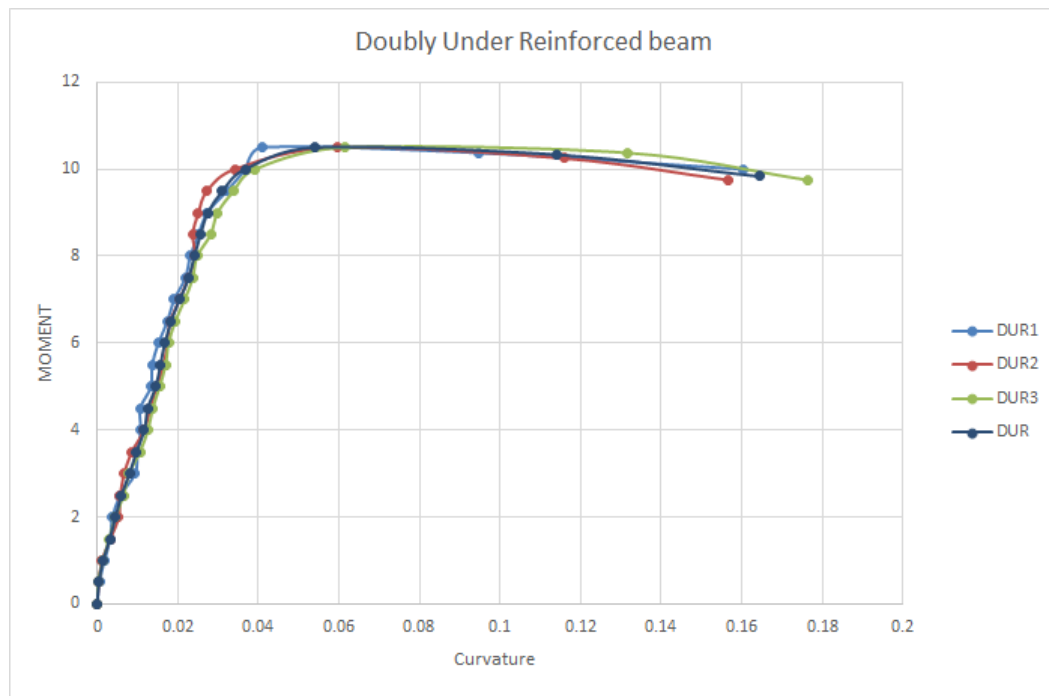


Figure 5.18: Moment-Curvature Doubly Under Reinforced

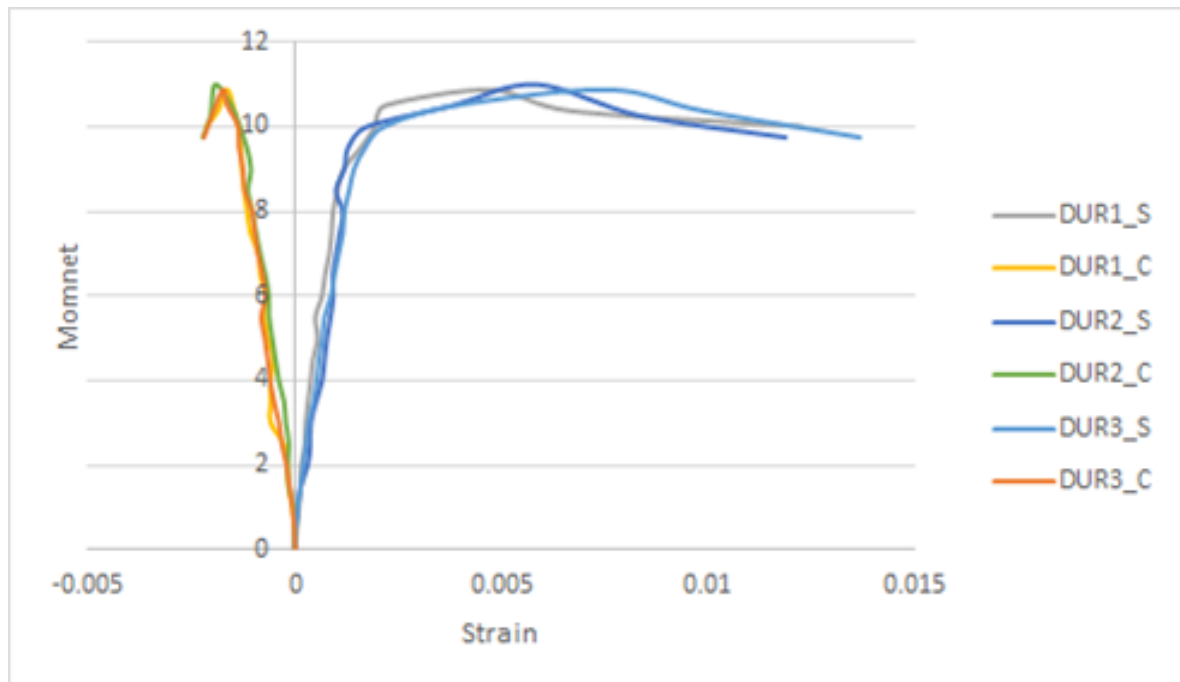


Figure 5.19: Compression Strain and Tensile Strain in Doubly Under Reinforced Beam

Table 5.17 shows Moment and Curvature for doubly over reinforced beam-1. In this case Ultimate Moment and Curvature was observed 13.5 kNm and 0.745 rad/m respectively. At the 68 kN load first crack was observed. Table 5.18 shows Moment-Curvature for Over Reinforced beam-2. For beam-2 ultimate Moment and Curvature was observed 13.5 kNm and 0.749 rad/m respectively. Here, first crack was occurred at 72 kN load. And Table 5.19 shows the Moment Curvature for Doubly Over Reinforced beam-3. 13.5 kNm and 0.693 rad/m were the ultimate moment and curvature for beam-3. Fig. 5.20 and Fig. 5.21 shows the Moment-Curvature relationship for all three Doubly Over Reinforced beams and it also shows the strain in RC element at the top and bottom reinforcement level. Table 5.20 shows average Moment and Curvature for doubly over reinforced section. Average ultimate moment was observed 13.5 kNm and ultimate curvature was observed 0.728 rad/m.

Table 5.17: Moment-Curvature for Doubly Over Reinforced Beam-1

Load (kN)	M (kNm)	Top Strain \times 10^{-3}	Bottom Strain \times 10^{-3}	$\phi \times 10^{-2}$ (rad/m)
0	0	0	0	0
4	0.5	-0.027	0.013	0.044
8	1	-0.067	0.033	0.111
12	1.5	-0.100	0.053	0.170
16	2	-0.087	0.147	0.259
20	2.5	-0.160	0.227	0.430
24	3	-0.160	0.280	0.489
28	3.5	-0.227	0.367	0.659
32	4	-0.233	0.527	0.844
36	4.5	-0.273	0.580	0.948
40	5	-0.300	0.667	1.074
44	5.5	-0.280	0.673	1.059
48	6	-0.347	0.733	1.200
52	6.5	-0.407	0.787	1.326
56	7	-0.473	0.880	1.504
60	7.5	-0.487	0.827	1.459
64	8	-0.607	0.880	1.652
68	8.5	-0.693	0.993	1.874
72	9	-0.713	1.000	1.904
76	9.5	-0.760	1.047	2.007
80	10	-0.807	1.047	2.059
84	10.5	-0.820	1.107	2.141
88	11	-0.940	1.207	2.385
92	11.5	-1.007	1.273	2.533
96	12	-1.173	1.620	3.104
100	12.5	-1.353	1.627	3.311
104	13	-1.433	2.873	4.785
108	13.5	-1.660	5.013	7.415
106	13.25	-2.007	8.507	11.681
98	12.25	-2.107	11.567	15.193

Table 5.18: Moment-Curvature for Doubly Over Reinforced Beam-2

Load (kN)	M (kNm)	Top Strain $\times 10^{-3}$	Bottom Strain $\times 10^{-3}$	$\phi \times 10^{-2}$ (rad/m)
0	0	0	0	0
4	0.5	-0.020	0.040	0.067
8	1	-0.053	0.080	0.148
12	1.5	-0.100	0.127	0.252
16	2	-0.087	0.213	0.333
20	2.5	-0.073	0.193	0.296
24	3	-0.140	0.267	0.452
28	3.5	-0.233	0.353	0.652
32	4	-0.333	0.427	0.844
36	4.5	-0.240	0.533	0.859
40	5	-0.320	0.440	0.844
44	5.5	-0.280	0.533	0.904
48	6	-0.460	0.593	1.170
52	6.5	-0.613	0.613	1.363
56	7	-0.713	0.747	1.622
60	7.5	-0.767	0.747	1.681
64	8	-0.767	0.800	1.741
68	8.5	-0.867	0.873	1.933
72	9	-0.927	0.853	1.978
76	9.5	-0.973	0.940	2.126
80	10	-1.007	1.013	2.244
84	10.5	-1.013	1.073	2.319
88	11	-1.087	1.127	2.459
92	11.5	-1.253	1.207	2.733
96	12	-1.373	1.613	3.319
100	12.5	-1.453	1.727	3.533
104	13	-1.480	3.553	5.593
108	13.5	-1.713	5.027	7.489
107	13.375	-2.053	8.793	12.052
100	12.5	-2.120	13.000	16.800

Table 5.19: Moment-Curvature for Doubly Over Reinforced Beam-3

Load (kN)	M (kNm)	Top Strain \times 10^{-3}	Bottom Strain \times 10^{-3}	$\phi \times 10^{-2}$ (rad/m)
0	0	0	0	0
4	0.5	-0.013	0.033	0.052
8	1	-0.060	0.060	0.133
12	1.5	-0.100	0.147	0.274
16	2	-0.127	0.100	0.252
20	2.5	-0.087	0.253	0.378
24	3	-0.180	0.280	0.511
28	3.5	-0.233	0.387	0.689
32	4	-0.340	0.473	0.904
36	4.5	-0.313	0.567	0.978
40	5	-0.373	0.633	1.119
44	5.5	-0.427	0.720	1.274
48	6	-0.447	0.780	1.363
52	6.5	-0.507	0.820	1.474
56	7	-0.567	0.880	1.607
60	7.5	-0.627	0.933	1.733
64	8	-0.607	0.987	1.770
68	8.5	-0.647	0.967	1.793
72	9	-0.667	1.013	1.867
76	9.5	-0.807	1.047	2.059
80	10	-0.907	1.173	2.311
84	10.5	-0.967	1.227	2.437
88	11	-1.167	1.573	3.044
92	11.5	-1.240	1.747	3.319
96	12	-1.307	1.827	3.481
100	12.5	-1.360	1.980	3.711
104	13	-1.400	2.833	4.704
108	13.5	-1.620	4.647	6.963
106	13.25	-2.013	8.747	11.956
97	12.125	-2.160	11.720	15.422

Table 5.20: Average Moment-Curvature for Doubly Over Reinforced RC Beam.

Load (kN)	M (kNm)	Top Strain \times 10^{-3}	Bottom Strain \times 10^{-3}	$C \times 10^{-2}$ (rad/m)
0	0	0	0	0
4	0.5	-0.020	0.029	0.054
8	1	-0.060	0.058	0.131
12	1.5	-0.100	0.109	0.232
16	2	-0.100	0.153	0.281
20	2.5	-0.107	0.224	0.368
24	3	-0.160	0.276	0.484
28	3.5	-0.231	0.369	0.667
32	4	-0.302	0.476	0.864
36	4.5	-0.276	0.560	0.928
40	5	-0.331	0.580	1.012
44	5.5	-0.329	0.642	1.079
48	6	-0.418	0.702	1.244
52	6.5	-0.509	0.740	1.388
56	7	-0.584	0.836	1.578
60	7.5	-0.627	0.836	1.625
64	8	-0.660	0.889	1.721
68	8.5	-0.736	0.944	1.867
72	9	-0.769	0.956	1.916
76	9.5	-0.847	1.011	2.064
80	10	-0.907	1.078	2.205
84	10.5	-0.933	1.136	2.299
88	11	-1.064	1.302	2.630
92	11.5	-1.167	1.409	2.862
96	12	-1.284	1.687	3.301
100	12.5	-1.389	1.778	3.519
104	13	-1.438	3.087	5.027
108	13.5	-1.664	4.896	7.289
106.33	13.25	-2.024	8.682	11.896
98.33	12.125	-2.129	12.096	15.805

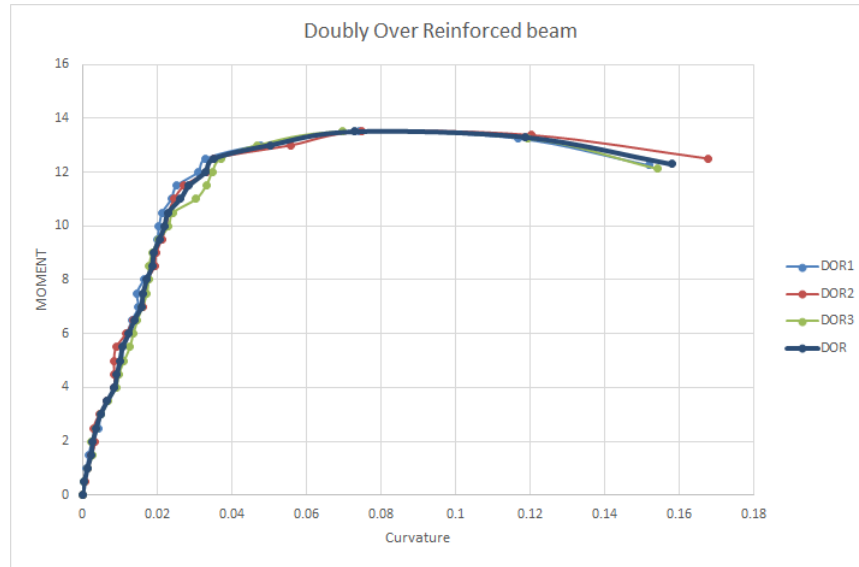


Figure 5.20: Moment-Curvature Doubly Over Reinforced

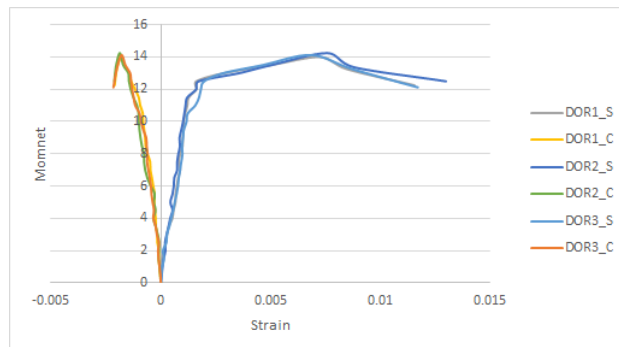


Figure 5.21: Compression Strain and Tensile Strain in Doubly Over Reinforced Beam

5.8 Summary

This chapter includes the concepts of the experimental evaluation of Moment-Curvature relationship. It also deals with the experimental program. The experimental program was designed in such way so that the experimental results can be compared with

the analytical results. Here, test setup, instrumentation for measuring curvature, testing of the concrete cubes, cylinder and beams to find out the concrete properties and testing of RC specimens were discussed in detail. The experimental curvature obtained from the testing of the RC specimens were also included in this chapter. From the Moment-Curvature one can estimate the deflection, stiffness, and ductility of the beam. Post peak behaviour of the beams can also be predicted.

Chapter 6

Results and Discussion

6.1 General

This chapter deals with the comparison of the analytical results for all four type (Singly Under Reinforced, Singly Over Reinforced, Doubly Under Reinforced and Doubly Over Reinforced) of beam elements with the experimental moment-curvature. This also include the stress-strain diagrams for selected model.

6.2 Stress-Strain Curves

Various existing stress-strain models were used to evaluate Moment-Curvature by using strain compatibility method. IS 456 model, Hognestad model, Kent and Park Model and IRC model were unconfined models. Cusson Model and Mander Model for confined concrete was used. Fig. 6.1 shows stress-strain curves obtain from these models.

IS code model follows the parabolic path up to the peak strain than it follow straight horizontal line up to the failure. Degradation in strength after the peak was not considered in to the model. But Hognestad include damage parameter in his model. So hognestad model shows degradation after the peak. In Kent and Park model ascending part of the stress-strain curve is represented by a second-degree

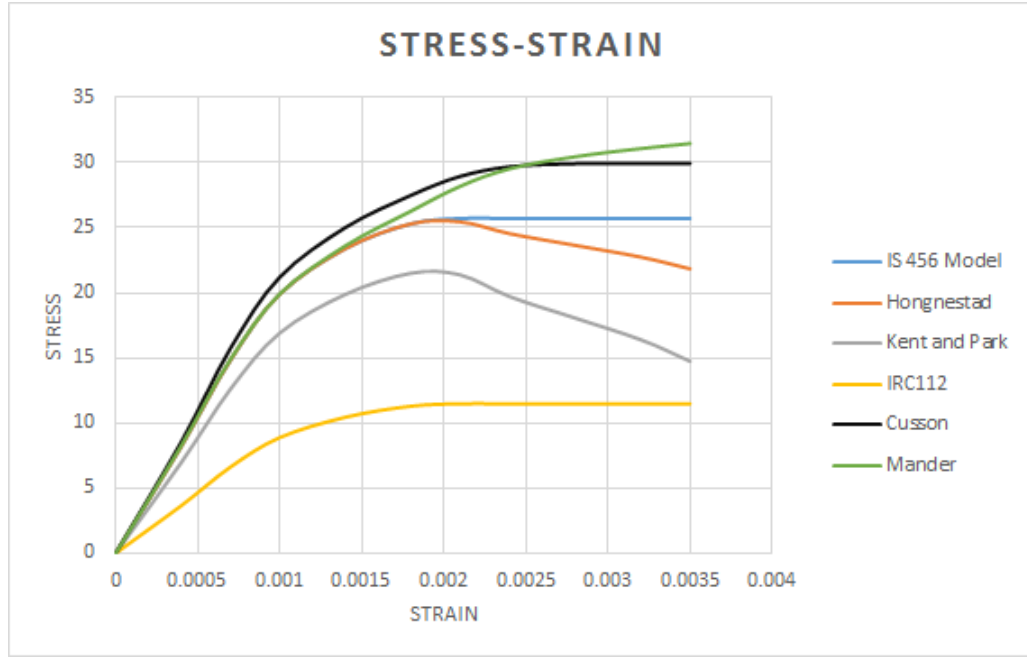


Figure 6.1: Stress-Strain Models

of parabola and here the confining steel has no effect on the shape of this portion. Descending branch depends on the concrete cylinder strength. Stress-strain curve is parabolic in the ascending portion then it follows horizontal line up to failure in the case of material model proposed in IRC112. Fig 6.1 also shows the stress-strain curve obtain by using Cusson Model and Mander Model.

6.3 Experimental and Analytical Comparison of Moment-Curvature

Fig 6.2 shows analytical as well as experimental Moment-Curvature for singly under reinforced beam. Experimental curvature are closer to the analytical values obtain by using IRC model up to the yield, after yielding it follows the value obtains by Hongnestad model. Experimental curvature was parabolic up to the peak than it follows almost straight horizontal line.

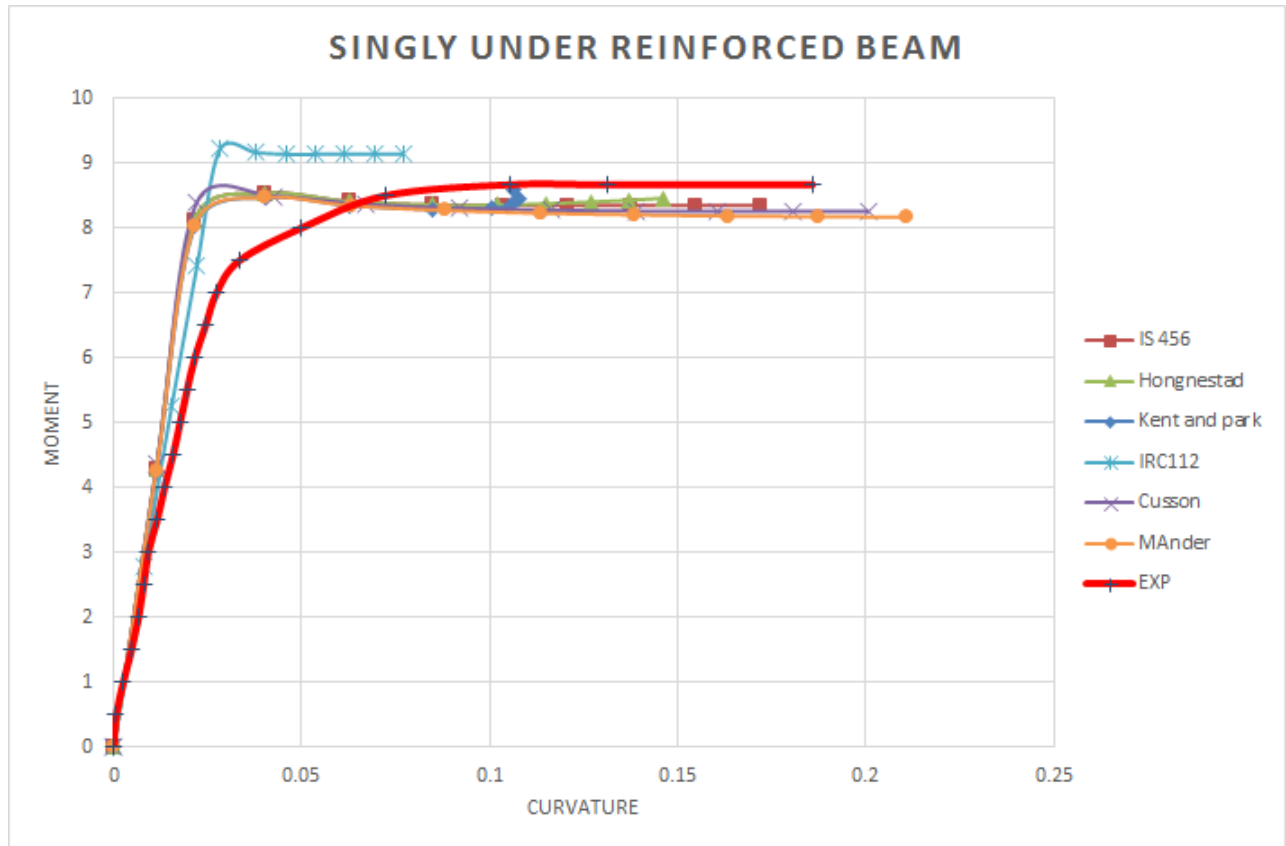


Figure 6.2: Moment-Curvature for Singly Under Reinforced Beam

Till the yielding only hairline cracks were observed but after the yielding of the reinforcement, as the moment was increased cracks were propagated. Cracking of concrete reduced the rigidity of the section due to these deflection of the beam was increased rapidly. Here, it is observed that the experimental Moment-Curvature was almost linear till the yielding then there was a large increment in curvature occurs at nearly constant bending moment. The slowly rise of the bending moment is due to the increment in to the lever arm, That represent tension failure.

Experimental values are observed very closer to the analytical value so only flexure failure was there. In case of shear failure drop in moment carrying capacity of the RC beam was observed.

If the ratio of analytical moment obtain by using IRC model to the experimental

moment was found out. It is observed around 1.05 and ratio of analytical curvature obtain by using IRC model to the experimental curvature was observed 0.8. These values are closer than 1.

If the ratio of ultimate moment evaluated by using IS code model to the experimental ultimate moment was found around 0.96. and ratio of ultimate analytical curvature to the experimental was found 0.97.

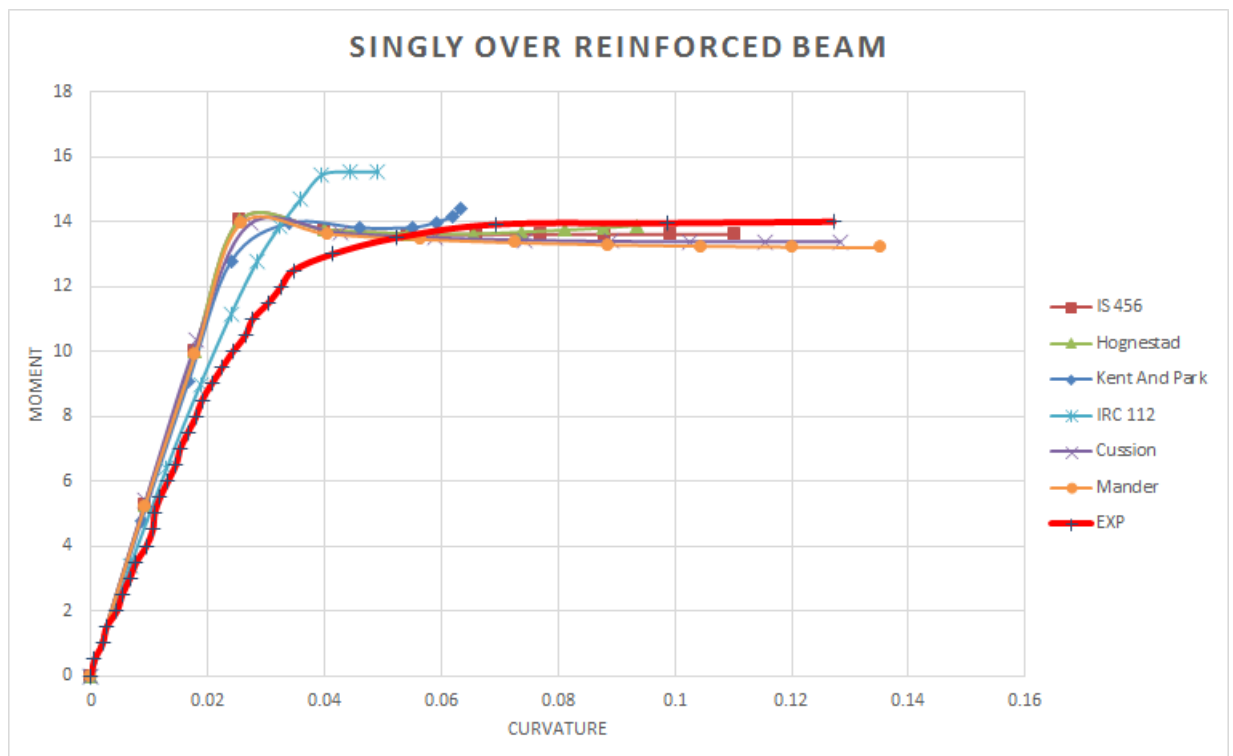


Figure 6.3: Moment-Curvature for Singly Over Reinforced Beam

Fig. 6.3 shows comparison of analytical as well as experimental Moment-Curvature for Singly Over Reinforced Beam. Here, also the analytical Moment-Curvature values obtained by using IRC model are closer to the experimental values up to the yield than it follows the value obtained by IS code model. Experimental curvature was parabolic up to the peak then it follows horizontal line. In the case of Singly Over Reinforced slope of the Moment-Curvature curve in the elastic region is less compared to the under

reinforced beam. Flexural rigidity of the over reinforced section is less compare to the under reinforced beam.

In analytical Moment-Curvature, after the peak there was minor drop in the strength was observed. Here also experimental values are observed very closer to the analytical value so only flexure failure is there. Crushing of the concrete was observed here.

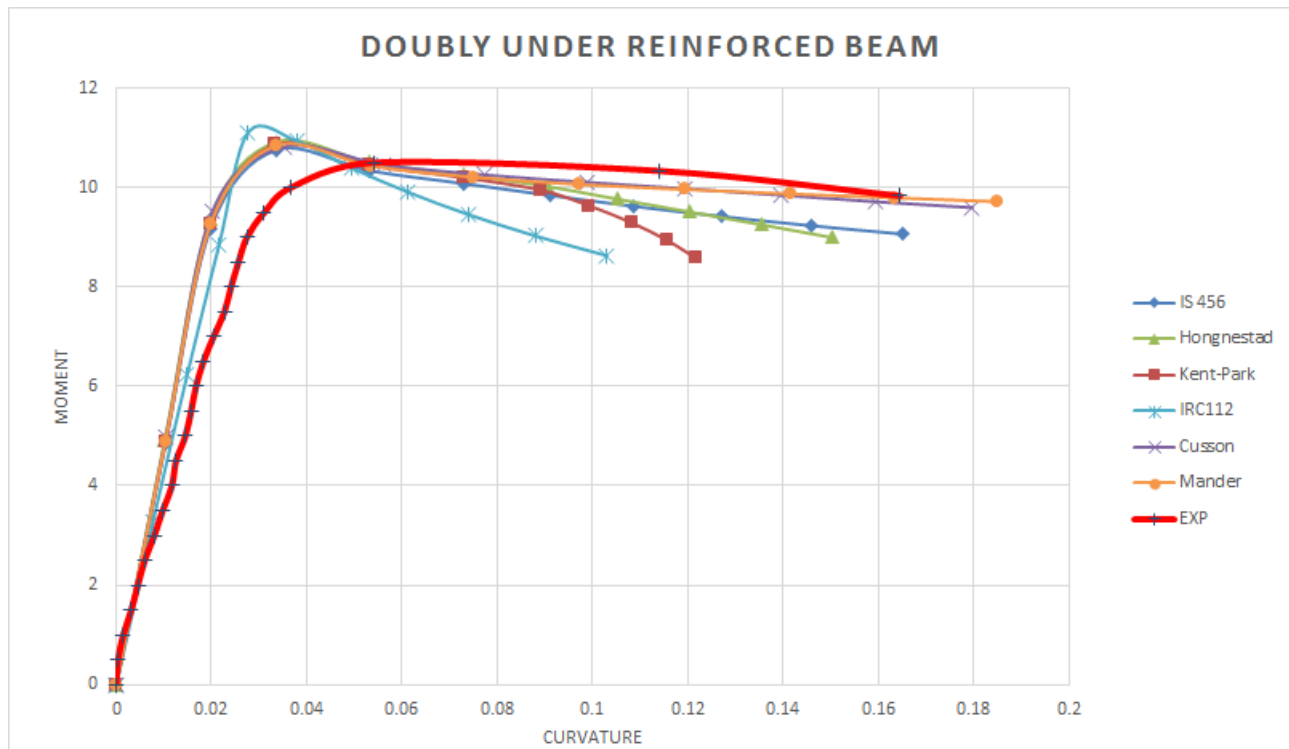


Figure 6.4: Moment-Curvature for Doubly Under Reinforced Beam

If the ratio of analytical moment obtain by using IRC model to the experimental moment was found out. It is observed around 1.022 and ratio of analytical curvature obtain by using IRC model to the experimental curvature was observed 0.814. These values are closer than 1.

If the ratio of ultimate moment evaluated by using IS code model to the experimental ultimate moment was found around 0.978 and ratio of ultimate analytical

curvature to the experimental was found 0.95.

Fig. 6.4 shows Moment-Curvature for Doubly Under Reinforced Beam. Analytical Moment-Curvature values obtain by using IRC model are closer to the experimental values up to the yield than it follows the value obtains by Mander and Cusson model. Experimental curvature was parabolic up to the peak then drop was observed in to strength. Here, Moment-Curvature become nonlinear when the concrete enters the inelastic part of the stress-strain curve. Here curing of the concrete was observed and after the curing sudden drop in the strength was observed.

0.96 is the ratio of analytical yielding moment which was obtain by using IRC 112 to the experimental method. and 1.185 is the ratio of analytical yielding curvature which was obtain by using IRC 112 to the experimental method. 0.967 and 1.05 is the ratio of the analytical moment to ultimate experimental moment and analytical curvature to ultimate experimental curvature respectively for doubly under reinforced beam.

Fig 6.5 shows Analytical and experimental Moment-Curvature for Doubly Over Reinforced Beam. Here also Experimental Moment-Curvature follow the analytical value obtain from the IRC model till the yielding was reached. After yielding it follows the values obtain by using Mander model and Cusson model. Experimental curvature was almost linear up to the peak then degradation in strength was observed in to Moment-Caring capacity. Here also curing of the concrete was observed and after the curing sudden drop in the strength as well as rapid increase in to the deflection was observed. Here flexural rigidity were almost same as in case of Doubly Under Reinforced section.

1.11 is the ratio of analytical yielding moment which was obtain by using IRC 112 to the experimental method. and 1.16 is the ratio of analytical yielding curvature which was obtain by using IRC 112 to the experimental method. 0.85 and 1.073 is ratio of the analytical moment to ultimate experimental moment and analytical curvature to ultimate experimental curvature respectively for doubly over reinforced beam.

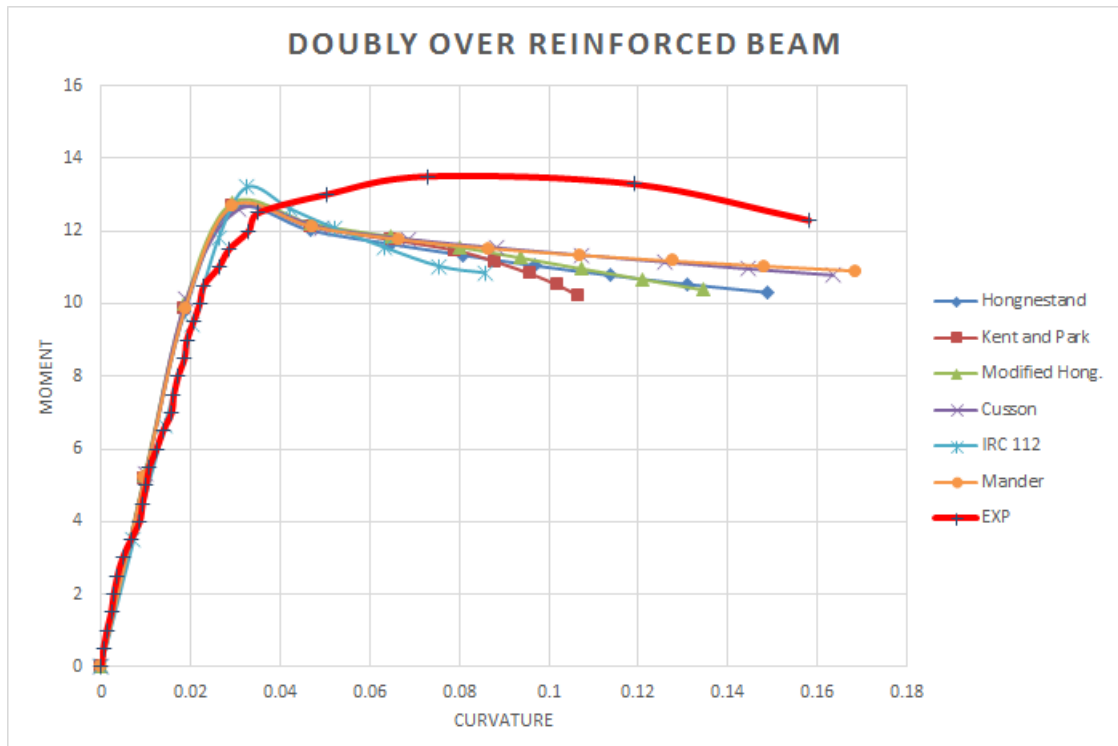


Figure 6.5: Moment-Curvature for Doubly Over Reinforced Beam

The tensile and compressive strains of reinforcement and concrete were measured at every load increment. The strain measurements against the moment for Singly Under Reinforced (SUR), Singly Over Reinforced (SOR), Doubly Under Reinforced (DUR) and Doubly Over Reinforced (DOR) are shown in the Fig 6.6. The negative values represent the compressive strain in the concrete, while the tensile strain in the reinforcement are shown in positive values.

The higher strains in beam may be due to higher deflection due to low modulus of elasticity. The strain were liner in beams until yielding of steel and then rapidly increased before failure. The higher strains in concrete beams also show that good bond between steel and concrete existed till the yielding of steel. the strain, before final failure failure may have been having higher than the strains mentioned here.

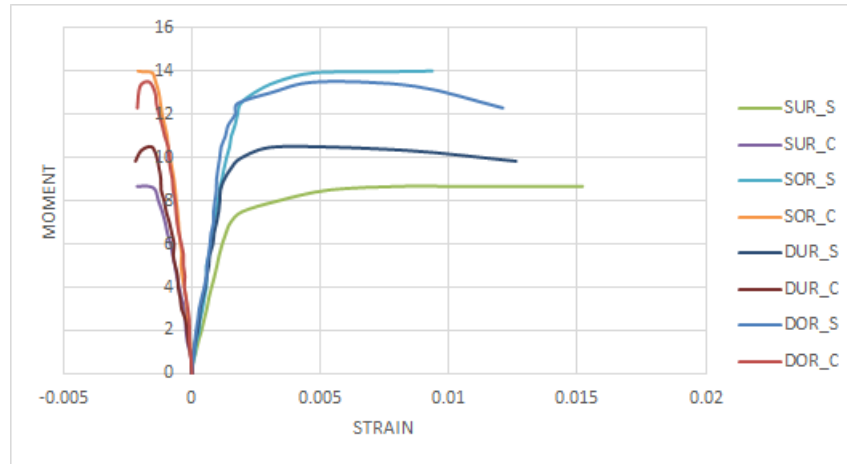


Figure 6.6: Compressive and tensile strain in concrete and steel respectively

6.4 Summary

This chapter include the comparison of experimental and analytical Moment-Curvature for RC beam elements. The strain profile was also discussed in this chapter. Analytical results by IRC model was found closer to the experimental results till the yielding and after yielding experimental results are closer to the analytical results obtain by using IS 456 model for singly reinforced beam and in case of Doubly Reinforced after the yielding, experimental results were closer to the analytical solution obtain by using Mander and Cusson Model.

Chapter 7

Summary and Conclusions

7.1 Summary

In the present study a Matlab program was developed to determine the Moment-Curvature relationship for rectangular RC beam elements by using transform area method as well as strain compatibility method. Transform area method is the approximate method and strain compatibility method is the accurate but iterative method. For evaluation of moment-curvature relationship by strain compatibility method existing material models were used as a stress block.

Experimental program was design to evaluate Moment Curvature relationship for RC rectangular beams. In experimental program casting of twelve reinforced concrete beam element were carried out. In present study singly reinforced as well as doubly reinforced RC specimens were design by limit state method. For measuring curvature, strain was measure at the top and bottom reinforcement level. Moment-Curvature obtain from the experiments was compared with the analytical results obtained from the computer program.

Attempt was also made to evaluate Moment-Curvature relationship for by using various available computational tools. In present study Response 2000 and RC-Analysis were used.

7.2 Conclusions

Following are the important conclusions made from the present study:

- By comparing the analytical results and experimental results it is observed that in the case of Singly Reinforced section the experimental Moment-Curvature follows the analytical results obtain by using IRC 112 model till the yielding of reinforcement. After this the experimental results were found closer to the analytical results obtain by IS 456.
- In the case of Doubly Reinforced section the experimental Moment-Curvature were found closer to the analytical results obtain by using IRC 112 model till the yielding of reinforcement. After this the experimental results follow the analytical results obtain by Mander and Cusson model.
- As the strain was increased, flexure rigidity of beam was decreased and deflection of the beam was increased.
- For both singly reinforced and doubly reinforced section crushing failure of the concrete was observed with the tension failure of RC beam. But in case of under reinforced section tensile cracks were observed first and then crushing failure was occurred. But in case of over reinforced crushing failure was observed first then tensile failure was observed.
- By increasing the amount of tension reinforcement there is a increase in the moment capacity of the section; however the ductility of the structure reduces drastically which is not at all desirable.
- With the increase in the grade of concrete there is a marginal increase in the moment capacity of the section but a substantial increase in the ductility of the section.

7.3 Future Scope of Work

- Moment-Curvature will be evaluated by considering the flexure as well as shear failure.
- Various parametric study will be to estimate the effects of parameters (grade of concrete, cover, grade of steel) on the Moment-Curvature relationship.
- Moment-Curvature relationship can be evaluated for Reinforced Concrete rectangular, square and circular column by using layer approach.
- Experimental evaluation of Moment-Curvature for RC Column elements.
- Moment-Curvature relationship can be developed by considering various support condition for RC elements.
- Moment-Curvature will be evaluated for 2D Frame.

References

- [1] Menon D. "Reinforced Concrete Design", Third edition.
- [2] Mander, J., Priestley, M. J. N., and Park, R. (1988). "Theoretical stress-strain model for confined concrete." *Journal of structural engineering*, 114, 1804.
- [3] Park, R., and Paulay, T. (1975). *Reinforced concrete structures*, John Wiley and Sons, New York.
- [4] Kent, D.C., and Park, R. (1971). "Flexural members with confined concrete." *Journal of the Structural Division, Proc. of the American Society of Civil Engineers*, 97(ST7), 1969-1990.
- [5] Li, B., Park, R., and Tanaka, H. (2000). "Constitutive behavior of high-strength concrete under dynamic loads." *ACI Structural Journal*, 97(4), 619-629.
- [6] Mukherjee, A. , Bagadi, S.P., and Rai, G. L., (2009) "Semianalytical Modeling of Concrete Beams Rehabilitated with Externally Prestressed Composites" *Journal of Composites for construction ASCE*, Volume 13, No.-2, April 1, 2009, 71-84.
- [7] IS: 456:2000 Code of Practice for Plain and Reinforced Concrete. Bureau of Indian Standards. New Delhi. 2000.
- [8] IS: 112-2011 Code of Practice for Concrete Road Bridges. Bureau of Indian Standards. New Delhi. 2011.
- [9] Mander, J.B., Priestley, M.J.N., and Park, R. (1988) "Theoretical stress-strain model of confined concrete." *J. Struct. Eng.*, 114(8), 1804-1826.

- [10] Popovics, S. (1973). "A numerical approach to the complete stress-strain curves of concrete." *Cement and Concrete Research*, 3(5), 583-599.
- [11] Scott, B.D., Park, R., and Priestley, M.J.N. (1982). "Stress-strain behavior of concrete confined by overlapping hoops at low and high strain rates." *J. American Concrete Institute*, 79, 13-27.
- [12] Thorenfeldt, E., Tomaszewicz, A., and Jensen, J.J. (1987). "Mechanical properties of high-strength concrete and application in design." *Proc. of the Symposium on Utilization of High-Strength Concrete*, Tapir, Trondheim, Norway, 149-159.
- [13] Whitney, C.S. (1942). "Plastic theory of reinforced concrete design." *Proceedings ASCE, Transactions ASCE*, 107, 251-326.
- [14] Cusson, D., and Paultre, P. (1995). "Stress-strain model for confined high strength concrete." *J. Struct. Eng.*, 121(3), 468-477.
- [15] Razvi, S., and Saatcioglu, M. (1999). "Confinement model for highstrength concrete." *J. Struct. Eng.*, 125(3), 281-289.
- [16] Hyo-Gyoung Kwak , Sun-Pil Kim, "Nonlinear analysis of RC beam on Moment curvature relationship", *Computers and Structures* (2002) 615-628.
- [17] Srikanth, at. el., " Moment Curvature of reinforced concrete beams using various confinement Models and Experimental validation.", *Asian journal of Civil engineering*, vol. 8, No. 3 (2007) 247-265
- [18] Monita Olivia, Parthasarathi Mandal, "Curvature Ductility of Reinforced Concrete beam"
- [19] Ersoy, U. and Ozcebe, G. (1998). "Moment-Curvature relationship of confined concrete", *Teknik Dergi*, vol. 9, no. 4, pp. 1799-827
- [20] Suarez V. A. and Hurtado J. C. RC-Anlaysia. Virtual Laboratory for Earthquake Engineering, 2008.

- [21] Kowalsky M. J. and Priestley M. J. N. "Improved analytical model for shear strength of circular reinforced concrete columns in seismic regions." ACI Structural Journal, 97(3), 2000.
- [22] Sheikh S. A., "Analytical Moment-Curvature relationship for tied concrete columns," Journal of Structural Engineering, Vol 118, No-2, February 1992.
- [23] Kaklauskas et al. "Eliminating shrinkage effect from Moment-Curvature and tension stiffening relationships of reinforced concrete member", Journal of Structural Engineering, Vol. 137, No-12, December 1, 2011.
- [24] Fafitis. A. and Shah S. P. (1985). "Lateral reinforcement for high-strength concrete columns." ACI Spec. Pub. SP 87-12. Am. Concrete Inst. (ACI). 213-232.
- [25] Noor, Munaz A., "Beam ductility experiment using grade 500 steel."

Appendix A

Matlab Program by Transform Area Method

Moment-Curvature Relationship for Doubly Reinforced by Transform
Area Method

```
Ast=input('Enter the bottom Reinforcement area(mm2):')
Asc=input('Enter the top reinforcement area(mm2):')
ecu=input('Enter the Extreme compression strain:')
f=input('Modulus of rupture:')
Fy=input('yield strength of steel:')
b=input('width of the beam:')
D=input('depth of the beam:')
Fc=input('Cylinder strength of concrete:')
Ec=input('Modulus of the elasticity of concrete:')
Es=input('Modulus of the elasticity of concrete:')
di=input('Clear Cover:')
diab=input('diameter of top bar:')
diat=input('diameter of botom bar:')
M1=0
```

```

phi1=0
d=D-di
As=Ast+Asc

%step 1:
%First Crack

n=Es/Ec
M=[]
phi=[]
M=[M;M1]
phi=[phi;phi1]
%Using transformed area
A=b*D+(n-1)*As
Y=((b*D*D/2)+(Ast*(D-(di+diab/2)))+(Asc*(di+diat/2)))/(A)
I=((b*D^3)/12)+(b*D*((D/2-Y)^2))+
    (Ast*((D-(di+diab/2))-Y)^2)+(Asc*((di+diat/2)-Y)^2)
M2=(f*I)*10^-6/(Y)
phi2=(f/(Ec*Y))*10^3
M=[M;M2]
phi=[phi;phi2]

%step 2
%At first Yield

del_t=Ast/(b*D)
del_c=Asc/(b*D)
K=((del_t+del_c)^2*n^2)+2*((del_t+(del_c*di/D))*n))^0.5-(del_t+del_c)*n
kd=K*D

```

```

es=Fy/Es
ec=es*(kd)/(d-kd)
fc=ec*Ec
esc=ec*(kd-di)/(kd)
fs=esc*Es
Cc=(fc*b*kd)/2
Cs=Asc*fs
C=Cc+Cs
j=(Cs*(di+diat)+(Cc*kd/3))/(C)
jd=d-j
M3=Fy*Ast*jd*10^-6
phi3=(10^3*es)/(d*(1-K))
M=[M;M3]
phi=[phi;phi3]

%At Ultimate

a=Fy*(Ast-Asc)/(0.85*Fc*b)
c=a/0.85
ess=ecu*(c-di)/(c)
fss=ess*Es
M4=(0.85*Fc*a*b*(d-a/2)+Asc*fss*(d-di))*10^-6
phi4=ecu*10^3/c
M=[M;M4]
phi=[phi;phi4]
plot(phi,M),grid
xlabel('Curvature of the section (phi)');
ylabel('Moment of resistance of the section (M) in kN-m');
title('Moment Curvature Relation For Over Reinforced section');

```


Moment-Curvature Relationship for Singly Reinforced by Transform Area Method

```

Ast=input('Enter the bottom Reinforcement area(mm2):')
ecu=input('Enter the Extreme compression strain:')
f=input('Modulus of rupture:')
Fy=input('yield strength of steel:')
b=input('width of the beam:')
D=input('depth of the beam:')
Fc=input('Cylinder strength of concrete:')
Ec=input('Modulus of the elasticity of concrete:')
Es=input('Modulus of the elasticity of concrete:')
di=input('Clear Cover:')
diab=input('diameter of top bar:')
diat=input('diameter of botom bar:')
M1=0
phi1=0
d=D-di
Ast=As
%step 1:
%First Crack
n=Es/Ec
M=[]
phi=[]
M=[M;M1]
phi=[phi;phi1]
%Using transformed area
A=b*D+(n-1)*Ast
Y=((b*D*D/2)+(As*(D-(di+diab/2))))/(A)
I=((b*D^3)/12)+(b*D*((D/2-Y)^2))+(As*(((D-di+diab/2))-Y)^2))

```

```

M2=(f*I)*10^-6/(Y)
phi2=(f/(Ec*Y))*10^3
M=[M;M2]
phi=[phi;phi2]

%step 2
%At first Yield

del_t=As/(b*D)
J=solve(K^2+2*n*del_t*K-2*n*del_t == 0)
K=input('Value of K from eq. K^2+2*n*del*K - 2*n*del = 0')
kd=K*d
es=Fy/Es
ec=es*(kd)/(d-kd)
fc=ec*Ec
Cc=(fc*b*kd)/2
C=Cc
jd=d-(kd/3)
M3=Fy*As*jd*10^-6
phi3=(10^3*es)/(d*(1-K))
M=[M;M3]
phi=[phi;phi3]

%At Ultimate

a=Fy*(As)/(0.85*Fc*b)
c=a/0.85
M4=As*Fy*(d-0.5*a)*10^-6
phi4=ecu*10^3/c

```

```
M=[M;M4]
phi=[phi;phi4]

plot(phi,M),grid
xlabel('Curvature of the section (phi)');
ylabel('Moment of resistance of the section (M) in kN-m');
title('Moment Curvature Relation For Over Reinforced section');
```

Appendix B

Matlab Program by Strain Compatibility Method

Moment-Curvature Relationship for Singly Reinforced Beam

```
clc
syms epsi_int z alpha gamma fc c_c X_u epsi_sh epsi_su fsu r m x
b=input('width of the beam:')
D=input('depth of the beam:')
Asc=input('Enter the top Reinforcement area(mm2):')
Ast=input('Enter the bottom Reinforcement area(mm2):')
co=input('Clear Cover:')
fcc=input('Cube strength of concrete:')
ecu=input('Enter the Extreme compression strain:')
fy=input('yield strength of steel:')
fc=input('Cylinder strength of concrete:')
Es=input('Modulus of the elasticity of concrete:')
sh=input('Spacing of Stirrups:')
fsu=input('Ultimate strength of steel:')
s_d=input('diameter of stirrups:')
```

```

b_s=input('diameter of bottom bar:')
dprime=h-co
d=h-2*co
b=B-2*co
deff=h-co-s_d-b_s/2
b_b=b-s_d
d_d=d-s_d
epsi_y=(fy/E_s)
epsi_sh=16*epsi_y
M=[]
phi=[]
for (i=1:10)
    epsi_int=(epsi_ult/10)*i
    X_u=0.5*dprime
    if (epsi_int<0.002)
        fc=((2*epsi_int/0.002)-(epsi_int/0.002)^2)*fcc
    else (0.002 <= epsi_int <= 0.004)
        fc=fcc
    end

    alpha=fc/fcc
    gamma=0.5
    for(j=1:5000)

        c_c=alpha*fcc*B*X_u*10^-3
        epsi_s=epsi_int*((deff-X_u)/(X_u))
        if (epsi_s<epsi_y)
            f_s=epsi_s*E_s
        else (epsi_y <= epsi_s < epsi_sh)

```

```

        f_s=fy
    end
    T=Ast*f_s*10^-3
    p=abs(c_c-T)

    if (p<=0.05)
        Mu=c_c*(deff-gamma*X_u)*10^-3+T*X_u*10^-3
        M(i+1)=Mu
        phiu=(epsi_int*10^3)/(X_u)
        phi(i+1)=phiu
        break;
    else
        X_u=X_u-0.01
    end

    j=j+1
end
i=i+1
end
plot(phi,M),grid
xlabel('Curvature of the section (phi)');
ylabel('Moment of resistance of the section (M) in kN-m');
title('Moment Curvature Relation For Over Reinforced section');

```

Moment-Curvature Relationship for Doubly Reinforced Beam

```

clc
syms epsi_int z alpha gamma fc c_c X_u epsi_sh epsi_su fsu r m x
b=input('width of the beam:')
D=input('depth of the beam:')
Asc=input('Enter the top Reinforcement area(mm2):')
Ast=input('Enter the bottom Reinforcement area(mm2):')
co=input('Clear Cover:')
fcc=input('Cube strength of concrete:')
ecu=input('Enter the Extreme compression strain:')
fy=input('yield strength of steel:')
fc=input('Cylinder strength of concrete:')
Es=input('Modulus of the elasticity of concrete:')
sh=input('Spacing of Stirrups:')
fsu=input('Ultimate strength of steel:')
s_d=input('diameter of stirrups:')
b_s=input('diameter of bottom bar:')
dprime=h-co
d=h-2*co
b=B-2*co
deff=h-co-s_d-b_s/2
b_b=b-s_d
d_d=d-s_d
epsi_y=(fy/E_s)
epsi_sh=1.5*epsi_y
M=[]
phi=[]
for (i=1:10)
    epsi_int=(epsi_ult/10)*i

```

```

X_u=0.5*dprime
if (epsi_int<0.002)
    fc=((2*epsi_int/0.002)-(epsi_int/0.002)^2)*fcc
else (0.002 <= epsi_int <= 0.004)
    fc=fcc
end

alpha=fc/fcc
gamma=0.5
for(j=1:5000)

    c_c=alpha*fcc*B*X_u*10^-3
    epsi_s=epsi_int*((deff-X_u)/(X_u))
    if (epsi_s<epsi_y)
        f_s=epsi_s*E_s
    else (epsi_y <= epsi_s < epsi_sh)
        f_s=fy
    end
    epsi_sc=epsi_int*((X_u-co)/(X_u))
    if (epsi_sc<epsi_y)
        f_sc=epsi_sc*E_s
    else (epsi_y <= epsi_sc < epsi_sh)
        f_sc=fy
    end
    c_t= Asc*f_sc*10^-3
    c=c_c+c_t
    T=Ast*f_s*10^-3
    p=abs(c-T)

    if (p<=0.05)

```



```

        Mu=c_c*(deff-gamma*X_u)*10^-3+c_t*(X_u-co-s_d)*10^-3+T*X_u*10^-3
        M(i+1)=Mu
        phiu=(epsi_int*10^3)/(X_u)
        phi(i+1)=phiu
        break;
    else
        X_u=X_u-0.01
    end

    j=j+1
end
i=i+1
end
plot(phi,M),grid
xlabel('Curvature of the section (phi)');
ylabel('Moment of resistance of the section (M) in kN-m');
title('Moment Curvature Relation For Over Reinforced section');

```

Appendix C

Experimental Results

Strain was measured by mechanical strain gauges. Average strain from top three strain gauge was consider as the compressive strain and average strain from bottom three strain gauge, tensile strain was evaluated. Here $\varepsilon_1, \varepsilon_3, \varepsilon_5$ were represent top strain. And $\varepsilon_2, \varepsilon_4, \varepsilon_6$ shows bottom strain. ε_c and ε_t repentant average compressive strain and average tensile strain. Fig. 5.9 shows the positions of the strain gauges.

Table C.1: Strain in Singly Under Reinforced Beam-1

Load (kN)	ε_1	ε_2	ε_3	ε_4	ε_5	ε_6	ε_c	ε_t
0	0	0	0	0	0	0	0	0
4	-0.02	0.06	-0.02	0.04	-0.02	0.06	-0.020	0.053
8	-0.08	0.12	-0.1	0.1	-0.06	0.12	-0.080	0.113
12	-0.2	0.14	-0.16	0.18	-0.14	0.16	-0.167	0.160
16	-0.18	0.2	-0.18	0.28	-0.2	0.26	-0.187	0.247
20	-0.3	0.6	-0.2	0.36	-0.26	0.26	-0.253	0.407
24	-0.24	0.7	-0.3	0.48	-0.28	0.28	-0.273	0.487
28	-0.32	0.9	-0.4	0.6	-0.38	0.36	-0.367	0.620
32	-0.4	1.04	-0.46	0.8	-0.46	0.38	-0.440	0.740
36	-0.48	1.12	-0.54	0.86	-0.58	0.44	-0.533	0.807
40	-0.56	1.2	-0.62	0.84	-0.64	0.46	-0.607	0.833
44	-0.68	1.42	-0.7	0.86	-0.76	0.54	-0.713	0.940
48	-0.64	1.58	-0.76	0.94	-0.86	0.68	-0.753	1.067
52	-0.84	1.82	-0.86	1.06	-0.98	0.82	-0.893	1.233
56	-0.94	1.8	-0.92	1.18	-1.08	1.4	-0.980	1.460
60	-1.2	2.74	-1.02	1.48	-1.12	1.4	-1.113	1.873
64	-1.48	4.36	-1.3	3.6	-1.28	2.74	-1.353	3.567
68	-1.7	9.88	-1.44	5.58	-1.32	4.42	-1.487	6.627
70	-1.64	11.76	-1.8	8.82	-1.7	6.4	-1.713	8.993
70	-2.22	14.26	-1.9	11.6	-1.98	7.62	-2.033	11.160
70	-2	19.76	-2.24	16.3	-2.08	14.74	-2.107	16.933

Table C.2: Strain in Singly Under Reinforced Beam-2

Load (kN)	ε_1	ε_2	ε_3	ε_4	ε_5	ε_6	ε_c	ε_t
0	0	0	0	0	0	0	0	0
4	-0.02	0.02	0	0.04	-0.02	0.04	-0.013	0.033
8	-0.12	0.26	-0.08	0.2	-0.1	0.16	-0.100	0.207
12	-0.16	0.58	-0.22	0.36	-0.2	0.24	-0.193	0.393
16	-0.26	0.78	-0.4	0.38	-0.22	0.36	-0.293	0.507
20	-0.1	0.94	-0.38	0.48	-0.5	0.16	-0.327	0.527
24	-0.2	0.92	-0.16	0.34	-0.34	0.2	-0.233	0.487
28	-0.24	1.36	-0.4	0.44	-0.5	0.32	-0.380	0.707
32	-0.36	0.96	-0.56	0.66	-0.66	0.32	-0.527	0.647
36	-0.5	1.1	-0.68	0.78	-0.74	0.4	-0.640	0.760
40	-0.62	1.18	-0.78	0.92	-0.78	0.54	-0.727	0.880
44	-0.74	1.34	-0.94	1.04	-0.74	0.72	-0.807	1.033
48	-0.86	1.4	-1.04	1.2	-0.82	0.82	-0.907	1.140
52	-0.98	1.5	-1.14	1.2	-0.94	1.16	-1.020	1.287
56	-1.04	1.6	-1.18	1.38	-1.14	1.36	-1.120	1.447
60	-1.14	1.66	-1.38	1.62	-1.16	1.46	-1.227	1.580
64	-1.22	2.34	-1.4	1.76	-1.42	2.36	-1.347	2.153
68	-1.38	2.9	-1.44	3.12	-1.34	2.76	-1.387	2.927
69	-1.52	10.12	-2.08	5.8	-1.58	4.68	-1.727	6.867
69	-1.7	11.12	-1.98	10.32	-2.46	8.32	-2.047	9.920
69	-1.84	11.62	-2.44	18.1	-2.06	15.54	-2.113	15.087

Table C.3: Strain in Singly Reinforced Beam 3

Load (kN)	ε_1	ε_2	ε_3	ε_4	ε_5	ε_6	ε_c	ε_t
0	0	0	0	0	0	0	0	0
4	-0.02	0.02	-0.02	0.04	-0.02	0.04	-0.02	0.033
8	-0.08	0.1	-0.08	0.1	-0.08	0.14	-0.080	0.113
12	-0.16	0.12	-0.26	0.18	-0.2	0.26	-0.207	0.187
16	-0.18	0.18	-0.22	0.42	-0.3	0.46	-0.233	0.353
20	-0.3	0.62	-0.24	0.28	-0.1	0.54	-0.213	0.480
24	-0.38	0.84	-0.38	0.4	-0.24	1.02	-0.333	0.753
28	-0.6	0.72	-0.5	0.6	-0.4	0.6	-0.500	0.640
32	-0.7	1.2	-0.66	0.62	-0.2	0.86	-0.520	0.893
36	-0.8	1.76	-0.8	0.76	-0.22	0.64	-0.607	1.053
40	-0.86	1.88	-0.88	0.88	-0.28	0.84	-0.673	1.200
44	-0.96	1.96	-0.92	0.96	-0.32	0.7	-0.733	1.207
48	-1.02	2.04	-0.98	1.06	-0.52	0.82	-0.840	1.307
52	-1.16	2.18	-1.1	1.18	-0.62	0.92	-0.960	1.427
56	-1.18	2.32	-1.2	1.32	-0.72	1.14	-1.033	1.593
60	-1.3	2.8	-1.26	1.4	-0.86	3.06	-1.140	2.420
64	-1.36	5.74	-1.3	1.62	-1	5.7	-1.220	4.353
68	-1.58	10.8	-1.78	2	-0.9	6.58	-1.420	6.460
69	-1.92	10.72	-1.7	4.4	-1.08	10.82	-1.567	8.647
69	-2	12.14	-2	4.62	-2.22	11.6	-2.073	9.453
69	-2.24	17.7	-2.3	6.74	-2	16.3	-2.180	13.580

Table C.4: Strain in Singly Over Reinforced Beam-1

Load (kN)	ε_1	ε_2	ε_3	ε_4	ε_5	ε_6	ε_c	ε_t
0	0	0	0	0	0	0	0	0
4	-0.02	0.04	0	0.04	-0.02	0.02	-0.013	0.033
8	-0.04	0.16	-0.1	0.12	-0.1	0.1	-0.080	0.127
12	-0.06	0.22	-0.06	0.2	-0.12	0.18	-0.080	0.200
16	-0.14	0.34	-0.1	0.26	-0.1	0.32	-0.113	0.307
20	-0.18	0.26	-0.16	0.3	-0.14	0.32	-0.160	0.293
24	-0.16	0.46	-0.12	0.38	-0.16	0.36	-0.147	0.400
28	-0.18	0.54	-0.2	0.44	-0.28	0.5	-0.220	0.493
32	-0.22	0.42	-0.24	0.5	-0.38	0.68	-0.280	0.533
36	-0.46	0.5	-0.48	0.52	-0.48	0.6	-0.473	0.540
40	-0.5	0.46	-0.5	0.46	-0.46	0.48	-0.487	0.467
44	-0.32	0.62	-0.42	0.56	-0.38	0.58	-0.373	0.587
48	-0.42	0.66	-0.46	0.68	-0.4	0.7	-0.427	0.680
52	-0.46	0.74	-0.62	0.78	-0.46	0.8	-0.513	0.773
56	-0.54	0.82	-0.5	0.84	-0.52	0.86	-0.520	0.840
60	-0.6	0.88	-0.52	0.88	-0.56	0.9	-0.560	0.887
64	-0.56	0.96	-0.6	0.94	-0.64	0.98	-0.600	0.960
68	-0.62	1.02	-0.62	1.02	-0.54	1.06	-0.593	1.033
72	-0.5	1.06	-0.5	1.06	-0.66	1.16	-0.553	1.093
76	-0.64	1.16	-0.66	1.12	-0.7	1.04	-0.667	1.107
80	-0.7	1.28	-0.74	1.26	-0.74	1.22	-0.727	1.253
84	-0.8	1.36	-0.76	1.36	-0.8	1.3	-0.787	1.340
88	-0.74	1.44	-0.82	1.46	-0.84	1.42	-0.800	1.440
92	-0.96	1.54	-0.9	1.56	-0.94	1.48	-0.933	1.527
96	-1.06	1.52	-1	1.62	-1.06	1.26	-1.040	1.467
100	-1.02	1.4	-1.06	1.46	-1.02	1.36	-1.033	1.407
104	-0.98	1.56	-1	1.54	-1.04	2.16	-1.007	1.753
108	-1.06	2.38	-1.18	1.46	-1.22	2.48	-1.153	2.107
112	-1.22	2.82	-1.22	2.26	-1.26	4.62	-1.233	3.233
113	-1.64	6.56	-1.64	4.64	-1.7	10.66	-1.660	7.287
113	-2.06	8.76	-2.06	7	-2.06	13.02	-2.060	9.593

Table C.5: Strain in Singly Over reinforced Beam-2

Load (kN)	ε_1	ε_2	ε_3	ε_4	ε_6	ε_c	ε_t	ε_1
0	0	0	0	0	0	0	0	0
4	-0.02	0.04	-0.02	0.1	-0.04	0.02	-0.027	0.053
8	0	0.12	-0.04	0.12	-0.12	0.04	-0.053	0.093
12	-0.02	0.08	-0.06	0.14	-0.08	0.14	-0.053	0.120
16	-0.08	0.2	-0.06	0.26	-0.16	0.4	-0.100	0.287
20	-0.1	0.28	-0.14	0.38	-0.32	0.34	-0.187	0.333
24	-0.14	0.34	-0.22	0.5	-0.36	0.4	-0.240	0.413
28	-0.1	0.46	-0.26	0.42	-0.28	0.46	-0.213	0.447
32	-0.22	0.72	-0.3	0.68	-0.36	0.68	-0.293	0.693
36	-0.18	0.56	-0.26	0.76	-0.3	0.72	-0.247	0.680
40	-0.3	0.62	-0.34	0.9	-0.36	0.74	-0.333	0.753
44	-0.34	0.68	-0.44	0.96	-0.42	0.8	-0.400	0.813
48	-0.38	0.8	-0.42	1.04	-0.48	0.88	-0.427	0.907
52	-0.48	0.9	-0.46	1.1	-0.54	0.94	-0.493	0.980
56	-0.5	1	-0.5	1	-0.52	1	-0.507	1.000
60	-0.56	0.98	-0.54	1.28	-0.62	1.08	-0.573	1.113
64	-0.66	1.1	-0.6	1.34	-0.66	1.16	-0.640	1.200
68	-0.72	1.14	-0.7	1.42	-0.82	1.14	-0.747	1.233
72	-0.78	1.22	-0.8	1.6	-0.96	1.24	-0.847	1.353
76	-0.84	1.3	-0.94	1.84	-1.08	1.38	-0.953	1.507
80	-0.82	1.38	-1.06	1.9	-1.22	1.44	-1.033	1.573
84	-0.84	1.48	-1.14	2.1	-1.36	1.6	-1.113	1.727
88	-0.9	1.6	-1.2	2.18	-1.46	1.76	-1.187	1.847
92	-0.96	1.74	-1.34	2.28	-1.52	2.06	-1.273	2.027
96	-1.12	1.88	-1.42	2.38	-1.44	2.26	-1.327	2.173
100	-1.3	1.98	-1.48	2.48	-1.56	2.8	-1.447	2.420
104	-1.48	3.6	-1.56	2.6	-1.62	2.92	-1.553	3.040
108	-1.7	5	-1.62	5.06	-1.64	3.14	-1.653	4.400
110	-1.7	7.44	-1.66	6.2	-1.68	3.74	-1.680	5.793
109	-1.8	11.18	-2.08	8.24	-2.1	4.24	-1.993	7.887
110	-2.04	13.38	-2.1	9.6	-2.12	5.6	-2.087	9.527

Table C.6: Strain in Singly Over reinforced Beam-3

Load (kN)	ε_1	ε_2	ε_3	ε_4	ε_5	ε_6	ε_c	ε_t
0	0	0	0	0	0	0	0	0
4	-0.02	0.02	-0.02	0.04	-0.02	0.04	-0.020	0.033
8	-0.06	0.14	-0.04	0.14	-0.1	0.14	-0.067	0.140
12	-0.1	0.2	-0.08	0.16	-0.12	0.18	-0.100	0.180
16	-0.2	0.32	-0.12	0.28	-0.1	0.22	-0.140	0.273
20	-0.22	0.24	-0.16	0.36	-0.14	0.34	-0.173	0.313
24	-0.28	0.44	-0.12	0.4	-0.16	0.44	-0.187	0.427
28	-0.32	0.52	-0.1	0.48	-0.28	0.5	-0.233	0.500
32	-0.4	0.4	-0.24	0.36	-0.38	0.56	-0.340	0.440
36	-0.32	0.48	-0.44	0.6	-0.48	0.48	-0.413	0.520
40	-0.36	0.44	-0.54	0.46	-0.46	0.48	-0.453	0.460
44	-0.42	0.6	-0.5	0.7	-0.38	0.52	-0.433	0.607
48	-0.46	0.64	-0.58	0.68	-0.46	0.58	-0.500	0.633
52	-0.5	0.7	-0.54	0.74	-0.48	0.6	-0.507	0.680
56	-0.54	0.74	-0.56	0.78	-0.54	0.66	-0.547	0.727
60	-0.56	0.82	-0.66	0.86	-0.44	0.74	-0.553	0.807
64	-0.58	0.9	-0.62	0.9	-0.6	0.82	-0.600	0.873
68	-0.62	0.9	-0.7	0.96	-0.54	0.9	-0.620	0.920
72	-0.68	1.04	-0.78	1.06	-0.66	1.02	-0.707	1.040
76	-0.78	1.14	-0.66	1.16	-0.7	1.08	-0.713	1.127
80	-0.86	1.2	-0.74	1.22	-0.78	1.18	-0.793	1.200
84	-0.92	1.28	-0.86	1.38	-0.86	1.28	-0.880	1.313
88	-0.96	1.36	-0.96	1.26	-0.84	1.28	-0.920	1.300
92	-1.04	1.5	-1.14	1.44	-0.8	1.46	-0.993	1.467
96	-1.12	1.96	-1.26	1.52	-1.02	1.54	-1.133	1.673
100	-1.18	2.38	-1.4	1.56	-1.04	1.64	-1.207	1.860
104	-1.28	4.24	-1.52	1.62	-1.14	1.66	-1.313	2.507
108	-1.48	6.36	-1.62	1.86	-1.22	1.88	-1.440	3.367
112	-1.58	6.8	-1.82	3.26	-1.72	5.28	-1.707	5.113
113	-1.76	7.54	-1.96	4.64	-1.94	5.66	-1.887	5.947
113	-2.04	9.74	-2.14	8	-2.26	9.02	-2.147	8.920

Table C.7: Strain in Doubly Under Reinforced Beam-1

Load(kN)	ε_1	ε_2	ε_3	ε_4	ε_5	ε_6	ε_c	ε_t
0	0	0	0	0	0	0	0	0
4	-0.02	0.02	0	0.06	-0.02	0.02	-0.013	0.033
8	-0.06	0.12	-0.04	0.1	-0.12	0.04	-0.073	0.087
12	-0.14	0.14	-0.18	0.14	-0.18	0.08	-0.167	0.120
16	-0.2	0.18	-0.14	0.16	-0.24	0.1	-0.193	0.147
20	-0.3	0.22	-0.28	0.32	-0.26	0.16	-0.280	0.233
24	-0.32	0.26	-0.32	0.36	-1.14	0.14	-0.593	0.253
28	-0.38	0.32	-0.44	0.4	-0.96	0.2	-0.593	0.307
32	-0.46	0.38	-0.52	0.5	-0.82	0.24	-0.600	0.373
36	-0.52	0.42	-0.6	0.58	-0.48	0.28	-0.533	0.427
40	-0.6	0.62	-0.68	0.68	-0.7	0.32	-0.660	0.540
44	-0.7	0.7	-0.76	0.4	-0.76	0.36	-0.740	0.487
48	-0.48	0.98	-0.8	0.5	-0.88	0.46	-0.720	0.647
52	-0.74	1.06	-0.88	0.62	-0.92	0.48	-0.847	0.720
56	-0.76	1.16	-1.02	0.7	-0.9	0.62	-0.893	0.827
60	-1.06	1.12	-1.08	0.84	-1.12	0.68	-1.087	0.880
64	-1.12	1.22	-1.16	0.76	-1.22	0.76	-1.167	0.913
68	-1.16	1.3	-1.24	0.88	-1.32	0.88	-1.240	1.020
72	-1.22	1.46	-1.28	1	-1.38	1.04	-1.293	1.167
76	-1.24	1.4	-1.44	2.16	-1.26	1.18	-1.313	1.580
80	-1.4	2.22	-1.34	2.06	-1.42	1.5	-1.387	1.927
84	-1.42	2.42	-1.54	2.48	-1.56	1.64	-1.507	2.180
87	-1.66	5.76	-1.64	6.72	-1.68	1.86	-1.660	4.780
83	-1.92	6.84	-1.88	8.88	-1.82	4.26	-1.873	6.660
80	-2.18	11	-2.22	18.02	-2.08	7.84	-2.160	12.287

Table C.8: Strain in Doubly Under Reinforced Beam-2

Load (kN)	ε_1	ε_2	ε_3	ε_4	ε_5	ε_6	ε_c	ε_t
0	0	0	0	0	0	0	0	0
4	-0.02	0.02	-0.02	0	-0.02	0.02	-0.020	0.013
8	-0.06	0.06	-0.04	0.04	-0.04	0.08	-0.047	0.060
12	-0.2	0.12	-0.14	0.1	-0.14	0.18	-0.160	0.133
16	-0.14	0.24	-0.1	0.26	-0.3	0.4	-0.180	0.300
20	-0.16	0.32	-0.16	0.32	-0.14	0.44	-0.153	0.360
24	-0.2	0.38	-0.26	0.36	-0.22	0.38	-0.227	0.373
28	-0.26	0.52	-0.38	0.5	-0.18	0.48	-0.273	0.500
32	-0.32	0.58	-0.46	0.64	-0.42	0.72	-0.400	0.647
36	-0.46	0.66	-0.52	0.7	-0.46	0.76	-0.480	0.707
40	-0.56	0.72	-0.56	0.76	-0.56	0.82	-0.560	0.767
44	-0.62	0.84	-0.66	0.84	-0.62	0.88	-0.633	0.853
48	-0.54	0.94	-0.68	0.9	-0.7	0.92	-0.640	0.920
52	-0.64	0.88	-0.74	0.86	-0.8	0.98	-0.727	0.907
56	-0.72	0.96	-0.92	0.96	-0.9	1.06	-0.847	0.993
60	-0.86	1.06	-1	1.04	-1	1.14	-0.953	1.080
64	-0.96	1.1	-1.06	1.16	-1.1	1.18	-1.040	1.147
68	-1.06	1.12	-1.14	0.98	-1.24	0.86	-1.147	0.987
72	-0.98	1.36	-0.96	1.18	-1.28	1.02	-1.073	1.187
76	-1.02	1.46	-1.12	1.32	-1.38	1.06	-1.173	1.280
80	-1.1	1.62	-1.42	2.44	-1.5	1.14	-1.340	1.733
84	-1.18	3.04	-1.7	2.82	-1.76	5.58	-1.547	3.813
88	-1.9	4.38	-2	4.36	-1.92	8.76	-1.940	5.833
82	-2	6.46	-2.06	6.44	-2.1	12.22	-2.053	8.373
78	-2.18	8.62	-2.22	8.6	-2.32	18.38	-2.240	11.867

Table C.9: Strain in Doubly Under Reinforced Beam-3

Load (kN)	ε_1	ε_2	ε_3	ε_4	ε_5	ε_6	ε_c	ε_t
0	0	0	0	0	0	0	0	0
4	0	-0.02	-0.02	0	-0.04	0.02	-0.020	0.000
8	-0.06	0.04	-0.04	0.08	-0.12	0.04	-0.073	0.053
12	-0.1	0.14	-0.12	0.14	-0.2	0.1	-0.140	0.127
16	-0.2	0.18	-0.18	0.24	-0.26	0.16	-0.213	0.193
20	-0.24	0.24	-0.3	0.34	-0.44	0.2	-0.327	0.260
24	-0.34	0.32	-0.4	0.42	-0.44	0.22	-0.393	0.320
28	-0.48	0.52	-0.54	0.54	-0.52	0.26	-0.513	0.440
32	-0.56	0.68	-0.68	0.52	-0.6	0.36	-0.613	0.520
36	-0.62	0.72	-0.74	0.6	-0.64	0.4	-0.667	0.573
40	-0.64	0.78	-0.88	0.7	-0.7	0.48	-0.740	0.653
44	-0.72	0.8	-0.98	0.86	-0.76	0.46	-0.820	0.707
48	-0.68	0.86	-0.66	1.14	-0.84	0.6	-0.727	0.867
52	-0.68	0.96	-0.76	1.2	-0.94	0.68	-0.793	0.947
56	-0.84	1.02	-0.86	1.26	-1.02	0.86	-0.907	1.047
60	-0.92	1.12	-0.92	1.38	-1.1	0.96	-0.980	1.153
64	-0.96	1.24	-1	1.32	-1.18	1	-1.047	1.187
68	-1.08	1.3	-1.26	1.54	-1.34	1.08	-1.227	1.307
72	-1.14	1.4	-1.36	1.64	-1.3	1.22	-1.267	1.420
76	-1.24	1.38	-1.44	2.34	-1.4	1.34	-1.360	1.687
80	-1.34	1.52	-1.46	2.42	-1.34	2.5	-1.380	2.147
84	-1.66	2.32	-1.68	6.7	-1.6	2.64	-1.647	3.887
87	-1.76	5.6	-1.82	12.22	-1.66	4.86	-1.747	7.560
83	-2.02	6.9	-2.06	15.44	-1.86	7.26	-1.980	9.867
78	-2.28	12.06	-2.34	19.08	-2.02	9.84	-2.213	13.660

Table C.10: Strain in Doubly Over Reinforced Beam-1

Load (kN)	ε_1	ε_2	ε_3	ε_4	ε_5	ε_6	ε_c	ε_t
0	0	0	0	0	0	0	0	0
4	-0.02	0	-0.02	0.02	-0.04	0.02	-0.027	0.013
8	-0.04	0.02	-0.04	0.04	-0.12	0.04	-0.067	0.033
12	-0.16	0.04	-0.06	0.06	-0.08	0.06	-0.100	0.053
16	-0.1	0.12	-0.1	0.18	-0.06	0.14	-0.087	0.147
20	-0.26	0.08	-0.14	0.2	-0.08	0.4	-0.160	0.227
24	-0.14	0.2	-0.18	0.3	-0.16	0.34	-0.160	0.280
28	-0.16	0.28	-0.2	0.42	-0.32	0.4	-0.227	0.367
32	-0.04	0.34	-0.3	0.78	-0.36	0.46	-0.233	0.527
36	-0.28	0.46	-0.26	0.6	-0.28	0.68	-0.273	0.580
40	-0.24	0.6	-0.3	0.68	-0.36	0.72	-0.300	0.667
44	-0.26	0.56	-0.28	0.72	-0.3	0.74	-0.280	0.673
48	-0.36	0.58	-0.34	0.8	-0.34	0.82	-0.347	0.733
52	-0.42	0.62	-0.42	0.88	-0.38	0.86	-0.407	0.787
56	-0.52	0.66	-0.46	1	-0.44	0.98	-0.473	0.880
60	-0.56	0.74	-0.5	0.72	-0.4	1.02	-0.487	0.827
64	-0.62	0.8	-0.72	0.78	-0.48	1.06	-0.607	0.880
68	-0.72	0.86	-0.74	0.86	-0.62	1.26	-0.693	0.993
72	-0.76	0.9	-0.72	0.96	-0.66	1.14	-0.713	1.000
76	-0.78	0.96	-0.76	0.94	-0.74	1.24	-0.760	1.047
80	-0.78	1.08	-0.84	0.9	-0.8	1.16	-0.807	1.047
84	-0.84	1.08	-0.8	0.94	-0.82	1.3	-0.820	1.107
88	-0.92	1.22	-0.94	1.02	-0.96	1.38	-0.940	1.207
92	-0.88	1.34	-1.06	1.18	-1.08	1.3	-1.007	1.273
96	-1.16	1.42	-1.14	1.38	-1.22	2.06	-1.173	1.620
100	-1.28	1.58	-1.3	1.52	-1.48	1.78	-1.353	1.627
104	-1.4	1.8	-1.44	3.76	-1.46	3.06	-1.433	2.873
108	-1.64	4.18	-1.66	6.12	-1.68	4.74	-1.660	5.013
112	-1.8	8.38	-1.88	8.16	-1.78	5.24	-1.820	7.260
106	-1.84	9.4	-2.08	9.52	-2.1	6.6	-2.007	8.507
98	-2.1	15.58	-2.1	10.52	-2.12	8.6	-2.107	11.567

Table C.11: Strain in Doubly Over Reinforced Beam-2

Load(kN)	ε_1	ε_2	ε_3	ε_4	ε_5	ε_6	ε_c	ε_t
0	0	0	0	0	0	0	0	0
4	0	0.04	-0.04	0.02	-0.02	0.06	-0.020	0.040
8	-0.02	0.06	-0.08	0.08	-0.06	0.1	-0.053	0.080
12	-0.02	0	-0.26	0.18	-0.02	0.2	-0.100	0.127
16	-0.04	0.1	-0.18	0.3	-0.04	0.24	-0.087	0.213
20	-0.1	0.14	-0.1	0.14	-0.02	0.3	-0.073	0.193
24	-0.14	0.16	-0.18	0.24	-0.1	0.4	-0.140	0.267
28	-0.2	0.26	-0.24	0.34	-0.26	0.46	-0.233	0.353
32	-0.4	0.32	-0.3	0.4	-0.3	0.56	-0.333	0.427
36	-0.18	0.42	-0.32	0.52	-0.22	0.66	-0.240	0.533
40	-0.4	0.46	-0.26	0.4	-0.3	0.46	-0.320	0.440
44	-0.32	0.56	-0.28	0.44	-0.24	0.6	-0.280	0.533
48	-0.64	0.6	-0.4	0.44	-0.34	0.74	-0.460	0.593
52	-0.7	0.52	-0.72	0.5	-0.42	0.82	-0.613	0.613
56	-0.76	0.66	-0.82	0.72	-0.56	0.86	-0.713	0.747
60	-0.84	0.72	-0.86	0.74	-0.6	0.78	-0.767	0.747
64	-0.86	0.8	-0.8	0.78	-0.64	0.82	-0.767	0.800
68	-0.94	0.88	-0.96	0.86	-0.7	0.88	-0.867	0.873
72	-0.98	0.82	-1.04	0.78	-0.76	0.96	-0.927	0.853
76	-1.06	0.92	-1	0.9	-0.86	1	-0.973	0.940
80	-1.02	1	-1.04	1	-0.96	1.04	-1.007	1.013
84	-1.06	1.04	-1.08	1.12	-0.9	1.06	-1.013	1.073
88	-1.08	1.06	-1.16	1.18	-1.02	1.14	-1.087	1.127
92	-1.36	1.14	-1.24	1.3	-1.16	1.18	-1.253	1.207
96	-1.4	1.3	-1.3	2.24	-1.42	1.3	-1.373	1.613
100	-1.5	1.38	-1.34	2.38	-1.52	1.42	-1.453	1.727
104	-1.6	1.52	-1.44	6.48	-1.4	2.66	-1.480	3.553
108	-1.86	3.9	-1.66	7.84	-1.62	3.34	-1.713	5.027
114	-2.02	7.1	-1.88	10.88	-1.72	4.84	-1.873	7.607
107	-2.04	8.12	-2.08	12.24	-2.04	6.02	-2.053	8.793
100	-2.2	14.3	-2.1	16.24	-2.06	8.46	-2.120	13.000

Table C.12: Strain in Doubly Over Reinforced Beam-3

Load (kN)	ε_1	ε_2	ε_3	ε_4	ε_5	ε_6	ε_c	ε_t
0	0	0	0	0	0	0	0	0
4	-0.02	0.06	0	0.04	-0.02	0	-0.013	0.033
8	-0.04	0.08	-0.04	0.08	-0.1	0.02	-0.060	0.060
12	-0.14	0.18	-0.1	0.2	-0.06	0.06	-0.100	0.147
16	-0.2	0.08	-0.14	0.12	-0.04	0.1	-0.127	0.100
20	-0.04	0.24	-0.16	0.32	-0.06	0.2	-0.087	0.253
24	-0.22	0.26	-0.18	0.24	-0.14	0.34	-0.180	0.280
28	-0.16	0.36	-0.24	0.44	-0.3	0.36	-0.233	0.387
32	-0.38	0.46	-0.3	0.54	-0.34	0.42	-0.340	0.473
36	-0.42	0.54	-0.26	0.6	-0.26	0.56	-0.313	0.567
40	-0.5	0.56	-0.28	0.68	-0.34	0.66	-0.373	0.633
44	-0.62	0.64	-0.38	0.8	-0.28	0.72	-0.427	0.720
48	-0.5	0.72	-0.46	0.8	-0.38	0.82	-0.447	0.780
52	-0.58	0.76	-0.52	0.84	-0.42	0.86	-0.507	0.820
56	-0.62	0.82	-0.6	0.88	-0.48	0.94	-0.567	0.880
60	-0.7	0.88	-0.66	0.9	-0.52	1.02	-0.627	0.933
64	-0.56	0.82	-0.72	1	-0.54	1.14	-0.607	0.987
68	-0.64	0.88	-0.7	0.92	-0.6	1.1	-0.647	0.967
72	-0.68	0.98	-0.68	0.84	-0.64	1.22	-0.667	1.013
76	-0.78	0.96	-0.84	0.98	-0.8	1.2	-0.807	1.047
80	-0.84	1.14	-0.94	1.04	-0.94	1.34	-0.907	1.173
84	-0.82	1.3	-1.02	1.12	-1.06	1.26	-0.967	1.227
88	-1.14	1.38	-1.16	1.32	-1.2	2.02	-1.167	1.573
92	-1.22	1.5	-1.24	1.54	-1.26	2.2	-1.240	1.747
96	-1.3	1.58	-1.28	1.6	-1.34	2.3	-1.307	1.827
100	-1.34	1.7	-1.32	1.74	-1.42	2.5	-1.360	1.980
104	-1.36	1.78	-1.4	3.7	-1.44	3.02	-1.400	2.833
108	-1.66	4.18	-1.54	5.06	-1.66	4.7	-1.620	4.647
113	-1.68	8.26	-1.94	7.1	-1.76	5.2	-1.793	6.853
106	-1.9	10.36	-2.06	9.32	-2.08	6.56	-2.013	8.747
97	-2.1	14.54	-2.28	12.06	-2.1	8.56	-2.160	11.720